Utrecht University
Institute for Theoretical Physics
MSc Theoretical Physics

The Information Paradox for One-sided Black Hole Evaporation in AdS

Author:
Stefani Stefanova

Supervisors:
Ro Jefferson
Umut Gursoy

December, 2024

Contents

Abstract

The black hole information paradox has been troubling the minds of physicists since the discovery of Hawking radiation. The contradiction between Hawking's result and the unitarity postulate of quantum mechanics, reached a potential resolution in favor of unitarity, with the discovery of AdS/CFT, which promised that black holes in AdS must evolve unitarily due to their dual description being manifestly unitary.

However, studying the black hole information paradox in AdS can be tricky, with black holes above a certain mass being unable to evaporate due to the usual reflective boundary conditions. One particular paper that sparked hope for resolving both this evaporation issue and the information paradox, proposes a method for black hole evaporation via different boundary conditions, which allow the emitted Hawking radiation to be absorbed into an auxiliary bath. This evaporation process is shown to be unitary in the gravitational theory, with the innovative incorporation of regions behind the event horizon, which contribute to the entropy of the Hawking radiation. However, the dual description of this evaporation model is not as well-understood.

In this work, we motivate the need for an auxiliary absorbing system by verifying that radiation cannot be absorbed into the holographic boundary. We review the previous work on why coupling the bath to one side of the double-sided black hole does indeed lead to one-sided black hole evaporation, and motivate why the method is unitary, at least in the gravity theory.

A simple toy-model for the black hole evaporation in the dual theory is then proposed, which mimics the proposed evaporation protocol in the bulk. We show that if the bath, which is described as a local operation, acts as a unitary operator, it cannot achieve the claimed one-sided black hole evaporation. However, a non-unitary local operation of the bath has been used to derive an LOCC (Local Operations Classical Communication) operation that can achieve the one-sided black hole evaporation.

Acknowledgements

The first thank you goes to my supervisor, Ro Jefferson. It is rare to find in one person both a supervisor from whom you can learn so much, but also one of the most encouraging and supportive people; a mentor not just when it comes to solving physics problems, but in general. Ro, thank you so much for offering me the project, for teaching me what research is all about and for being such an awesome supervisor!

Thank you to my second supervisor Umut Gursoy for always making time to chat and offer insight about the project...even when it was early in the morning or late in the evening.

Thank you to my family back home in Bulgaria. I would not be here if it wasn't for all your support and encouragement! I can't wait to come home and hug you all! But a very special thank you goes to my mom, who brought me to math and physics classes for years, waiting for me for hours, often in the cold winters, staying up late to help me with homework, always believing in me...Thank you for always encouraging me to follow my dreams, even though they didn't seem as serious to other people, coming from a little girl. I know it mustn't have been easy for you to send me to study abroad, yet you still did it to help me achieve my goals. I do not know what I have to do to repay you for all your sacrifices...I love you!

The next thank you goes to Peter, who came into my life when I least expected, who made me realize that those notions about relationships, which I had started labeling as childish, can be real; who stood by me no matter how stressed and grumpy I was when work wasn't going well, who cheered me up every day, no matter how stressed he was too, and believed in me when I couldn't...I appreciate you so much and I feel so lucky! And I am not saying all of this just because you make the best coffee...maybe...

Another big thank you goes to Tim (aka The Bestie) who has been cheering me up and encouraging me for the past 8 years. With every year I realize how rare it is to find such a great friendship and I am very appreciative! Thanks for all the suppawt! I can't wait to see how much weirder this friendship will get over the years. I mean, as a start, I think we do need to put our CCV language into writing! And yes, I do HAVE TO say: my black holes will totally destroy your lasers...

Thank you to all my friends, for all the support and fun times! Thank you to all the peeps in Utrecht: Jaffar, Mike, Nicole, Meri (to name a few!) You have made this degree such an enjoyable experience!

I also want to thank the Dutch side of my family for all their support, for accepting me into their family and for making me feel so at home!

And thank you to all my teachers at Utrecht University! You have made me fall in love with physics all over again!

1 Introduction

1.1 Black Hole Thermodynamics

The notion of black hole entropy is at the heart of black hole thermodynamics. Its discovery is mostly accredited to Jacob Bekenstein, who is associated with the famous Bekenstein-Hawking entropy formula. However, it should be noted that this realization was greatly motivated by his PhD supervisor John Wheeler who was first to raise the question about the effect of black holes on the entropy of the Universe. It was in the early 70s when Wheeler started pondering what happens to the entropy of the Universe when matter falls into a black hole and disappears forever. This so-called *Wheeler's demon*, named by Bekenstein, was responsible for a violation of the second law of thermodynamics. Every time matter fell into a black hole, its entropy, however high, would disappear behind the horizon, hence lowering the entropy of the Universe.

This concern was a consequence of the black hole *no-hair theorem*, also named by Bekenstein[1], which states that black holes can be described entirely only by their mass, charge and angular momentum, so any specific properties of matter that falls into a black hole are lost to an outside observer. The no-hair theorem was a consequence of the uniqueness theorems developed by Brandon Carter and Werner Israel [1, 2], which led to the *Carter-Israel conjecture*. It stated that the solution, exterior to an event horizon, formed from gravitational collapse in a flat spacetime, eventually approaches the Kerr-Newman solution, which is, in turn, entirely described by the mass, charge and angular momentum parameters. It is a generalization which followed from work done in the late 60s by Israel, who showed that this is true for the simplified case of the Schwarzschild metric [3].

Soon (merely several months) after it originated, Bekenstein proposed a resolution to Wheeler's demon [4]. His revolutionary idea, however instinctive to physicists now, was that black holes have entropy themselves. When matter falls in, its entropy is not lost from the Universe, but gets added to the black hole, whose entropy increases.

It was in that same year (1971) that Steven Hawking developed the black hole *area theorem*,

[1] It is commonly believed that Wheeler coined the name, though in an interview he revealed it was indeed Bekenstein who did.

according to which the area of a black hole is never decreasing, i.e. $\mathrm{d}A/\mathrm{d}t \geq 0$ always holds true[5]. This is now referred to as the second law of black hole thermodynamics.[2]He considered the merging of two black holes to form one bigger Kerr black hole, and showed that the area of the event horizon of the resulting Kerr black hole is at least as big as the sum of the areas of the event horizons of the two individual black holes that were used to form it; i.e. $A_{\mathrm{Kerr}} \geq A_1 + A_2$.

It is interesting to note that around the same time, Sir Roger Penrose and Roger Floyd also reached a somewhat similar result, although via a different route. They studied if it would be possible to extract energy from a black hole - a puzzle which Penrose had already proposed mechanisms for, though it was later that him and Floyd showed that it was indeed possible for the case of the Kerr black hole solution[6]. They considered a test particle entering the ergosphere, which is the region between the event horizon of the Kerr black hole and the so-called ergosurface, defined as the radius at which particles remain stationary to an outside observer if they travel at the speed of light. Because this region is outside the event horizon, particles can enter and escape it. If a test particle enters the ergosphere, it can split into two particles, one of which must have negative mass, as required by energy conservation. It is this particle that falls into the black hole, while the positive mass particle escapes with energy greater than the energy of the original test particle. Penrose and Floyd showed that although the mass of the black hole decreases in this so-called *Penrose process*, the area of its event horizon cannot decrease, hence recovering the area theorem.

Having ascribed entropy to black holes, and motivated by Hawking's area theorem, Bekenstein suggested that the black hole entropy is proportional to the area of its event horizon such that

$$S_{\mathrm{BH}} \propto \frac{k_{\mathrm{B}} A}{\ell_{\mathrm{P}}^2} \,, \tag{1.1}$$

with a proportionality constant (credited to Wheeler) of $\mathcal{O}(\ell_{\mathrm{P}}^{-2})$, where ℓ_{P} is the Planck length, given by $\ell_{\mathrm{P}} = \sqrt{\hbar G/c^3}$, and k_{B} is Boltzmann's constant [7]. This is in great contrast to the familiar entropy of ordinary matter, which scale with the volume of the system, rather with its surface area. Furthermore, this law implied a deep connection between different theories in physics, namely thermodynamics (due to S_{BH}), gravity (due to A) and quantum mechanics (due to ℓ_{P}), which breaks in the classical limit of $\hbar \to 0$. Combined with Hawking's area theorem, this implied that the entropy of a black hole is increasing monotonically since

$$\frac{\mathrm{d}A}{\mathrm{d}t} \geq 0 \;\Rightarrow\; \frac{\mathrm{d}S_{\mathrm{BH}}}{\mathrm{d}t} \geq 0 \,. \tag{1.2}$$

Bekenstein later (1973) interpreted this entropy as Shannon entropy, meaning it quantified the level of uncertainty, or the lack of information about the internal structure of black holes [8]. He conjured that the required increase in the entropy of the Universe (including black holes and any matter falling into them) is a direct consequence of the loss of information about the initial conditions of any infalling matter. When it falls into a black hole, any information about the properties of the matter gets lost as the black hole evolves into a thermodynamic equilibrium, due to the no-hair theorem, hence increasing the entropy of the black hole. Despite the loss

[2]To avoid confusion, note that this law was derived before the discovery of Hawking radiation and no black hole evaporation was taken into account. The law was purely classical, hence only matter falling into the black hole was accounted for, and did not take into account any quantum effects, such as the existence of Hawking radiation.

of entropy of the black hole exterior due to the matter crossing the event horizon, the loss of information associated with the initial conditions being irrecoverable to an outside observer, is reflected in an greater increase of the black hole entropy. Although the black hole entropy increases in the process, for this to lead to an overall increase in the entropy of the Universe, it needs to be able to compensate for the decrease in the entropy outside the black hole, which occurs once the matter has crossed the event horizon, making its entropy inaccessible to the rest of the Universe.

Bekenstein raised a further question which seemed to violate Hawking's area law, namely that the black hole entropy is always increasing; i.e. $\mathrm{d}S_{\mathrm{BH}}/\mathrm{d}t \geq 0$. He suggested that it would be possible to gain information about the black hole, hence lowering its entropy, by simply obtaining information about any infalling matter prior to its fall into the black hole. This would lower the entropy of the black hole, while increasing the entropy outside of it. To reconcile this with Hawking's area theorem, Bekenstein proposed that both the black hole and matter entropies need to be taken into account in properly defining an entropy law in accordance with the second law with thermodynamics[8]. In this way, Wheeler's demon was resolved by generalizing the area law, such that the change in the entropy of a black hole, combined with the change in the entropy of the outside matter, must never decrease, such that

$$\frac{\mathrm{d}S_{\mathrm{total}}}{\mathrm{d}t} = \frac{\mathrm{d}S_{\mathrm{BH}}}{\mathrm{d}t} + \frac{\mathrm{d}S_{\mathrm{matter}}}{\mathrm{d}t} \geq 0 \,. \tag{1.3}$$

This is known as the generalized second law of black hole thermodynamics and meant that even though the entropy of matter gets lost when falling into a black hole, the increase in the area of the event horizon causes the entropy of the black hole to increase sufficiently so as to, overall, increase the entropy of the Universe.

Bekenstein's work faced a step back, following the realization that an earlier (1971) thought experiment proposed by Robert Geroch (another one of Wheeler's PhD students) violated the generalized second law, which meant that Bekenstein had to reconsider his equation. Geroch's thought experiment, known as *Geroch's heat engine*, considered a heat engine, which made use of a Schwarzschild black hole as an energy sink. It involved a massless box and a massless rope used to slowly lower the box very close to the event horizon of a black hole. The box, filled with radiation, is opened once close to the event horizon, releasing the radiation into the black hole. The weight of the radiation in the box was used to do work on the box, generated by the gravitational field. Geroch showed that the amount of work that can be extracted is precisely the energy of the radiation dropped, meaning that the energy of the black hole remains unchanged, while the energy of the radiation is converted to energy in the reservoir. The main concern arose with the result that this process can be used to run a Carnot cycle with perfect efficiency, in which case the temperature of the black hole was zero. Geroch's belief that black holes are systems of zero temperature violated the generalized second law of black hole thermodynamics, which assigned a positive entropy to black holes. It meant that the entropy of matter falling into a black hole would be lost; i.e. $\mathrm{d}S_{\mathrm{matter}}/\mathrm{d}t < 0$, while the entropy of the black hole would remain unchanged; i.e. $\mathrm{d}S_{\mathrm{BH}}/\mathrm{d}t = 0$, which would, naturally, lead to a violation of the second law of thermodynamics if the generalized law of black hole thermodynamics (1.3) was to hold true.

In attempt to salvage the situation, Bekenstein imposed that the proportionality constant

of the entropy-area formula contained an additional factor of $1/\hbar$, so

$$S_{\rm BH} \propto \frac{k_{\rm B}}{\hbar}\frac{A}{\ell_{\rm P}^2}\,, \tag{1.4}$$

This implied a that black holes have enormous entropies and raised concern among the physics community, with most physicists objecting to Bekenstein's entropy law (including Hawking), except for his supervisor Wheeler. It seemed counterintuitive for an objet containing no atoms or molecules, but just a singularity, to have such an enormous entropy.

In 1973, in response to Bekenstein's claim of an entropy-area relation[7], Hawking and Carter, together with James Bardeen formulated the laws of black hole thermodynamics, in accordance with the ordinary laws of thermodynamics[9], given by

The zeroth law : For a stationary black hole, the event horizon has a constant surface gravity, κ.
The first law : Perturbations of stationary black holes can be quantified via

$$\mathrm{d}E = \frac{\kappa}{8\pi}s\,\mathrm{d}A + \Omega\,\mathrm{d}J + \Phi\,\mathrm{d}Q\,, \tag{1.5}$$

where E is the total energy of the black hole, A is the area of the event horizon, Ω is the angular velocity, J is the angular momentum, Φ is the electrostatic potential and Q is the electric charge.
The second law : The area of the event horizon is never decreasing; i.e.

$$\frac{\mathrm{d}A}{\mathrm{d}t} \geq 0\,. \tag{1.6}$$

The third law : A black hole cannot be formed with a zero surface gravity, so all black holes must have $\kappa > 0$.

There was, indeed, a strong analogy with the ordinary laws of thermodynamics, but the paper still contained some flaws, one of which was about the temperature of the black hole, which was at absolute zero, implying they had no thermodynamic entropy.[3] This was based on the classical result that a black hole could not be in a thermodynamic equilibrium with radiation at any non-zero temperature, because although radiation can always enter the black hole, no radiation can be emitted from it (at least in the classical picture). This issue was soon to be fixed with the incorporation of quantum mechanics.

A progress followed with Bekenstein's proposal, in response to Hawking, Carter and Bardeen, that black holes have temperature and hence also a thermodynamic entropy. He was first to assign a temperature to black holes, which was proportional to the surface gravity[8]. However, the notion of black hole temperature kept baffling physicists, such as Hawking, who were faced with the choice that either black holes have no temperature and hence no thermodynamic entropy, which violated the second law of thermodynamics, or they had a temperature, meaning they could emit particles - an idea just as silly at the time, since no

[3]Note that the entropy that Bekenstein ascribed to black holes was Shannon entropy and should not be confused with the thermodynamic entropy. These different notions of entropy and their distinctive property under unitary evolution will be reviewed in Chapter 3.

particles were expected to be able to escape the gravitational pull of a black hole once behind its event horizon.

Things took a turn the following year (1974), when Hawking discovered that black holes can indeed radiate[10], and hence do have a temperature, as previously proposed by Bekenstein. Hawking's approach involved studying a massless scalar field in an asymptotically flat spacetime around a spherically symmetric collapsing star, and using quantum field theory on the spacetime before and after a black hole forms. The basic idea behind his calculation involved taking a positive-frequency wave on the future null infinity I^+, corresponding to a particle at late times, and propagating it backwards through spacetime. Hawking showed that the curvature of the Schwarzschild spacetime will cause part of the wave to scatter back towards the past null infinity I^- with the same positive frequency, while the other part propagates backwards into the star, through the origin and again out towards the past null infinity I^-. He wrote the scalar field in terms of solutions representing ingoing and outgoing waves crossing the horizon, and obtained an expression for the number of particles that would be created (and emitted) to the future infinity of the collapsing star, which was shown to be infinite in some frequency range. Hawking identified this infinite number of particles with a steady emission rate at late times, implying that the black hole will emit particles and eventually evaporate completely. Comparing absorption and emission, Hawking was able to show that the radiation was thermal, with a temperature proportional to the surface gravity, namely

$$T = \frac{\hbar}{ck_{\mathrm{B}}}\frac{\kappa}{2\pi} \,. \tag{1.7}$$

Following his discovery of the quantum nature of black holes, in the following year of 1975, Hawking showed that the black hole temperature is inversely proportional to the mass M of the black hole for the case of the Schwarzschild solution, such that

$$T = \frac{c^3\hbar}{Gk_{\mathrm{B}}}\frac{1}{8\pi M} \,, \tag{1.8}$$

deeming these black holes thermodynamically unstable[11]. However, it was another equation that stole the spotlight in Hawking's paper, namely the famous Bekenstein-Hawking entropy formula

$$S_{\mathrm{BH}} = \frac{k_{\mathrm{B}}c^3}{G\hbar}\frac{A}{4} \,. \tag{1.9}$$

While in accordance with the entropy equation proposed by Bekenstein, namely the proportionality to the area, Hawking had now fixed the proportionality constant. The main difference between their approaches was that Hawking tried to incorporate quantum mechanics into general relativity, while Bekenstein's approach was to combine general relativity and thermodynamics. Although Bekenstein's generalized second law was valid is many thought experiments, there was no proof of the law, and there were also cases (more *gedanken* experiments), in which it appeared to be violated. These violations occurred precisely due to the assumption that black holes do not radiate, which was immediately resolved with the discovery of the thermal emissions by Hawking, who also provided a proof of the generalized second law.

The formulation of Hawking's radiation only became more precise in the following years. Several months after his original proposal, Hawking worked on providing an explanation as to

how a black hole can actually emit these particles, which were not allowed to escape it classically. Being a quantum process, Hawking interpreted the emission of Hawking radiation as the quantum tunneling of particles across the event horizon[12]. A black hole could evaporate if a spontaneous creation of a pair of particles and anti-particles occurred in the gravitational field of the black hole, such that the particle with negative energy fell back into the black hole, while the other one escaped out to infinity as Hawking radiation. It was soon after that, that Hawking used quantum field theory to show that vacuum fluctuations cause such pairs of particles and anti-particles to be continuously created and annihilated. It is only when the pair is produced in the vicinity of a black hole event horizon, it is possible for it to be separated, with one of them falling into the black hole, while the other one escapes[13].

The discovery of Hawking radiation immediately seemed to have a direct implication on the area law (1.6), which appeared to be violated. In the process of emitting Hawking radiation, a black hole would evaporate, decreasing the area of its event horizon[14]. What is more, the generalized second law of black hole thermodynamics (1.3) now also faced a problem, since once completely evaporated, the entropy of the black hole would vanish, causing the Universe to lose entropy. Since the black hole evaporation is inherently a quantum mechanical process, while both the area law and the generalized second law were, so far, purely classical results, it meant that they had to be modified.

The key was, as pointed out by Bekenstein[15], to assign entropy to the Hawking radiation, such that the entropy of the emitted radiation is enough to overcompensate for the loss in entropy of the black hole, as seen in the decrease of its surface area. The final (quantized) version of the generalized second law of black hole thermodynamics hence required that the total entropy of the black hole, together with the total entropy of the Hawking radiation, should be non-decreasing, hence increasing the entropy of the Universe.

Although a lot of the basics of black hole thermodynamics had been well-established at this point, a Pandora's box had been opened as soon as Hawking radiation was discovered, leading to the famous black hole information paradox.[4]

1.2 The Information Paradox

The Information paradox began with the discovery of Hawking radiation. If one were to imagine a black hole formed from the gravitational collapse of matter in a pure state, then this initial black hole, being in a pure state, would have a vanishing von Neumann entropy. [5] However, as Hawking discovered, black holes emit thermal radiation, which is not pure. This means that after the complete evaporation of the initially-pure black hole, one would be left with only thermal radiation, which is in a mixed state. However, the evolution from a pure to a mixed state is not a unitary process since the von Neumann entropy, which is a quantum entropy, is invariant under a unitary evolution. For the black hole evaporation to be a unitary process, the final entropy of the Hawking radiation needs to somehow be purified, so that the von Neumann entropy of the system is brought back to zero. But why is the entropy of the Hawking radiation non-zero? The reason lies with the fact that Hawking modes are entangled, with a combined von Neumann entropy of zero. However, with the creation of

[4] A much more comprehensive review of the history of black hole thermodynamics can be found in [4].

[5] This is just a definition for the von Neumann entropy of a pure state. Properties of the von Neumann entropy will be discussed in Chapter 3.

each Hawking pair, one of the Hawking modes remains trapped behind the horizon, while the other one escapes to infinity. This leads to a continuously increasing von Neumann entropy of the emitted Hawking radiation, as illustrated by the green line in Figure 1.1. As the black hole evaporates, its mass decreases and the area of its event horizon shrinks, causing its thermodynamic entropy to decrease. This has been illustrated by the black curve in Figure 1.1, where a the blue curve has been used to illustrate what a unitary evolution would look like for the von Neumann entropy of the Hawking radiation. Such unitary evolution curve, namely one bringing the von Neumann entropy back to its original value is called a Page curve.

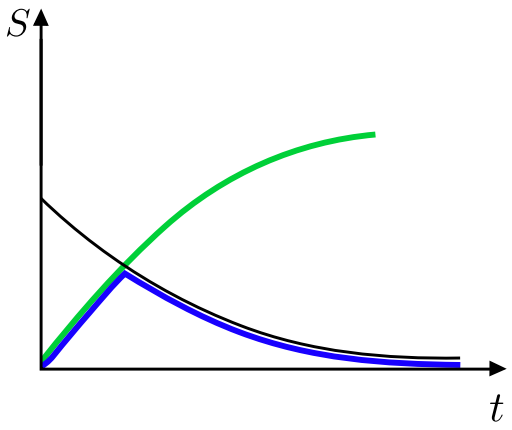

Figure 1.1: (green) The monotonically increasing entanglement entropy of the emitted Hawking radiation due to the increasing number of unpaired hawking modes. (black) The thermodynamic black hole entropy, which decreases as the black hole evaporates, due to the area of the event horizon getting smaller. (blue) A Page curve for the entropy of the Hawking radiation, which would bring the entropy back to its initial value, expected from a unitary evaporation model.

This discrepancy between the unitary evolution expectation in quantum mechanics and the non-unitary result following Hawking calculations established the Information paradox. There have been multiple attempts to resolve the paradox, such as the black hole Complementarity [16], which was later shown to be self-contradicting by [17], which introduced the so-called AMPS or *Firewall* paradox, hence bringing the information paradox the back to the drawing boards.

In recent years, there has been a lot of progress in the context of AdS, following the development of the AdS/CFT correspondence, which settled the issue in favor of unitarity and conservation of information. It meant that black hole evaporation in AdS must be a unitary process, since its dual description, namely the CFT that lives on the holographic boundary, is inherently a unitary theory. However, as we will see in this thesis, studying black holes in AdS, despite resolving some ambiguities about the expected unitary evolution, present other issues.

Structure of Thesis

The aim of this thesis is to review recent developments in resolving the Information Paradox, as well as raise some potential questions about their description.

In Chapter 1, we introduced the history of black hole thermodynamics, which gave rise to the Information Paradox. The paradox was explained, as well as how the discovery of AdS/CFT helped resolve some debates surrounding it.

In Chapter 2, we review aspects of the AdS/CFT correspondence. After describing the basic features of AdS spacetimes, the dynamics of a scalar field in AdS is reviewed, which is shown to depend on the signature of the metric. We show that while in Euclidean AdS, there does not exist a normalizable solution, in Lorentzian signature, one of the solutions is normalizable. We then review some features of CFTs, such as the state-operator map, and we give an example, in which we summarize some results for the massless free boson. After describing both AdS and CFT, the AdS/CFT duality is reviewed.

In Chapter 3, we introduce entanglement entropy in quantum mechanics, which is then derived for a general quantum field theory. We show how the AdS/CFT correspondence can be applied to the entanglement entropy, and introduce the RT prescription, as well as a short review of its derivation. Subsequent generalizations of the RT formula are stated, including the latest version of the generalized gravitational entanglement entropy.

In Chapter 4, we use the theoretical background from Chapter 2 to study black holes in AdS. We explain the motivation for studying black holes in AdS, as well as the issues surrounding these solutions, due to the nature of the AdS geometry and its reflective boundary conditions. We explain why large black holes do not evaporate in AdS, with all the Hawking radiation bouncing off the AdS boundary, and why making them smaller presents further issues. With that in mind, we show that changing these boundary conditions to being absorptive into the holographic boundary is not possible, since any particle that escapes the bulk will no longer have a description at the holographic boundary. This is used to motivate the need for an auxiliary system, where the Hawking radiation could be absorbed, hence allowing the black holes to evaporate.

In Chapter 5, we review one such recent model in the context of JT gravity [18], which proposes the attachment of an auxiliary bath to the AdS boundary, making one-sided black hole evaporation into the bath possible. To explain this model, we first review features of JT gravity, and use its semiclassical description to review how coupling to the bath achieves the evaporation protocol. The discussion in Chapter 3 is then used to explain how the proposed black hole evaporation model was used to produce a unitary Page for both the evaporating black hole and the emitted Hawking radiation, hence leading to a possible resolution to the Information paradox. We then look for a way to describe this one-sided black hole evaporation model, but using a toy-model for the boundary theory, namely working in the TFD formalism. We model the bath in the gravity theory as an operator in the dual theory, and we find such an operation which successfully reproduces all the expected results in the dual theory. However, this operation is shown to be non-unitary and we argue that a unitary bath operation may not be possible, at least with the way the bath is described to act on the bulk. As will be explained, this does not exclude the possibility for a global unitary bath operation, although the way that the bath is coupled to the bulk might have to be different. We also show that the one-sided evaporation can be modeled via an LOCC protocol, which uses the bath as a way to transfer classical information.

2
AdS/CFT

The AdS/CFT duality provides a powerful tool for studying the Information paradox. Due to the unitary evolution of the CFT on the holographic boundary, AdS/CFT also guarantees a unitary evolution inside the bulk, where one could choose to study how black holes evaporate. In this chapter, we will discuss aspects of the AdS/CFT correspondence, which will be used later in the thesis. In Section 2.1, we will review the basic features of AdS spacetimes, such as the dynamics of a scalar field in AdS, which will be shown to depend on the signature of the metric. We show that while in Euclidean AdS, there does not exist a normalizable solution, in Lorentzian signature, one of the solutions is normalizable. In Section 2.2, we will review some features of CFTs, such as the state-operator map, and review the massless free boson theory. In Section 2.3, we will review the correspondence between these two descriptions. Although it will not include any new calculations, the results in this chapter will be used for calculations later on in the thesis.

2.1 Anti-de Sitter Spacetime

2.1.1 Coordinates

Anti-de Sitter (AdS) spacetime is a maximally symmetric spacetime and a solution to Einstein's equations with a negative cosmological constant. A $(d+1)$-dimensional AdS spacetime, namely AdS_{d+1}, can be obtained from a submanifold of $(d+2)$-dimensional Minkowski spacetime with a $(2,d)$ signature $\mathbb{R}^{d,2}$, described by

$$\mathrm{d}s^2 = -\mathrm{d}T_1^2 - \mathrm{d}T_2^2 + \mathrm{d}X_1^2 + \ldots + \mathrm{d}X_d^2 \,. \tag{2.1}$$

AdS_{d+1} is then defined as the submanifold

$$T_1^2 + T_2^2 - X_1^2 - \ldots - X_d^2 = \ell_{\mathrm{AdS}}^2 \,, \tag{2.2}$$

where ℓ_{AdS} is referred to as the AdS radius (i.e. radius of curvature). The cosmological constant depends on the AdS radius, such that $\Lambda = -\frac{d(d+1)}{2\ell_{\text{AdS}}^2}$. There are different sets of coordinates that can be used to describe the AdS spacetime[19]. A common choice are the so-called *global coordinates* $(\tau, \tilde{\rho}, \Omega_i)$, defined as

$$\begin{aligned} T_1 &= \ell_{\text{AdS}} \cos\tau \cosh\tilde{\rho} \,, \\ T_2 &= \ell_{\text{AdS}} \sin\tau \cosh\tilde{\rho} \,, \\ X_i &= \ell_{\text{AdS}} \Omega_i \sinh\tilde{\rho} \,, \end{aligned} \tag{2.3}$$

where the Ω_i with $i \in \{1, \ldots, d\}$ parameterize the $\mathbb{S}^{d-1}$ sphere and $\sum_i \Omega_i^2 = 1$. The global coordinates cover the entire AdS_{d+1} spacetime. In these coordinates, the AdS_{d+1} metric (2.1) can be written as

$$\mathrm{d}s^2 = \ell_{\text{AdS}}^2(-\cosh^2\tilde{\rho}\,\mathrm{d}\tau^2 + \mathrm{d}\tilde{\rho}^2 + \sinh^2\tilde{\rho}\,\mathrm{d}\Omega_{d-1}^2) \,. \tag{2.4}$$

Here $0 \leq \tau < 2\pi$, $\tilde{\rho} \geq 0$ and $\mathrm{d}\Omega_{d-1}^2$ is the sphere metric on $\mathbb{S}^{d-1}$. The periodicity of the τ coordinate indicates the presence of closed timelike curves. To resolve this issue, we "unwrap" the time circle and take $-\infty < \tau < \infty$ to obtain the so-called *universal cover* of AdS without closed timelike curves[19].

The metric (2.1) is also often written in terms of the coordinates (t, r, Ω_i), which are also often referred to as global coordinates due to their full coverage of the AdS spacetime. They are defined as

$$\begin{aligned} T_1 &= \sqrt{\ell_{\text{AdS}}^2 + r^2}\cos(t/\ell_{\text{AdS}}) \,, \\ T_2 &= \sqrt{\ell_{\text{AdS}}^2 + r^2}\sin(t/\ell_{\text{AdS}}) \,, \\ X^2 &= X_1^2 + \ldots + X_d^2 = r^2 \,, \end{aligned} \tag{2.5}$$

in which case it takes the form

$$\mathrm{d}s^2 = -\left(1 + \frac{r^2}{\ell_{\text{AdS}}^2}\right)\mathrm{d}t^2 + \left(1 + \frac{r^2}{\ell_{\text{AdS}}^2}\right)^{-1}\mathrm{d}r^2 + r^2\mathrm{d}\Omega_{d-1}^2 \,. \tag{2.6}$$

Here $r \in [0, \infty)$, $t \in (-\infty, \infty)$ and the two sets of coordinates can be related via $r = \ell_{\text{AdS}} \sinh\rho$ and $t = \ell_{\text{AdS}}\tau$.

To study the causal structure of AdS_{d+1}, it is useful [6] to make a further change of variables $r = \ell_{\text{AdS}} \tan\rho$, where $\rho \in [0, \pi/2]$, in which case the metric becomes

$$\mathrm{d}s^2 = \frac{\ell_{\text{AdS}}^2}{\cos^2\rho}(-\mathrm{d}t^2 + \mathrm{d}\rho^2 + \sin^2\rho\,\mathrm{d}\Omega_{d-1}^2) \,. \tag{2.7}$$

The causal structure is invariant under a conformal scaling of the metric. A scaling transformation to remove the Weyl factor $\ell_{\text{AdS}}^2/\cos^2\rho$ shows that AdS_{d+1} has $\mathbb{R} \times \mathbb{S}^{d-1}$ topology and hence the same causal structure as a cylinder, as illustrated in Figure 2.1 (left). In these coordinates, the boundary is located at $\rho = \pi/2$ ($r = \infty$). [7]

[6] For example, in Section 4, we will focus on the $\text{AdS}_3/\text{CFT}_2$ duality and use this metric because the cylindrical structure of AdS_3 makes it easier to see that the metric of the boundary CFT_2 is just the flat Minkowski metric.

[7] As we will see later in this chapter, this is the so-called conformal boundary, which plays an important role in the AdS/CFT correspondence, being the boundary where the CFT lives.

Another convenient set of coordinates are the *Poincaré coordinates*, defined via

$$\begin{aligned} T_1 &= \frac{\ell_{\text{AdS}}^2}{2r}\left(1+\frac{r^2}{\ell_{\text{AdS}}^4}\left(\ell_{\text{AdS}}^2+\vec{x}^2-t^2\right)\right) , \\ T_2 &= \frac{r}{\ell_{\text{AdS}}}t , \\ T_2 &= \frac{r}{\ell_{\text{AdS}}}x_i , \\ T_1 &= \frac{\ell_{\text{AdS}}^2}{2r}\left(1-\frac{r^2}{\ell_{\text{AdS}}^4}\left(\ell_{\text{AdS}}^2-\vec{x}^2+t^2\right)\right) . \end{aligned} \tag{2.8}$$

The coordinates cover only a portion of the AdS spacetime, called the *Poincaré patch*. This can be seen in Figure 2.1 (right) which shows that the Poincaré patch covers only half of the spacetime covered by the global coordinates. In these coordinates, the metric (2.1) can be written as

$$\mathrm{d}s^2 = \frac{r^2}{\ell_{\text{AdS}}^2}\left(-\mathrm{d}t^2+\mathrm{d}\vec{x}^2\right)+\frac{\ell_{\text{AdS}}^2}{r^2}\mathrm{d}r^2 . \tag{2.9}$$

A further change of variables $z = \ell_{\text{AdS}}^2/r$ allows us to write the metric as

$$\mathrm{d}s^2 = \frac{\ell_{\text{AdS}}^2}{z^2}\left(\mathrm{d}z^2-\mathrm{d}t^2+\mathrm{d}\vec{x}^2\right) = \frac{\ell_{\text{AdS}}^2}{z^2}\left(\mathrm{d}z^2+\eta_{\mu\nu}\mathrm{d}x^\mu\mathrm{d}x^\nu\right) , \tag{2.10}$$

where $x^\mu = (t, \vec{x})$ and $\eta_{\mu\nu} = \text{diag}(-,+,\ldots,+)$. In these coordinates, the conformal boundary is located at $z = 0$. In what follows we will set $\ell_{\text{AdS}} = 1$ for simplicity.

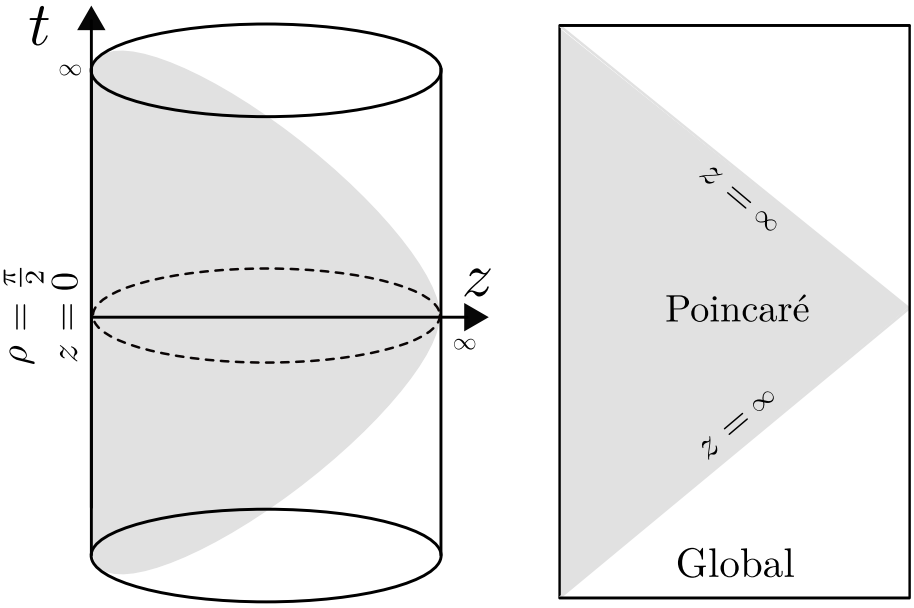

Figure 2.1: (left) In the Poincaré Patch (grey), the holographic boundary is at $z = 0$, which is equivalent to $\rho = \pi/2$ in the global coordinates. right) A slice through the AdS_3 spacetime, showing that the Poincaré Patch covers half of the full spacetime.

2.1.2 Scalar field theory in Poincaré AdS

In this section, we will study the dynamics of a massive scalar in AdS_{d+1}. We will see that in the Euclidean case there exist normalizable and non-normalizable bulk solutions, but the

normalizable solution blows up at the centre of the bulk and is hence not physical. This issue is not present in the Lorentzian case, where the normalizable solution is also regular everywhere in the bulk [20]. The notion of normalizability will be explained in more detail later, but it has to do with the regularity of the action, when evaluated on the particular solution. In what follows, we will derive these results, starting with the Euclidean case.

A. Dynamics in Euclidean signature

For convenience, we will work in the Poincaré patch with metric defined in (2.10) and set $\ell_{\text{AdS}} = 1$. Since we are considering the Euclidean case, we will Wick-rotate from Lorentzian time t to Euclidean time τ by setting $t = -i\tau$, in which case the metric becomes

$$\mathrm{d}s^2 = \frac{1}{z^2}\left(\mathrm{d}z^2 + \mathrm{d}\tau^2 + \mathrm{d}\vec{x}^2\right) = \frac{1}{z^2}\left(\mathrm{d}z^2 + \delta_{ab}\mathrm{d}x^a\mathrm{d}x^b\right) , \tag{2.11}$$

where $x^a = (\tau, \vec{x})$ with $a \in [0, d]$ and $\delta_{ab} = \mathrm{diag}(+, \ldots, +)$. In these coordinates, the action for a scalar field ϕ of mass m is given by

$$\begin{aligned} S &= \frac{1}{2}\int \mathrm{d}^{d+1}x\,\sqrt{g}\,(\partial_\mu\phi\partial_\nu\phi g^{\mu\nu} + m^2\phi^2) \\ &= \frac{1}{2}\int \mathrm{d}^d x\mathrm{d}z\; z^{-d+1}\left((\partial_z\phi)^2 + (\partial_a\phi)^2 + \frac{m^2}{z^2}\phi^2\right) , \end{aligned} \tag{2.12}$$

where we have used that $g = \det(g_{\mu\nu})$ and in Poincaré coordinates, $g = z^{-2(d+1)}$. To obtain the equation of motion for ϕ, we vary the action with respect to ϕ and set $\delta S/\delta\phi = 0$ to get

$$\frac{1}{\sqrt{-g}}\partial_\mu(\sqrt{-g}g^{\mu\nu}\partial_\nu\phi) = m^2\phi , \tag{2.13}$$

which gives

$$z^2\partial_z^2\phi - (d-1)z\partial_z\phi + z^2\partial_a^2\phi = m^2\phi . \tag{2.14}$$

To solve the above equation, it is convenient to perform a Fourier decomposition in the x^a directions and use a plane-wave ansatz of the form $\phi(z, x) = \mathrm{e}^{ik.x}f_k(z)$, where $k.x = \delta_{ab}k^a x^b$ [21]. The equation can now be written as

$$z^2\partial_z^2 f_k - (d-1)z\partial_z f_k - (k^2z^2 + m^2)f_k = 0 , \tag{2.15}$$

where $k^2 = \delta_{ab}k^a k^b$. This is can be written in the form of the modified Bessel equation by doing a change of variable $f_k = z^{d/2}g_k$, which yields

$$z^2\partial_z^2 g_k + z\partial_z g_k - \left(\frac{d^2}{4} + k^2z^2 + m^2\right)g_k = 0 . \tag{2.16}$$

Taking $g_k = g_k(kz)$, where $k = |k| = \sqrt{k^2}$, one finds two independent solutions in terms of the modified Bessel functions of the first and second kind, given by

$$g_k(kz) = a_k K_\nu(z|k|) + b_k I_\nu(z|k|) , \tag{2.17}$$

where a_k and b_k are integration constants, and we have defined $\nu = \sqrt{d^2/4 + m^2}$[22]. Hence, we arrive at

$$f_k(z) = a_k z^{\frac{d}{2}} K_\nu(z|k|) + b_k z^{\frac{d}{2}} I_\nu(z|k|) \, . \tag{2.18}$$

Note that since each mode depends on the parameter k, the full solution for the scalar field is obtained by the superposition of all of them, and so takes the form

$$\phi(z, x) = \int \frac{\mathrm{d}^d k}{(2\pi)^d} \mathrm{e}^{ik.x} f_k(z) \, , \tag{2.19}$$

where $\phi(z, x)$ is the Fourier transform of $f_k(z)$. We have to impose that the solution remains regular everywhere in the bulk, including the centre of the bulk at $z \to \infty$ and boundary, located at $z \to 0$. To check this regularity, we will use the asymptotic behaviour of the Bessel functions for $\nu > 0$, given by

$$K_\nu(z|k|) \sim \frac{\Gamma(\nu)}{2} \left(\frac{2}{z|k|} \right)^\nu \, , \tag{2.20}$$

$$I_\nu(z|k|) \sim \frac{1}{\Gamma(\nu + 1)} \left(\frac{z|k|}{2} \right)^\nu \, , \tag{2.21}$$

which allow us to write the solution (2.18) near the boundary behaves as

$$f_k(z) \sim A_k z^{\Delta_-} + B_k z^{\Delta_+} \, , \tag{2.22}$$

where we have defined

$$\Delta_\pm = \frac{d}{2} \pm \nu = \frac{d}{2} \pm \sqrt{\frac{d^2}{4} + m^2} \tag{2.23}$$

and

$$A_k = a_k \frac{\Gamma(\nu)}{2} \left(\frac{|k|}{2} \right)^\nu , \tag{2.24}$$

$$B_k = b_k \frac{1}{\Gamma(\nu + 1)} \left(\frac{2}{|k|} \right)^\nu \, . \tag{2.25}$$

In position space, one can therefore write the full scalar field solution near the boundary ($z \to 0$) as

$$\phi(z, x) \to A(x) z^{\Delta_-} + B(x) z^{\Delta_+} \, , \tag{2.26}$$

where $A(x)$ and $B(x)$ and the Fourier transforms of A_k and B_k respectively.[8] The Δ_+ is the so-called *normalizable* mode, while Δ_- is a *non-normalizable* mode. This normalizability criterion will be discussed in more detail later on. Having checked the behaviour near the boundary, it remains to check the behaviour of the solution near the centre of the bulk, where $z \to \infty$. Using the asymptotic behaviour of the Bessel functions, one finds that

$$K_\nu(z|k|) \sim \mathrm{e}^{-z|k|} \, , \tag{2.27}$$

$$I_\nu(z|k|) \sim \mathrm{e}^{z|k|} \, . \tag{2.28}$$

[8]Note that we can deduce these scalings much quicker from (2.14) with an ansatz $\phi(z, x) = f(z)g(x)$ and ignoring terms of $O(z^2)$ since we are only interested in the behaviour of the field near the boundary at $z = 0$.

While the first solution $K_\nu(z|k|)$ remains regular at the centre of the bulk, the second solution $I_\nu(z|k|)$ diverges exponentially. Hence, in order to impose regularity in the interior, we need to omit this solution by setting $b_k = 0$. Hence, $B(x) = 0$ and near boundary

$$\phi(z, x) \to A(x) z^{\Delta_-} \ , \tag{2.29}$$

meaning that in the Euclidean signature only the non-normalizable solution is admissible. This is not the case in Lorentzian spacetime. In what follows, we will repeat the above analysis to Lorentzian signature, and show that in this case, there exists a solution which is normalizable at the boundary, while also being regular everywhere in the bulk.

B. Dynamics in Lorentzian signature

In Lorentzian spacetime there are, again, two possible solutions - a normalizable and a non-normalizable one, but unlike the Euclidean case, where the normalizable mode was not physical at the origin, the normalizable mode is now well-defined throughout the whole bulk. In this case, the metric is

$$\mathrm{d}s^2 = \frac{1}{z^2}\left(\mathrm{d}z^2 - \mathrm{d}t^2 + \mathrm{d}\vec{x}^2\right) = \frac{1}{z^2}\left(\mathrm{d}z^2 + \eta_{ab}\mathrm{d}x^a\mathrm{d}x^b\right) \ , \tag{2.30}$$

where η_{ab} is the standard Minkowski metric. Following the same procedure as before, we find that the equation of motion for f_k is the same as in (2.18), but now $k^2 = \eta_{ab}k^a k^b$. Now the solution depends on whether $k^2 > 0$ or $k^2 < 0$[23]. For the case $k^2 > 0$, the results are the same as the Euclidean case, and there is no regular normalizable solution. However, for the case when $k^2 < 0$, the situation is more complicated and we have a regular normalizable solution appearing as well. Again, there are two independent solutions, but now they are in terms of the Bessel functions $\{J_\nu(z|k|), J_{-\nu}(z|k|)\}$ if ν is a non-integer, and in terms of $\{J_\nu(z|k|), Y_\nu(z|k|)\}$ otherwise. Hence,

$$f_k(z) = \begin{cases} d_k z^{\frac{d}{2}} J_\nu(z|k|) + c_k z^{\frac{d}{2}} J_{-\nu}(z|k|) & \text{if } \nu \notin \mathbb{Z} \\ d_k z^{\frac{d}{2}} J_\nu(z|k|) + c_k z^{\frac{d}{2}} Y_\nu(z|k|) & \text{if } \nu \in \mathbb{Z} \ . \end{cases} \tag{2.31}$$

Let's consider the case when ν is an integer. At the centre of the bulk (as $z \to \infty$), the Bessel functions with $\nu > 0$ are regular, so both sets of solutions remain regular. Approaching the boundary as $z \to 0$, the Bessel functions with $\nu > 0$ behave as

$$J_\nu(z|k|) \sim \frac{1}{\Gamma(\nu+1)}\left(\frac{z|k|}{2}\right)^\nu \ , \tag{2.32}$$

$$Y_\nu(z|k|) \sim -\frac{\Gamma(\nu)}{\pi}\left(\frac{2}{z|k|}\right)^\nu \ , \tag{2.33}$$

so the boundary limit of (2.31) becomes

$$f_k(z) \sim C_k z^{\Delta_-} + D_k z^{\Delta_+} \ , \tag{2.34}$$

where

$$C_k = -c_k \frac{\Gamma(\nu)}{\pi} \left(\frac{2}{|k|}\right)^{\nu} , \tag{2.35}$$

$$D_k = d_k \frac{1}{\Gamma(\nu+1)} \left(\frac{|k|}{2}\right)^{\nu} . \tag{2.36}$$

In position space, the scalar field solution near the boundary is

$$\phi(z,x) \to C(x) z^{\Delta_-} + D(x) z^{\Delta_+} , \tag{2.37}$$

where $C(x)$ and $D(x)$ are the Fourier transforms of c_k and d_k respectively. Similar discussion follows for the case when ν is not an integer. Hence, unlike the Euclidean case, now there is an additional solution which is both normalizable and regular. This solution will be important in Chapter 5.3, where it'll be used to model the radiation from a black hole in an asymptotically AdS spacetime. We will want to use a solution which is both normalizable near the boundary and regular everywhere in the bulk. Hence, for future bulk calculation we shall use the Lorentzian signature.

We wish to clarify the notion of normalizability of the bulk scalar solutions. In what follows, we will focus on the Lorentzoan signature. We claimed that Δ_+ is a *normalizable* mode, while Δ_- is a *non-normalizable* mode. This normalizability criterion comes from the normalizability requirement for the action when evaluated using the particular solution. One can check that the action (2.12) remains finite when the integral over z is evaluated from $z = 0$ to some cut-off $z = \epsilon$ using $\phi \sim z^{\Delta}$, provided that $\Delta > d/2$. Hence, the action is finite if $\Delta = \Delta_+$ and so it seems as if this is the only admissible mode.

However, there exist examples of the correspondence, where the boundary theory allows for operators of scaling dimension $\Delta < d/2$. Hence, in order to preserve the duality, there must be an oversight in the conclusion that $\Delta = \Delta_+$ is the only allowed solution. It turns out that in the range

$$-\frac{d^2}{4} < m^2 \leq -\frac{d^2}{4} + 1 , \tag{2.38}$$

the action is also finite for $\Delta = \Delta_-$. This can be shown with the following further analysis of the action. By performing integration by parts, the action (2.12) becomes

$$S = \frac{1}{2} \int \mathrm{d}^{d+1}x \sqrt{g}\, \phi(-\partial_\mu \partial^\mu + m^2)\phi + \frac{1}{2} \int \mathrm{d}^{d+1}x \sqrt{g}\, \partial_\mu(\phi \partial^\mu \phi) , \tag{2.39}$$

where the second term is a boundary term, which does not contribute to the equations of motion for ϕ. By ignoring the boundary term, the restriction on Δ changes [24]. In this case, the action becomes

$$S = \frac{1}{2} \int \mathrm{d}^d x \mathrm{d}z \sqrt{g}\, \phi(-z^2\partial_z^2 + (d-1)z\partial_z + z^2\partial_a^2\phi + m^2)\phi , \tag{2.40}$$

where we can recognize the equation of motion for ϕ. Using $\phi \sim z^{\Delta}$ and evaluating the integral over z from $z = 0$ to $z = \epsilon$, it can be seen that the boundary term in is non-zero, and in fact diverges, if $\Delta \leq d/2$ [25]. However, ignoring the boundary term, the action

converges for $\Delta \geq d/2 - 1$.[9] This modified bound implies that there can exist solutions with $d/2 - 1 \leq \Delta < d/2$, in which case $\Delta = \Delta_-$ is also an admissible solution. In this case, the requirement $\Delta \geq d/2 - 1$ corresponds to the upper bound for the mass in (2.38)). The lower bound arises from requiring that the scaling dimension $\Delta_\pm \in \mathbb{R}$, which imposes a further restriction on the mass of the scalar field, namely that

$$m^2 \geq -\frac{d^2}{4} \, . \tag{2.41}$$

This is known as the *Breitenlohner-Freedman bound* (BF). It implies that bulk particles of negative mass can have stable solutions.[10] Hence, in the range (2.38), both $\Delta\pm$ are allowed solutions, while for m^2 above this range, only Δ_+ is allowed.

Having described the dynamics in the bulk, in the next section, we will quickly review a few of the properties of conformal field theories, while focusing only on the parts which will be important in future calculations in the thesis.

2.2 Conformal Field Theory

A conformal field theory (CFT) is a relativistic quantum field theory with some additional symmetries. We will consider a CFT with a metric tensor $g_{\mu\nu}$ in d spacetime dimensions. Under a coordinate transformation $x^\mu \to x'^\mu$, the metric transforms as

$$g_{\mu\nu}(x) \to g'_{\mu\nu}(x') = \Omega^2(x) g_{\mu\nu}(x) \, . \tag{2.42}$$

A conformal field theory is invariant under this transformation and we say that a conformal transformation is one that leaves the metric invariant up to some factor $\Omega^2(x)$. An important feature of this invariance in Minkowski spacetime is that conformal transformations preserve the angles between curves crossing each other. This has an important consequence, namely that conformal transformations preserve the causal structure, so null/timelike/spacelike intervals remain null/timelike/spacelike separated.

2.2.1 CFT Algebra

The group of transformations that satisfies this property is called the *conformal group*. The conformal group in Minkowski spacetime contains as a subgroup the Poincaré group, which includes translations and Lorentz transformations. The conformal group contains two additional transformations[27], namely *dilatations* and the so-called *special conformal transformations*. The conformal group transformations and their respective generators are

[9] This is identical to a unitarity bound arising from the properties of the CFT. The CFT unitarity bound can be derived from demanding that matrix elements are positive definite, which yields that for a CFT$_d$, $\Delta \geq \frac{d-2}{2}$ [26].

[10] This is not the case in flat spacetime, where negative mass solutions are unstable.

$$\text{translations} : x'^{\mu} = x^{\mu} + a^{\mu} \qquad P_{\mu} = -i\partial_{\mu} \tag{2.43}$$

$$\text{rotations} : x'^{\mu} = M^{\mu}{}_{\nu} x^{\nu} \qquad L_{\mu\nu} = i(x_{\mu}\partial_{\nu} - x_{\nu}\partial_{\mu}) \tag{2.44}$$

$$\text{dilatations} : x'^{\mu} = \lambda\, x^{\mu} \qquad D = -x^{\mu}\partial_{\mu} \tag{2.45}$$

$$\text{SCTs} : x'^{\mu} = \frac{x^{\mu} - b^{\mu}x^2}{1 - 2b.x + b^2x^2} \qquad K_{\mu} = -i(2x_{\mu}x^{\nu}\partial_{\nu} - x^2\partial_{\mu})\ . \tag{2.46}$$

A special conformal transformation can be thought of as an inversion $x^{\mu} \to x^{\mu}/x^2$, followed by a translation $x^{\mu}/x^2 \to x^{\mu}/x^2 - b^{\mu}$, which is in turn followed by another inversion like the first one such that the full transformation can be expressed as

$$\frac{x'^{\mu}}{x'^2} = \frac{x^{\mu}}{x^2} - b^{\mu}\ . \tag{2.47}$$

The metric scale factor introduced from the special conformal transformation is given by

$$\Omega^2(x) = (1 - 2b.x + b^2x^2)^2\ . \tag{2.48}$$

The conformal group generators P_{μ}, $L_{\mu\nu}$, D and K_{μ} satisfy a set of commutation relations, which define the conformal algebra. If one defines a new set of generators, defined as

$$J_{\mu\nu} = L_{\mu\nu} \tag{2.49}$$

$$J_{-1,0} = D \tag{2.50}$$

$$J_{-1,\mu} = \frac{1}{2}(P_{\mu} - K_{\mu}) \tag{2.51}$$

$$J_{0,\mu} = \frac{1}{2}(P_{\mu} + K_{\mu})\ , \tag{2.52}$$

then the conformal algebra can be written as

$$[J_{ab}, J_{cd}] = i(\eta_{ad}J_{bc} + \eta_{bc}J_{ad} - \eta_{ac}J_{bd} - \eta_{bd}J_{ac})\ , \tag{2.53}$$

where $J_{ab} = -J_{ba}$ and η_{ab} is the usual Minkowski metric with $a, b \in \{-1, \ldots, d\}$. The conformal group is isomorphic to the group $SO(d, 2)$. For the remaining part of Section 2.2, we will focus on CFT_2 theories.

2.2.2 The state $\leftrightarrow$ operator map

It is operators and (local) states in the CFT that we primarily interested in, and in CFTs, there is a way to relate them, known as the *state-operator map*. While in a general QFT, local states and operators are very different objects, with states living on an entire spatial slice, while local operators being localized on a single spacetime point, in a CFT, there exists an isomorphism between these objects [28].

To make the state-operator correspondence more precise, we will use the notion of radial quantization. We can parameterize the CFT_2 theory in terms of the Cartesian plane coordinates (τ, x), which denote the time and space coordinate. One can also parameterize

the theory in terms of the complex cylinder coordinates $(w, \bar{w})$, defined as $w = x - i\tau$ and $\bar{w} = x + i\tau$, such that $x \in (0, 2\pi]$. The states live on spatial slices of the cylinder.

Another convenient way to parameterize the theory is to do a map from the complex cylinder to the complex plane $(z, \bar{z})$ via $z = \mathrm{e}^{iw}$ and $\bar{z} = \mathrm{e}^{i\bar{w}}$. While on the cylinder, the states lived on constant time slices, in the complex plane, they live on circles of constant radius [28]. This can be seen from the Hamiltonian generating time evolution on the cylinder, given by $H = \partial_\tau$, which is the dilatation operator in the complex plane coordinates, given by $D = z\partial_z + \bar{z}\partial_{\bar{z}}$. [11] Hence, the state in the infinite past $\tau = -\infty$ of the cylinder is mapped onto the complex plane at $z = \bar{z} = 0$. The state-operator map states that

$$|\mathcal{O}\rangle = \lim_{z,\bar{z}\to 0} \mathcal{O}(z, \bar{z})|0\rangle \ . \tag{2.54}$$

It should be noted that the state is defined by acting on the vacuum state with an operator at $z = \bar{z} = 0$, which means that the state on the cylinder is defined at $\tau = -\infty$. This is illustrated in Figure 2.2, where the state on the cylinder at $\tau = -\infty$ corresponds to an operator insertion at the origin of the complex plane.

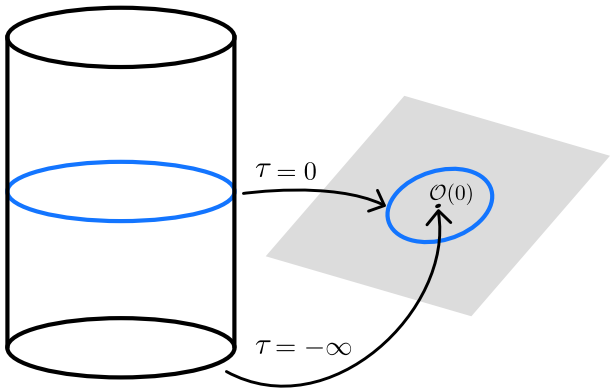

Figure 2.2: Constant time slices on the cylinder corresponding to constant radius circles on the complex plane. The state-operator map, states that operators inserted at the origin $z = \bar{z} = 0$ of the complex plane get mapped to stated at $\tau = -\infty$ on the cylinder. As states evolve on the cylinder, they correspond to circles of bigger radius on the complex plane, as shown in blue. Adapted from [29]

A nice derivation of the state-operator map can be found in [28], in terms of the path integral formulation of the wavefunction.

2.2.3 Operator product expansion

A concept of particular importance in CFTs is the *operator product expansion* (OPE). Even though it is also a concept in a general quantum field theory, the notion of a "field" in CFT is slightly more general, since the term also includes any operations (such as derivatives) of the usual fields.

[11] This has rather interesting implications for the dynamics in the complex plane. The Hamiltonian in the complex plane is the dilatation operator. Since $[D, P_\mu] = P_\mu$ and $[D, K_\mu] = -K_\mu$, comparing to the usual commutation relations between the Hamiltonian and the ladder operators, P_μ acts as a raising operator, while K_μ acts as a lowering operator [27].

The OPE is a statement about what happens when operators are very close to each other. For local operators $\mathcal{O}_i$, and only within time-ordered correlation functions, the OPE is defined as

$$\mathcal{O}_i(z,\bar{z})\mathcal{O}_j(w,\bar{w}) = \sum_k C_{ij}^k(z-w,\bar{z}-\bar{w})\mathcal{O}_k(w,\bar{w}) \ , \tag{2.55}$$

where the functions $C_{ij}^k(z-w,\bar{z}-\bar{w})$ depend only on the separation between the operators, due to translational invariance. We will not go into the derivation of the OPE, but one can see from its definition that it diverges for $z \to w$ (or $\bar{z} \to \bar{w}$).

A particular type of operator in CFT, called a *primary operator* is defined as an operator, whose OPE with the stress-energy tensor truncates at $(z-w)^{-2}$. Hence, the OPE of a primary operator $\mathcal{O}$ with the stress-energy tensor is defined as

$$T(z)\mathcal{O}(w,\bar{w}) = h\frac{\mathcal{O}(w,\bar{w})}{(z-w)^2} + \frac{\partial_w\mathcal{O}(w,\bar{w})}{z-w} \tag{2.56}$$

$$\bar{T}(\bar{z})\mathcal{O}(w,\bar{w}) = \bar{h}\frac{\mathcal{O}(w,\bar{w})}{(\bar{z}-\bar{w})^2} + \frac{\partial_{\bar{w}}\mathcal{O}(w,\bar{w})}{\bar{z}-\bar{w}} \ , \tag{2.57}$$

where $h, \bar{h}$ are called the *weights* of the operator. These are related to the scaling dimension of an operator, which can be written as $\Delta = h + \bar{h}$. Note, $h, \bar{h} \in \mathbb{R}$ and $h, \bar{h} \geq 0$ for a unitary CFT. Under a general finite conformal transformation, namely $z \to z'(z)$ and $\bar{z} \to \bar{z}'(\bar{z})$, primary operators transform as

$$\mathcal{O}(z,\bar{z}) \to \mathcal{O}'(z',\bar{z}') = \left(\frac{\partial z'}{\partial z}\right)^{-h}\left(\frac{\partial \bar{z}'}{\partial \bar{z}}\right)^{-\bar{h}}\mathcal{O}(z,\bar{z}) \tag{2.58}$$

The significance of the primary operators is that the spectrum of the weights $h, \bar{h}$ of primary operators is related to the spectrum of the masses of the particles in the field theory.

In the next section we will quickly review some basic aspects of an example CFT theory, namely that of the massless free boson, without preforming any derivations.

2.2.4 Example: The Massless Free Boson

The dynamics of the free boson is governed by the action

$$S = \frac{1}{2}g\int \mathrm{d}^2x \ \partial_\mu\varphi\partial^\mu\varphi \ , \tag{2.59}$$

where g is a normalization parameter, which will be specified later [27]. The correlation functions are given by

$$\langle\varphi(x)\varphi(y)\rangle = -\frac{1}{4\pi g}\ln|x-y|^2 \ , \tag{2.60}$$

which can be written in terms of the complex plane coordinates, introduced in the previous section, to give

$$\langle\varphi(z,\bar{z})\varphi(w,\bar{w})\rangle = -\frac{1}{4\pi g}\big\{\ln|z-w|^2 + \ln|\bar{z}-\bar{w}|^2\big\} \ . \tag{2.61}$$

Taking partial derivatives of (2.61), it can be split into holomorphic and anti-holomorphic contributions, given by

$$\begin{aligned}\langle \partial_z \varphi(z) \partial_w \varphi(w) \rangle &= -\frac{1}{4\pi g} \frac{1}{(z-w)^2} \\ \langle \partial_{\bar{z}} \varphi(\bar{z}) \partial_{\bar{w}} \varphi(\bar{w}) \rangle &= -\frac{1}{4\pi g} \frac{1}{(\bar{z}-\bar{w})^2} \ . \end{aligned} \tag{2.62}$$

Recall that to test if an operator in a primary operator, one needs to calculate its OPE with the stress-energy tensor. The stress-energy tensor for the theory under consideration can be written in terms of the complex plane coordinates as [27]

$$\begin{aligned} T(z) &= -2\pi g : \partial_z \varphi(z) \partial_z \varphi(z) : \\ T(\bar{z}) &= -2\pi g : \partial_{\bar{w}} \varphi(\bar{w}) \partial_{\bar{w}} \varphi(\bar{w}) : \ . \end{aligned} \tag{2.63}$$

It has been shown in [27] that by canonically quantizing the scalar field on the cylinder, the partial derivatives of the scalar field, appearing in the expression for the stress-energy tensor, can be written as

$$\begin{aligned} \partial_z \varphi(z, \bar{z}) &= -\frac{i}{\sqrt{4\pi g}} \sum_n a_n z^{-n-1} \\ \partial_{\bar{z}} \varphi(z, \bar{z}) &= -\frac{i}{\sqrt{4\pi g}} \sum_n \bar{a}_n \bar{z}^{-n-1} \ , \end{aligned} \tag{2.64}$$

where a_n and $\bar{a}_n$ are ladder operators for left- and right-moving excitations, and obey the following commutation relations

$$\begin{aligned} [a_m, a_n] &= [\bar{a}_m, \bar{a}_n] = m \delta_{m+n} \\ [a_m, \bar{a}_n] &= [\bar{a}_m, a_n] = 0 \ , \end{aligned} \tag{2.65}$$

where

$$\delta_{m+n} = \begin{cases} m & \text{if } m = -n \\ 0 & \text{otherwise} \ . \end{cases} \tag{2.66}$$

The creation/annihilation operators act on the CFT vacuum state, such that

$$a_n |0\rangle_{\text{CFT}} = \begin{cases} = 0 \text{ if } \ n > -1 \\ \neq 0 \text{ if } \ n \leq -1 \end{cases} \tag{2.67}$$

and similarly for $\bar{a}_n$. [12]

These features of the massless scalar boson CFT_2 theory will be used later in Chapter 4, to study the dual description of a massless scalar in AdS_3.

[12] Note that this action of the creation/annihilation operators is specific to the operator, and in particular to its weight $h, \bar{h}$. In the above example, namely the mode expansion of the operator $\partial_z \varphi$, the weight of that operator was $h = 1$, hence the factors of -1 in (2.67). For the mode expansion of a general operator of weight h, such that $\phi(z, \bar{z}) = -\sum_n b_{n,m} \ z^{-n-h} \bar{z}^{-m-\bar{h}}$, one must impose $b_{n,m}|0\rangle = 0$ for $n \geq -h$ and $m \geq -\bar{h}$. The reason for this requirement is the otherwise the state generated by the state-operator map will be non-singular (and hence not well-defined) at $z = \bar{z} = 0$ [30].

2.3 AdS/CFT Correspondence

2.3.1 Statement of the correspondence

The map between observables on both sides is given by the so-called AdS/CFT *dictionary*. There are two versions of the dictionary, namely the *differentiate* and the *extrapolate* dictionary. The differentiate dictionary is stated in terms of the equivalence between the bulk and boundary partition functions

$$Z_{\text{Bulk}}[\phi_0] = Z_{\text{CFT}}[\phi_0] \,, \tag{2.68}$$

where $\phi_0(x)$ is the boundary condition on the fields. Correlation functions of the CFT operators are then computed, as per usual, by differentiating the partition with respect to the sources

$$\langle \mathcal{O}(x_1) \dots \mathcal{O}(x_n) \rangle_{\text{CFT}} = \left[\frac{\delta}{\delta J(x_1)} \dots \frac{\delta}{\delta J(x_n)} Z_{\text{Bulk}}[J] \right]_{J=0} \,, \tag{2.69}$$

where we set the sources $J = 0$ at the end. On the other hand, the extrapolate dictionary evaluates the CFT correlators by first computing the bulk correlators and then pulling them to the boundary via

$$\langle \mathcal{O}(x_1) \dots \mathcal{O}(x_n) \rangle_{\text{CFT}} = \lim_{z \to 0} z^{-n\Delta} \langle \phi(x_1, z) \dots \phi(x_n, z) \rangle_{\text{Bulk}} \,. \tag{2.70}$$

It has been shown in [31] that (up to some proportionality constant) the two dictionaries compute the same CFT correlators i.e.

$$\left[\frac{\delta}{\delta J(x_1)} \dots \frac{\delta}{\delta J(x_n)} Z_{\text{Bulk}}[J] \right]_{J=0} \approx \lim_{z \to 0} z^{-n\Delta} \langle \phi(x_1, z) \dots \phi(x_n, z) \rangle_{\text{Bulk}} \,. \tag{2.71}$$

The AdS/CFT correspondence gives a relation between the mass m of the AdS bulk scalar field and the scaling dimension Δ of the operator $\mathcal{O}$ on boundary CFT theory, given by the roots of $m^2 = \Delta(\Delta - d)$, which are

$$\Delta_\pm = \frac{d}{2} \pm \sqrt{\frac{d^2}{4} + m^2} \,. \tag{2.72}$$

Hence, for a general massive scalar field in the bulk, there exist two solutions for the scaling dimensions of the dual operator $\mathcal{O}$ living on the boundary. These are the normalizable and non-normalizable solutions of the bulk field and have different interpretations in the CFT theory, as will be explained in the next section.

2.3.2 Boundary behaviour : the field $\leftrightarrow$ operator map

We wish to use the AdS bulk scalar field solution and the AdS/CFT duality to explain what it corresponds to in the CFT theory. To do that, it is convenient to consider the boundary limit of the scalar field solution, which behaves as

$$\phi(z, x) = A(x) z^\Delta + B(x) z^{d-\Delta} \,, \tag{2.73}$$

where we found that there are two possible solutions for the scaling dimension, namely the roots $\Delta_\pm$ of $\Delta(\Delta - d) = m^2$. Choosing a particular solution for Δ implies a different physical interpretation of the functions $A(x)$ and $B(x)$.

If we choose $\Delta = \Delta_+$, the term $\sim z^{d-\Delta_+} = z^{\Delta_-}$ is the dominant term in the limit $z \to 0$, since $\Delta_- < \Delta_+$. Hence, near the boundary, we find that

$$B(x) = \lim_{z\to 0} z^{-\Delta_-}\phi(z, x) \, . \tag{2.74}$$

By dimensional analysis [21], the function $A(x)$, corresponding to the normalizable mode, is identified with the vacuum expectation value of the dual field operator $\mathcal{O}$, of scaling dimension Δ_+, while $B(x)$ is identified as the source for this operator. In accordance with the extrapolate dictionary, this suggests that $B(x)$ sources the bulk field $\phi(z, x)$.

If we, instead, chose $\Delta = \Delta_-$, the roles of the functions $A(x)$ and $B(x)$ will be reversed, with $B(x)$ being identified as the vacuum expectation value of $\mathcal{O}$, and $A(x)$ as its source.

2.4 Conclusion

The AdS/CFT duality provides a powerful tool for studying the Information paradox. Due to the unitary evolution of the CFT on the holographic boundary, AdS/CFT also guarantees a unitary evolution inside the bulk, where one could choose to study how black holes evaporate. In this chapter, we discussed some aspects of the correspondence, which will be used in later chapters. In the next chapter, we will review the concept of entanglement and entanglement entropy in both quantum mechanics and quantum field theory. The results from Chapter 2 will be used in deriving the RT prescription for the holographic entanglement entropy.

3
Holographic Entanglement Entropy

In this chapter, we review aspects of the entanglement entropy. In Section 3.1, we introduce entanglement entropy in quantum mechanics, which is then derived for a general quantum field theory. In Section 3.2, we show how the AdS/CFT correspondence introduced in Chapter 2 can be applied to the entanglement entropy, and introduce the RT prescription, the derivation of which was reviewed in Section 3.3. Subsequent generalizations of the RT formula are mentioned in Section 3.4, including the latest version of the generalized gravitational entanglement entropy.

3.1 Entanglement Entropy

3.1.1 Basics

One of the, undoubtedly, coolest features of quantum field theory, absent in its classical counterpart, is the non-zero correlation between spatially separated field operators, arising from the superposition of quantum states [32]. This correlation can be explained as entanglement between distant regions, and it is this feature that presents one of the fundamental differences between quantum and classical physics. Before diving into the discussion on entanglement, it is helpful to recall and distinguish the different notions of entropy.

In classical statistical physics, entropy is often met in the form $S_B = k_B \ln \Omega$, where k_B is the Boltzmann constant and Ω is used to denote the number of available microstates for a system in a particular macrostate. This is the so-called *Boltzmann* entropy and assumes that each microstate is equally probably. For the case where miscrostates appear with different probabilities $\{p_i\}$ with $\sum_i p_i = 1$, the Boltzmann entropy is generalized to the so-called *Gibbs* entropy, defined as $S_G = -k_B \sum p_i \ln p_i$.[13] When $p_i = 1/\Omega$ (for an equal probability distribution), S_G reduces to S_B. In information theory, the so-called *Shannon* entropy entropy $H(p)$ is defined in the same way; i.e. for a discrete random variable X with probability distribution

[13]The dimensionless entropy is obtained by dropping the Boltzmann constant k_B.

$p(x)$, such that $\mathrm{P}(X = x) = p(x)$, Shannon's entropy is defined as[14]

$$H(p) = \sum_{x \in X} p(x) \log p(x) \ . \tag{3.1}$$

The *von Neumann* entropy (or quantum entropy) of a quantum state $\rho \in \mathcal{H}$ is a natural generalization of the Shannon entropy, defined as

$$H(\rho) = -\mathrm{Tr}[\rho \log \rho] \ . \tag{3.2}$$

Some of the properties of the von Neumann entropy include:

$$\begin{aligned} \text{Non-negativity} &: H(\rho) \geq 0 \text{ with } H(\rho) = 0 \text{ iff } \rho \text{ is pure} \\ \text{Upper bound} &: H(\rho) \leq \log \dim \mathcal{H} \\ \text{Invariance under isometries} &: H(\rho) = H(V \rho V^\dagger) \text{ for any isometry } V \ . \end{aligned} \tag{3.3}$$

We will be interested in evaluating the entropy in a QFT, where the dimensionality of the Hilbert space is infinite. Hence, for a QFT, the upper bound for the von Neumann entropy is $H(\rho) \leq \infty$.[15] We should also note that the last property has the important consequence that the von Neumann entropy is invariant under a unitary time evolution, namely i.e. $H(\rho) = H(U \rho U^\dagger)$. This is different from the thermodynamic entropy, which obeys the second law of thermodynamics and hence increases under a unitary time evolution. The distinction between the von Neumann (also referred to as *fine-grained*) entropy and the thermodynamic (also referred to as *coarse-grained*) entropy will be important later in Chapter 4 when discussing the entropy of an evaporating black hole and its Hawking radiation.

To quantify entanglement, we can consider a system at zero temperature, divided into two subsystems, namely A and B, where the latter is often referred to as the *complement* of A and written as $B = \bar{A}$, as illustrated in Figure 3.1 below.

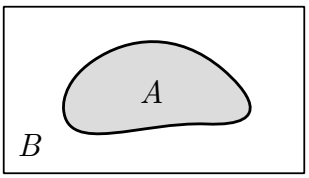

Figure 3.1: A bipartite system with two subsystems, A and B, where B is the complement of A, namely $B = \bar{A}$.

If the total system, described by a ground state $|\Psi\rangle$, is in a pure state, the density matrix is defined as[16]

$$\rho_{AB} = |\Psi\rangle\langle\Psi| \ . \tag{3.4}$$

To define the entropy of the subsystems A and B, it is assumed that the total Hilbert space factorizes into a direct product of the Hilbert spaces of the subsystems; i.e. $\mathcal{H}_{AB} = \mathcal{H}_A \otimes \mathcal{H}_B$.

[14] Note, in information theory, the log denotes the logarithm to base 2., whereas the definition in physics uses the natural logarithm ln.

[15] One should really think of the entropy as being UV sensitive and dependent on the cut-off scale, rather than being infinite.

[16] Recall that for a pure state ρ, $\mathrm{Tr}[\rho] = 1$ so we have assumed the state is normalized such that $\langle\Psi|\Psi\rangle = 1$.

The system A is described by the *reduced* density matrix ρ_A, obtained by tracing over the Hilbert space $\mathcal{H}_B$, such that

$$\rho_A = \mathrm{Tr}_B[\rho_{AB}] \ . \tag{3.5}$$

The *entanglement entropy* of the subsystem A with the subsystem B, which provides a measure of the entanglement between these two subsystems, is the von Neumann entropy of the reduced density matrix and is hence defined as

$$S_A = -\mathrm{Tr}_A[\rho_A \log \rho_A] \ , \tag{3.6}$$

which for a pure state ρ_{AB} is independent of which subsystem we pick; i.e. $S_A = S_B$.[17] The entanglement entropy vanishes for a pure state, so $S_{AB} = 0$.
Any *bipartite* (one that consists of two subsystems) pure state $|\Psi_{AB}\rangle \in \mathcal{H}_{\mathcal{AB}} = \mathcal{H}_A \otimes \mathcal{H}_B$ can be written as

$$|\Psi_{AB}\rangle = \sum_{i=1}^{\min(d_A,d_B)} \sqrt{p_i}\ |\psi_i\rangle_A \otimes |\psi_i\rangle_B \ , \tag{3.7}$$

where $d_A = \dim\ \mathcal{H}_A$ and $d_B = \dim\ \mathcal{H}_B$. The $p_i > 0$ satisfy $\sum_i p_i = 1$ and the basis vectors $\{|\psi_i\rangle_A\} \in \mathcal{H}_A$ and $\{|\psi_i\rangle_B\} \in \mathcal{H}_B$ form orthonormal basis for the subsystems A and B respectively. This is known as the *Schmidt decomposition*. A state is called *separable* if it can be written in the form $|\Psi_{AB}\rangle = |\psi_i\rangle_A \otimes |\psi_i\rangle_B$. A separable state has pure reduced density matrix ρ_A and hence a vanishing entanglement entropy. Hence, separable states are also referred to as *unentangled*. A state is called *entangled* (or *inseparable*) if it cannot be written in the form $|\Psi_{AB}\rangle = |\psi_i\rangle_A \otimes |\psi_i\rangle_B$ and has the form of (3.7). In the Schmidt decomposition, the reduced density matrix becomes

$$\rho_A = \sum_{i=1}^{d_A} p_i\ |\psi_i\rangle_{AA}\langle\psi_i| \tag{3.8}$$

and in this case, the entanglement entropy becomes the Shannon entropy

$$S_A = -\sum_{i=1}^{d_A} p_i \log p_i \ . \tag{3.9}$$

Thus, evaluating the entanglement entropy requires computing the reduced density matrix ρ_A and diagonalizing it to obtain its eigenvalues p_i. This is generally difficult to calculate, particularly in a quantum field theory with infinite degrees of freedom [34, 35]. Instead of having to deal with this diagonalization, a more convenient approach makes use of the so-called *replica trick*, first introduced in the context of entanglement entropy in [36]. This involves using another entanglement measure, namely the *Renyi* entropy, which is a one-parameter generalization of the entanglement entropy, defined as [37]

$$S_n(A) = \frac{1}{1-n} \log \mathrm{Tr}_A[\rho_A^n] \ , \tag{3.10}$$

[17] Note, this equality is no longer true of the total system is no longer a pure state. If the total state is mixed (e.g. at finite temperature), $S_A \neq S_B$ [33].

where n is an integer, commonly referred to as the *replica parameter*. The replica trick is a method for calculating the entanglement entropy, by utilizing this new type of Renyi entropy, which contains n copies of the density matrix. Indeed, in the limit $n \to 1$, the Renyi entropy reduces to the entanglement entropy; i.e.

$$S_A = \lim_{n\to 1} S_n(A) \ . \tag{3.11}$$

This can be seen from [38]

$$\begin{aligned}
\lim_{n\to 1} S_n(A) &= \lim_{n\to 1} \frac{1}{1-n} \log \mathrm{Tr}_A[\rho_A^n] \\
&= \lim_{n\to 1} \frac{1}{1-n} \log \sum_i p_i^n \\
&= \lim_{n\to 1} \frac{\log \sum_i p_i^n}{(1-n)} \frac{(1+n)}{(1+n)} \\
&= \lim_{n\to 1} \frac{\log \sum_i p_i^n + (1+n) \frac{\sum_i p_i^n \log p_i}{\log \sum_i p_i^n}}{-2n} \\
&= -\sum_i p_i \log p_i \\
&= S_A \ ,
\end{aligned} \tag{3.12}$$

where in the fourth line we have applied L'Hôpital's rule, defined as $\lim_{x\to c} \frac{f(x)}{g(x)} = \lim_{x\to c} \frac{f'(x)}{g'(x)}$, together with the logarithmic derivative, defined as $\frac{\mathrm{d}}{\mathrm{d}x} \log f(x) = \frac{1}{f(x)} \frac{\mathrm{d}f}{\mathrm{d}x}$. Another way that the entanglement entropy can be written as as $S_A = -\lim_{n\to 1} \partial_n \mathrm{Tr}[\rho_{\mathrm{A}}^{\mathrm{n}}]$, which can be shown from

$$-\lim_{n\to 1} \partial_n \mathrm{Tr}[\rho_{\mathrm{A}}^{\mathrm{n}}] = -\lim_{n\to 1} \partial_n \sum_i p_i^n = -\lim_{n\to 1} \sum_i p_i \log p_i = S(A) \tag{3.13}$$

In literature, both result from (3.12) and (3.13) are often combined to define the replica trick as one that utilizes the following step:

$$S_A = \lim_{n\to 1} \frac{1}{1-n} \log \mathrm{Tr}_A[\rho_A^n] = -\lim_{n\to 1} \partial_n \log \mathrm{Tr}_A[\rho_A^n] \ , \tag{3.14}$$

where the density matrix is normalized such that $\mathrm{Tr}_A[\rho_A] = 1$. Note, in the definition of the Renyi entropy, $n \in \mathbb{Z}_+$, but an analytic continuation to $n \in \mathbb{R}_+$ is assumed in taking the limit $n \to 1$.

The entanglement entropy at finite temperature $T = \beta^{-1}$ is defined by replacing (3.4) with the *thermal* density matrix defined as $\rho_{\mathrm{thermal}} = \mathrm{e}^{-\beta H}/Z$, where $Z = \mathrm{Tr}[\mathrm{e}^{-\beta H}]$ is the thermal partition function and H is the total Hamiltonian of the system. The thermodynamic entropy is defined in terms of the thermal partition function via

$$S(\beta) = (1 - \beta\partial_\beta) \log Z(\beta) \ . \tag{3.15}$$

The thermodynamic entropy will be used in Section 3.3 to evaluate the thermodynamic black hole entropy from the gravitational path integral.

3.1.2 Entanglement Entropy in a QFT: Euclidean Path Integral Representation

Obtaining the entanglement entropy is not that straightforward in QFT, as it was in the quantum mechanical description, since one needs to take into account the path integral formalism and the interpretation of what n copies of the density matrix signify is not that obvious. In this section, we will provide the schematic derivation of the QFT entanglement entropy, following closely the work in [37]. If we consider a $d-$dimensional QFT, the ground state wavefunctional $\Psi[\phi_0(\vec{x})] = \langle\phi_0(\vec{x})|\Psi\rangle$ has the following Euclidean path integral representation

$$\Psi[\phi_0(\vec{x})] = \int_{\tau=-\infty}^{\tau=0,\phi(0,\vec{x})=\phi_0(\vec{x})} \mathcal{D}\phi\ \mathrm{e}^{-I_E[\phi]} \ = \tag{3.16}$$

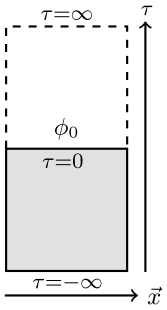

which is obtained by integrating from $\tau = -\infty$ to $\tau = 0$ and $\phi_0(\vec{x}) = \phi(\tau, \vec{x})$ is the eigenvalue of the field operator $\hat{\phi}(\tau, \vec{x})$ at $\tau = 0$ [37]. Similarly, the conjugate of the wavefunctional, namely $\Psi^*[\phi_0'(\vec{x})] = \langle\Psi|\phi_0'(\vec{x})\rangle$ has the following path integral representation:

$$\Psi^*[\phi_0'(\vec{x})] = \int_{\tau=0,\phi(0,\vec{x})=\phi_0'(\vec{x})}^{\tau=\infty} \mathcal{D}\phi\ \mathrm{e}^{-I_E[\phi]} \ = \tag{3.17}$$

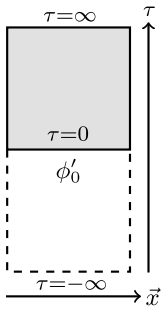

Assuming the system is at zero temperature and in a pure state, which is not necessarily normalized, the density matrix is given by

$$\rho = \frac{1}{Z}|\Psi\rangle\langle\Psi| \ , \tag{3.18}$$

where Z is the partition function obtained via integrating over the entire space, namely

$$Z = \int \mathcal{D}\phi_0(\tau = 0, \vec{x})\langle\phi_0|\Psi\rangle\langle\Psi|\phi_0\rangle \ . \tag{3.19}$$

For a general bipartite state ρ_{AB}, the reduced density matrix of the A subsystem is obtained by tracing over its complement $\bar{A} = B$, which will be equivalent to connecting along the B subsystem. In terms of the path integral representation, this is equivalent to gluing the wavefunctional (3.16) and it conjugate (3.17) along a boundary in the B subsystem; i.e. by integrating over $\phi^B(\tau = 0, \vec{x} \in B)$, where $\vec{x}$ is only in the B subsystem. The reduced density

matrix is then given by

$$\rho_A = \frac{1}{Z}\mathrm{Tr}_B[|\Psi\rangle\langle\Psi|] = \frac{1}{Z}\int \mathcal{D}\phi^B(\tau = 0, \vec{x} \in B)\langle\phi^B|\Psi\rangle\langle\Psi|\phi^B\rangle \ . \tag{3.20}$$

The reduced density matrix has two indices, specifying the boundary conditions at $\tau = 0^+$ and $\tau = 0^-$. This is more easily explained by solving for the elements of the reduced density matrix schematically [37]. A reduced density matrix with boundary conditions $\phi^A(\tau = 0^+) = \phi_b^A$ and $\phi^A(\tau = 0^-) = \phi_a^A$ (where $\phi_a^A, \phi_b^A \in A$), can be written as

$$\begin{aligned}
[\rho_A]_{ab} &= \langle\phi_a^A|\rho_A|\phi_b^A\rangle \\
&= \frac{1}{Z}\int \mathcal{D}\phi^B(\tau = 0, \vec{x} \in B)\ (\langle\phi_a^A| \otimes \langle\phi^B|)|\Psi\rangle\langle\Psi|(|\phi^B\rangle| \otimes |\phi_b^A\rangle) \\
&= \frac{1}{Z}\int \mathcal{D}\phi^B(\tau = 0, \vec{x} \in B)
\end{aligned}$$

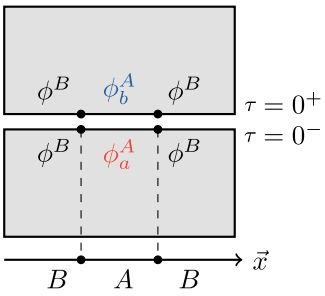

$$= \frac{1}{Z}$$

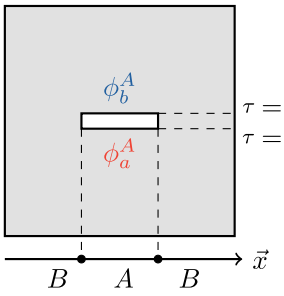

(3.21)

where tracing over the B subsystem just glues the wavefunctional and its conjugate together along the B subsystem, resulting in a path integral with a cut along the A subregion. To find $\mathrm{Tr}_A[\rho_A^n]$, requires taking n copies of (3.21), which involves a matrix multiplication, and hence the contraction of the matrix indices. One needs to remember that each of these n copies has different independent boundary conditions $\phi_{i\pm}^A \in A$ at $\tau = 0^\pm$. Taking the trace over this product of n copies is done by connecting the copies cyclically along the cuts (along A) such that

$$\mathrm{Tr}_A[\rho_A^n] = [\rho_A]_{\phi_1^A\phi_2^A}[\rho_A]_{\phi_2^A\phi_3^A}\ldots[\rho_A]_{\phi_n^A\phi_1^A} \ . \tag{3.22}$$

This decreases the number of independent boundary conditions, since now the boundary condition at $\tau = 0^-$ of any one sheet (representing the reduced density matrix (3.21)) is identified as the boundary condition at $\tau = 0^+$ of its adjacent sheet, such that all sheets are connected cyclically. This has been illustrated in Figure 3.2, where this n-fold cover is defined as Z_n, in terms of which we can write

$$\mathrm{Tr}_A[\rho_A^n] = \frac{1}{Z^n}\int_{(\tau,\vec{x})\in\mathcal{R}_n} \mathcal{D}\phi_1\mathcal{D}\phi_2\ldots\mathcal{D}\phi_n\ \mathrm{e}^{-I_E[\phi_1]-I_E[\phi_2]-\ldots-I_E[\phi_1]} = \frac{Z_n}{Z^n} \ , \tag{3.23}$$

where the partition function of the n-fold cover $\mathcal{M}_n$, namely Z_n should not be confused with the nth power of the partition function Z of the original manifold $\mathcal{M}$.

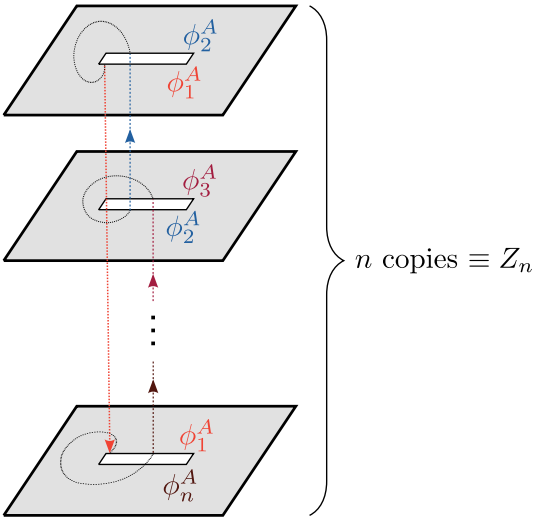

Figure 3.2: The partition function Z_n of the n-fold cover, which is often denoted as $\mathcal{M}_n$, consisting of n sheets, each representing the elements of one of the n copies of the reduced density matrix. The sheets are glued cyclically along their cuts (along A), which are labeled by the boundary conditions of the fields of A at the $\tau = 0^{\pm}$. Each line in the diagram shows a connection between consecutive sheets, which always connects regions of A with the same boundary conditions, such that the boundary condition of any one sheet at $\tau = 0^-$ (such as the ϕ_2^A boundary condition at $\tau = 0^-$ of the second sheet) is identified as the boundary condition at $\tau = 0^+$ (such as the ϕ_2^A boundary condition at $\tau = 0^+$ of the first sheet) of its adjacent sheet. Figure adapted from [37].

There are different ways if thinking about what the arrows in Figure 3.2 mean. One way is in terms of boundary conditions on the quantum fields, living on each of the sheets. There are boundary conditions on each of the cuts (at $\tau = 0^{\pm}$), with the arrows connecting regions with the same boundary conditions, and these boundary conditions are summed over. Another way to think about it as as simply gluing the manifold together along the cuts, which is invariant under the cyclic permutation of the fields. To find the entanglement entropy one can now use the result in (3.23) and apply the replica trick (3.14), which yields

$$\begin{aligned} S_A &= -\lim_{n\to 1} \partial_n \log \mathrm{Tr}_A[\rho_A^n] \\ &= -\lim_{n\to 1} \partial_n \log \frac{Z_n}{Z^n} \\ &= -\lim_{n\to 1} \partial_n (\log Z_n - n \log Z) \ . \end{aligned} \tag{3.24}$$

This is the formula used to calculate the entanglement entropy in a QFT. An example of this is the evaluation of the entanglement entropy in a flat CFT_2 [39], which has been shown to have an entanglement entropy across an interval of length l, given by

$$S_A = \frac{c}{3} \log \frac{l}{\epsilon} \ , \tag{3.25}$$

where c is the central charge of the CFT_2 and ϵ is a UV cut-off that needs to be imposed across the region A (where the interval l is located) and its complement $\bar{A}$, since there is

an infinite amount of entanglement across any boundary [18]. In this case, there would be an infinite amount of entanglement between the A and $\bar{A}$, so a cut-off is imposed at the interface between them.

The von Neumann entropy of a CFT is an important tool in the study of the black hole information paradox in the context of AdS/CFT, where the it is used to study the entanglement entropy of the Hawking radiation, with the hope of obtaining a Page curve and resolving the paradox. This thesis does not perform any calculations of CFT entanglement entropies, so a derivation of (3.25) will not be provided. However, in Section 5.2.4, (3.25) will be used to review the way the the CFT entanglement entropy can be used to calculate the entanglement entropy of the Hawking radiation, which will involve using an interval across spacetime regions with different metrics.

3.2 Ryu-Takayanagi conjecture

The Ryu-Takayanagi (RT) formula, named after Ryu and Takayanagi, was conjectured in the context of AdS/CFT, giving an expression for the entanglement entropy of a region in the CFT with the help of holography [40]. Since it assumes holography, the RT formula is referred to as a holographic entanglement entropy formula. This section will simply introduce the RT formula. A review of its later proof by Lewkowycz and Maldacena [41] will be presented in the next section.

As introduced in Section 2.3, one way to write the AdS/CFT correspondence is in terms of the differentiate dictionary (2.68), according to which the partition functions of the two theories are equivalent; i.e. $Z_{\text{Bulk}}[\mathcal{B}] = Z_{\text{CFT}}[\partial\mathcal{B}]$, where $\mathcal{B}$ is the bulk spacetime and the CFT lives on its boundary $\partial\mathcal{B}$. One can write the CFT partition function $Z_{\text{CFT}}[\partial\mathcal{B}]$ in terms of the bulk action $I_{\text{Bulk}}[\mathcal{B}]$ by using the *semiclassical* (also known as *saddle point*) approximation, which assumes that the partition function is dominated by the contribution from the on-shell bulk action; i.e.

$$Z_{\text{Bulk}}[\mathcal{B}] = \mathrm{e}^{-I_{\text{Bulk}}[\mathcal{B}]+\cdots} \approx \mathrm{e}^{-I_{\text{Bulk}}[\mathcal{B}]} \,, \tag{3.26}$$

where $I_{\text{Bulk}}[\mathcal{B}]$ is the on-shell gravitational action in the bulk. Substituting into the differentiate dictionary, one obtains the so-called GKP-W relation [42, 43], given by

$$Z_{\text{CFT}}[\partial\mathcal{B}] = \mathrm{e}^{-I_{\text{Bulk}}[\mathcal{B}]} \tag{3.27}$$

In order to use (3.27) to write the entanglement entropy (3.24) in terms of the bulk action, also requires an n-fold cover bulk solution $\mathcal{B}_n$, with a boundary $\partial\mathcal{B}_n$. Assuming the existence of such a spacetime, such that $Z_{\text{CFT}}[\partial\mathcal{B}_n] = \mathrm{e}^{-I_{\text{Bulk}}[\mathcal{B}_n]}$, one can re-write the replica trick entanglement entropy (3.24) for the case of the bulk theory, which yields

$$S_A = \lim_{n\to 1} \partial_n (I_{\text{Bulk}}[\mathcal{B}_n] - n I_{\text{Bulk}}[\mathcal{B}]) \,. \tag{3.28}$$

[18] One can think of this as arising from the way the correlation functions behave across a boundary. Since they are inversely proportional to the separation between the two points, correlation functions diverge at small distances, such as across a boundary. This high correlation across a boundary is indicative of the high entanglement between the two regions across the boundary.

This holographic entanglement entropy is a formula for the von Neumann entropy associated to a subregion on the dual CFT boundary of the bulk AdS theory. Ryu and Takayanagi conjectured that the formula takes the form

$$S_A = \frac{\mathcal{A}}{4G_N} \tag{3.29}$$

where $\mathcal{A}$ is the area of a static surface $\gamma_{\mathcal{A}}$ in the bulk that ends on the boundary of region $\mathcal{A}$, as illustrated in Figure 3.3. The surface $\gamma_{\mathcal{A}}$ is homologous to the region A and is such that it extremizes the area $\mathcal{A}$; hence being called a *minimal surface*. In the case there exist multiple extremal surfaces $\gamma_{\mathcal{A}}$, the one with the least area is chosen to compute the entropy.

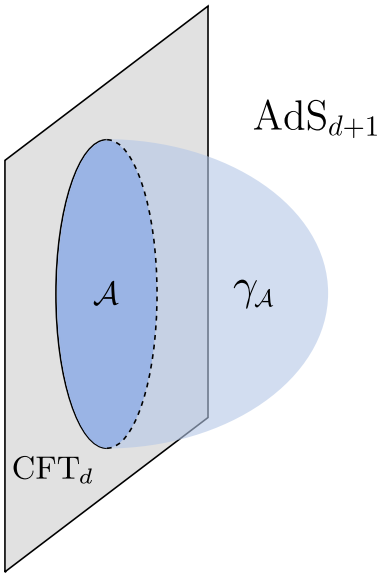

Figure 3.3: The RT formula states that the entanglement entropy of a region A in the CFT$_d$ theory can be calculated via the area of a static minimal surface (one with the minimum area) $\gamma_{\mathcal{A}}$, which extends from the holographic boundary into the AdS$_{d+1}$ bulk. Figure adapted from [37].

The RT formula can be used to reproduce the entanglement entropy (3.25) of for a flat CFT$_2$ theory [37]. However, a more interesting example of using the RT formula is for calculating the black hole entropy. The entropy appearing in the RT formula seems to resemble the black hole entropy area law, which can indeed be derived from the RT formula. Since the RT formula applies to static spacetime, one could use it to calculate the entropy of the usual Schwarzschild eternal black hole; i.e. one not formed by a gravitational collapse. If the black hole is placed in an asymptotically AdS spacetime, and the region A is chosen to cover the entire spacetime, it can be shown via the RT formula, that the surface $\gamma_{\mathcal{A}}$, which both minimizes the area and is homologous to A, is precisely the black hole event horizon.

Following the RT conjecture, a derivation of the RT formula was provided by Lewkowycz and Maldacena (LM) [41], with a simpler, more heuristic version later provided by Dong [44]. In the next section we will outline the key steps of the proof, following the work in [44], without going into details, since this thesis does not deal any explicit entropy calculations.

3.3 Generalized gravitational entropy

Lewkowycz and Maldacena (LM) provided a derivation of the RT area law for entanglement entropy in a general Euclidean spacetime, entirely from the Euclidean path integral formalism [41]. An earlier attempt to derive the RT conjecture was proposed in [45], which was later proved to be incorrect [46]. Before looking at the approach used in [44], it is nice to review an earlier work by Hawking and Gibbons (HG) [47], which used the Euclidean path integral formalism and correctly arrived at the black hole entropy area law. The LM proof was a generalization of the work done in the HG paper. While the HG paper used the assumption of a general U(1) symmetry, LM provided a result for a general Euclidean spacetime without a general U(1) symmetry.

3.3.1 Introduction to the gravitational path integral

The usual path integral in QFT is represented by the partition function

$$Z = \int \mathcal{D}\phi \, \mathrm{e}^{-I_E[\phi]} \tag{3.30}$$

where $I_E[\phi]$ is the Euclidean action and we integrate over all fields ϕ (except for the metric $g_{\mu\nu}$). In particular, the thermal partition function is defined as the Euclidean path integral with the boundary condition that the Euclidean time is periodic; i.e. $\tau \sim \tau + \beta$, so

$$Z(\beta) = \mathrm{Tr}[\mathrm{e}^{-\beta H}] = \int_{\phi(\tau)\sim\phi(\tau+\beta)} \mathcal{D}\phi \, \mathrm{e}^{-I_E[\phi]} \tag{3.31}$$

The periodicity β of the Euclidean time is related to the temperature of the QFT and is given by $\beta = 1/T$.[19]

The (quantum gravity) argument by Hawking and Gibbons was based on the idea of adding gravity to the path integral. In this case, the partition function has contributions from both gravity, via the Euclidean Einstein action, and also from the quantum fields. The gravitational path integral in d spacetime dimensions is given by (3.30), but now requires also to integrate over the geometry itself, which gives[20]

$$\begin{aligned} Z &= \int \mathcal{D}g\mathcal{D}\phi \, \mathrm{e}^{-I_E[g,\phi]} \\ I_E[g,\phi] &= -\frac{1}{16\pi}\int_{\mathcal{M}} \mathrm{d}^d x \, \sqrt{g}R + (\text{boundary term}) + (\text{coupling to } \phi) \, , \end{aligned} \tag{3.32}$$

where ϕ is used to denote a set of matter fields and $\mathcal{M}$ is a manifold with a boundary. It is important to note that in performing the integral, the manifold is not specified. Instead, the metric is treated as a field, which is integrated over. Since the manifold $\mathcal{M}$ has a boundary, a cut-off is imposed at some large constant $r = r_0$, which is where the manifold boundary $\partial\mathcal{M}$ is located. In the presence of a boundary, a boundary term, commonly known as the

[19] Recall the thermal partition function $Z = \mathrm{Tr}[\mathrm{e}^{-\beta H}]$, where $\beta = 1/T$. There are multiple ways to see why this is identified with the periodicity of the Euclidean time coordinate. One way is to consider the time evolution of the thermal Green function, $G_\beta(\tau, x) = -\mathrm{Tr}\left[\rho_{\mathrm{thermal}}\mathcal{O}(\tau, x)\mathcal{O}(0,0)\right]$, which can be shown to be periodic in Euclidean time, with periodicity β; i.e. $G_\beta(\tau, x) = G_\beta(\tau + \beta, x)$.

[20] We have implicitly set Newton's constant $G_N = 1$ here for simplicity.

Gibbons-Hawking-York (GHY) term needs to be added to the action. This was first shown by York in [48] and later by Gibbons and Hawing in [47]. Writing the GHY term explicitly, the Euclidean action (3.32) becomes

$$I_E[g,\phi] = -\frac{1}{16\pi}\int_{\mathcal{M}} \mathrm{d}^d x\, \sqrt{g}R - \frac{1}{8\pi}\int_{\partial\mathcal{M}} \mathrm{d}^{d-1}x\, \sqrt{h}K + (\text{coupling to } \phi)\,, \tag{3.33}$$

where $h = \det(h_{ij})$ is the induced metric on the boundary and $K = h^{ij}K_{ij}$ is the trace of the extrinsic curvature, defined as $K_{ij} = \nabla_{(i}n_{j)}$. The vector n_i is a unit inward-pointing normal to $\partial\mathcal{M}$, so $h_{ij}n^j = 0$. The GHY term arises from requiring the variation of the Euclidean action to be stationary around the classical solutions. Although the geometry is not fixed, the boundary conditions are specified. In analogy with the thermal partition function in QFT, the quantum gravity thermal partition function is subject to the boundary condition that the Euclidean time is periodic[21]

$$Z(\beta) = \int_{\tau\sim\tau+\beta} \mathcal{D}g\mathcal{D}\phi\, \mathrm{e}^{-I_E[g,\phi]} \tag{3.34}$$

The periodicity of the Euclidean time; i.e. $\tau \sim \tau + \beta$ for all $\beta \in \mathbb{R}$ is the underlying U(1) symmetry of the spacetime, represented by the U(1) operator $\mathrm{e}^{\beta H}$ where $H = \partial_\tau$ is the time translation generator. The Euclidean action is invariant under the translation $\tau \to \tau + \beta$, i.e. $I_E[g,\phi] \to I_E[g,\phi]$. It is this U(1) symmetry which is the key assumption of the Gibbons-Hawking paper which was later neglected by the LM paper.

This path integral is difficult to compute, but one can use the saddle point approximation, which assumes that the path integral is dominated by the extrema. The semiclassical approximation states that

$$Z(\beta) \sim \sum_{\text{saddles}} \mathrm{e}^{-I_E[g_0,\phi_0]+I^{(1)}+I^{(2)}+\dots}\,, \tag{3.35}$$

where $I_E[g_0,\phi_0]$ is action on the saddle point; i.e. the on-shell Euclidean action, with (g_0,ϕ_0) obeying the classical equations of motion. This gives the leading approximation and is of order $\mathcal{O}(G_N^{-1})$.[22] The next terms are the 1-loop, 2-loop and the subsequent higher-loop contributions, which are subleading corrections, including fluctuations $(\delta g, \delta\phi)$ of the quantum fields around their classical values; i.e. $g = g_0 + \delta g$ and $\phi = \phi_0 + \delta\phi$. These terms are of order $\mathcal{O}(G_N^0)$, $\mathcal{O}(G_N^1)$, etc. In what follows we take the leading contribution of the semi-classical approximation of the path integral and only use the first term; i.e. $Z(\beta) \sim \mathrm{e}^{-I_E[g_0,\phi_0]}$.

In order to evaluate the partition function, we need to evaluate the Euclidean action. The particular solution to the Euclidean Einstein action that Gibbons and Hawking focused on is the Euclidean Schwarzschild black hole solution. We will focus on the $d = 4$ case. The Euclidean black hole metric can be obtained from the Lorentzian Schwarzschild metric by doing a Wick rotation to Euclidean time. The Schwarzschild metric is

$$\mathrm{d}s_E^2 = -\left(1-\frac{r_s}{r}\right)\mathrm{d}t^2 + \left(1-\frac{r_s}{r}\right)^{-1}\mathrm{d}r^2 + r^2\mathrm{d}\Omega_2^2\,, \tag{3.36}$$

[21] (Spoiler Alert) The reason we are talking about the thermal partition function in the first place is because we would like to use it to compute the entropy later.

[22] That is since the gravitational action is of order $\mathcal{O}(G_N^{-1})$.

so performing a Wick rotation to Euclidean time via $t \to -i\tau$ gives the Euclidean black hole metric

$$\mathrm{d}s^2 = g_{\mu\nu}\mathrm{d}x^\mu \mathrm{d}x^\nu = \left(1 - \frac{r_s}{r}\right)\mathrm{d}\tau^2 + \left(1 - \frac{r_s}{r}\right)^{-1}\mathrm{d}r^2 + r^2\mathrm{d}\Omega_2^2 \,, \tag{3.37}$$

where $r_s = 2M$ and M is the black hole mass. The Euclidean time coordinate is now an angular coordinate which is periodic, with period β, so $\tau \sim \tau + \beta$. Unlike the more familiar Lorentzian black hole solution, which has a horizon at $r = r_s$ and a singularity at $r = 0$, the Euclidean black hole has no interior and no singularity. Instead, the radial coordinate is restricted to $r > r_s$, with the black hole origin being located at $r = r_s$. To avoid the conical singularity at $r = r_s$, we need to fix the periodicity of the Euclidean time coordinate to $\beta = 4\pi r_s$, so $\tau \sim \tau + 4\pi r_s$, or equivalently, $\tau \sim \tau + 8\pi M$.[23] This periodicity is precisely the inverse of the black hole temperature; i.e. $T = 1/8\pi M$.

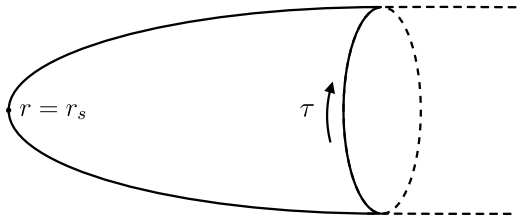

Figure 3.4: Euclidean black hole cigar geometry, periodic in Euclidean time; adapted from [49]

Now we wish to evaluate the action. The black hole solution is a vacuum solution, so we need to set $\bar{\phi} = 0$. The spacetime of the Euclidean black hole, as described by the metric in (3.37) has no boundary and is thus infinite. However, since in this case $R = 0$, we see that in the absence of a boundary, the action will vanish. Adding a boundary does fix this issue, because the GHY term in the action is no longer zero. Since only the GHY term contributes to the action in (3.33),

$$\log Z(\beta) = \frac{1}{8\pi}\int_{\partial\mathcal{M}} \mathrm{d}^{d-1}x\, \sqrt{h}K \,. \tag{3.38}$$

We imposed a radial cut-off at r_0, so the boundary hypersurface $\partial\mathcal{M}$ is at some fixed $r = r_0$ so $\mathrm{d}r = 0$. The metric on the boundary is thus

$$\mathrm{d}s_E^2\Big|_{\partial\mathcal{M}} = h_{ij}\mathrm{d}x^i\mathrm{d}x^j = \left(1 - \frac{r_s}{r_0}\right)\mathrm{d}\tau^2 + r_0^2\,\mathrm{d}\Omega_2^2 \,. \tag{3.39}$$

[23] To see this, we can consider the simple metric $\mathrm{d}s^2 = \mathrm{d}r^2 + r^2\mathrm{d}\theta^2$, which has a coordinate singularity at $r = 0$. Unlike a physical curvature singularity, a coordinate singularity can be removed via a coordinate transformation. By defining $x = r\cos\theta$ and $y = r\sin\theta$, we can rewrite the metric as $\mathrm{d}s^2 = \mathrm{d}x^2 + \mathrm{d}y^2$. For the coordinate transformation to be well defined, θ has to be periodic in 2π, or we end up with a conical singularity, instead of the Euclidean spacetime manifold. Now we wish to see how this works for the Euclidean black hole. We can do a coordinate transformation to the coordinate ρ, defined as $\mathrm{d}\rho^2 = (1 - \frac{r_s}{r})\mathrm{d}r^2$, in which case the metric (3.37) becomes $\mathrm{d}s^2 = \mathrm{d}\rho^2 + \rho^2\frac{\mathrm{d}\tau^2}{(2r_s)^2} + r^2\mathrm{d}\Omega_2^2$. In analogy with the previous example, imposing regularity at the $\rho = 0$ origin, $\frac{\tau}{2r_s}$ needs to have a period of 2π. Hence, $\tau \sim \tau + 4\pi r_s$.

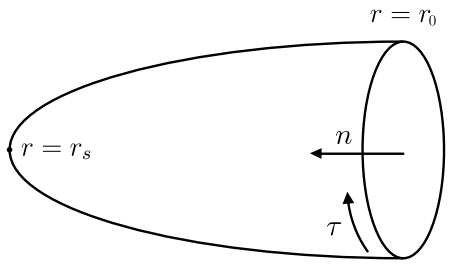

Figure 3.5: Euclidean black hole with a boundary at r_0 and the inward-pointing normal vector n; adapted from [49]

To evaluate the extrinsic curvature, we need to find the unit normal vector to the boundary. Since n is along the r direction, $n = n^\mu \partial_\mu = n^r \partial_r$. Imposing the unitarity condition $n^\mu n_\mu = 1$, leads to $n^r = 1/\sqrt{g_{rr}}$. Using the components of the induced metric, namely $h_{ij} = \text{diag}(1 - r_s/r_0, r_0^2, r_0^2 \sin\theta^2)$, the determinant of the metric is given by $h = \det(h_{ij}) = (1 - r_s/r_0) r_0^4 \sin\theta^2$. Hence, the extrinsic curvature can hence obtained via

$$\begin{aligned} K &= \nabla_\mu n^\mu \\ &= \nabla_r n^r \Big|_{r=r_0} \\ &= \frac{1}{r^2} \partial_r (r^2 n^r) \Big|_{r=r_0} \\ &= -\frac{2}{r_0} \sqrt{1 - \frac{r_s}{r_0}} - \frac{r_s}{2r_0^2} \frac{1}{\sqrt{1 - \frac{r_s}{r_0}}} \end{aligned} \tag{3.40}$$

The GHY term can now be evaluated via

$$\begin{aligned} -\frac{1}{8\pi} \int_{\partial\mathcal{M}} \mathrm{d}^{d-1}x \, \sqrt{h} K &= -\frac{1}{8\pi} \int_0^\beta \mathrm{d}\tau \int_0^{2\pi} \mathrm{d}\phi \int_0^{\pi/2} \mathrm{d}\theta \, \sqrt{h} K \\ &= -\beta \left(r_0 - \frac{3r_s}{4} \right) . \end{aligned} \tag{3.41}$$

As pointed out before, in the absence of a boundary, the action vanished, so a boundary was placed at some fixed $r = r_0$. The end goal of this calculation will be to compute the entropy of the Euclidean black hole. To do this only the black hole geometry needs to be taken into account without any of the asymptotically flat spacetime at large $r \gg r_0$. This requires taking the limit $r_0 \to \infty$. However, we can see from (3.41) that the GHY term $\to \infty$ as $r_0 \to \infty$. Hence, if we add a fixed boundary and we then take that cut-off to infinity, the action will go to infinity. To regulate this divergence and ensure that the action remains well-defined at large r, a further counterterm needs to be added to the action, given by [50]

$$\frac{1}{8\pi} \int_{\partial\mathcal{M}} \sqrt{h} K_0 = \beta \left(r_0 - \frac{r_s}{2} \right) , \tag{3.42}$$

where K_0 is the extrinsic curvature of $\partial\mathcal{M}$ embedded in a flat spacetime manifold with the flat metric

$$\mathrm{d}s_E^2 = \left(1 - \frac{r_s}{r_0} \right) \mathrm{d}\tau^2 + \mathrm{d}r^2 + r^2 \mathrm{d}\Omega_2^2 \tag{3.43}$$

In the evaluation of (3.42) terms of $\mathcal{O}(1/r_0)$ are neglected since we have take the limit of $r_0 \to \infty$. This counterterm acts as to cancel out the flat spacetime contribution to the integral. Hence,

$$I_E[g] = \frac{\beta r_s}{2} = \frac{\beta^2}{16\pi} \tag{3.44}$$

To obtain the entropy, one can use the standard relation from thermodynamics (3.15)

$$S(\beta) = (1 - \beta\partial_\beta) \log Z(\beta) = 4\pi M^2 = \frac{\mathcal{A}}{4} \,, \tag{3.45}$$

where we have used that the area of the event horizon is $\mathcal{A} = 4\pi r_s^2 = 16\pi M^2$. This is precisely the black hole entropy area law!

The work by Lewkowycz and Maldacena [41] is a generalization of the above computation, without the U(1) symmetry assumption, and it provided a proof of the RT formula. It should be noted that while the RT formula was motivated by the AdS/CFT duality, the derivation by Lewkowycz and Maldacena was gravitational. The outline of the derivation will be discussed in the next section, following the approach presented in [44].

3.3.2 Gravitational entanglement entropy - no U(1)

To proceed with the review of the derivation, we should recall some results in Section 3.2 from the semiclassical approximation, namely the expression for the entanglement entropy in terms of an n-fold cover bulk manifold $\mathcal{B}_n$, with a boundary $\partial\mathcal{B}_n$, given by

$$S_A = \lim_{n\to 1} \partial_n (I_{\text{Bulk}}[\mathcal{B}_n] - n I_{\text{Bulk}}[\mathcal{B}]) \,. \tag{3.46}$$

Note that the case we are considering now is a spacetime without a general U(1) symmetry. Instead, we consider a bulk manifold $\mathcal{B}$, whose boundary has just one U(1) symmetry, namely $\tau \sim \tau + 2\pi$, as illustrated in Figure 3.6 (left).

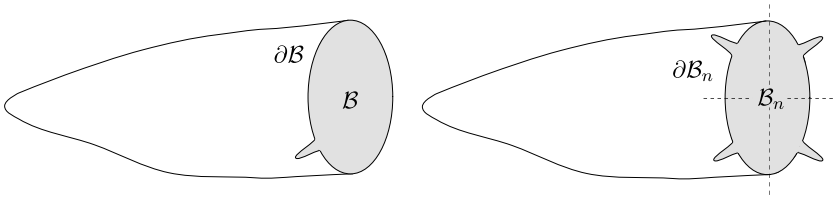

Figure 3.6: (left) A bulk manifold $\mathcal{B}$ with a boundary that has $\tau \sim \tau + 2\pi$ symmetry. (right) A bulk n-fold cover manifold $\mathcal{B}_n$ with a boundary that has $\tau \sim \tau + 2\pi n$ symmetry. adapted from [41]

With a boundary of the original manifold, invariant under $\tau \sim \tau + 2\pi$, the boundary of the n-fold cover manifold must have periodicity of $\tau \sim \tau + 2\pi n$, as illustrated in Figure 3.6 (right). This can be motivated using Figure 3.7 and Figure 3.2 by considering the n-fold cover and following the arrows as before. Starting from one of the sheets, a period of 2π will takes us to the sheet above it. Similarly, another period of 2π will take us to the next sheet above that one. To reach the original sheet, one needs to repeat this process n times, hence the periodicity of the n-fold cover boundary being $2\pi n$. This means that the boundary $\partial\mathcal{B}_n$ of the n-fold cover manifold $\mathcal{B}_n$ has a $\mathbb{Z}_n$ symmetry.

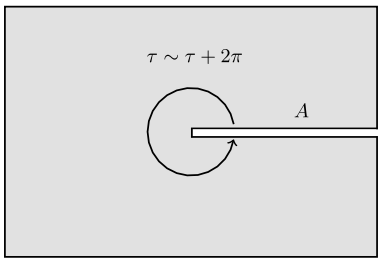

Figure 3.7: The single-sheet cover $\mathcal{B}$ with a cut along the A region; adapted from [37]

To derive of the entanglement entropy expression (3.46), we used the Renyi entropy, which is where the n copies of the n-fold cover came from. Recall that although the n-fold cover assumes that the parameter $n \in \mathbb{Z}_+$, in the evaluation of the right-hand side of (3.46), due to the partial derivative with respect to n, one needs to analytically continue to $n \in \mathbb{R}$ [37]. However, it is not immediately clear how deal with an n-fold cover partition function in the case where $n \in \mathbb{R}$. To circumvent this issue, the key assumption in [41] is that the $\mathbb{Z}_n$ symmetry of the boundary $\partial\mathcal{B}_n$ of the n-fold cover manifold $\mathcal{B}_n$, also extends into the bulk, such that $\mathcal{B}_n$ also has a $\mathbb{Z}_n$ symmetry. This analytic continuation into the bulk means that we can focus on the bulk orbifold

$$\hat{\mathcal{B}}_n := \mathcal{B}_n/\mathbb{Z}_n \ , \tag{3.47}$$

which is illustrated in Figure 3.8 (right). Note that although the boundary of this orbifold is the same as the boundary of the original manifold, namely $\partial\hat{\mathcal{B}}_n = \partial\mathcal{B}$, the bulk is not the same, due to the conical singularity along the cut, which means that $\hat{\mathcal{B}}_n \neq \mathcal{B}$.

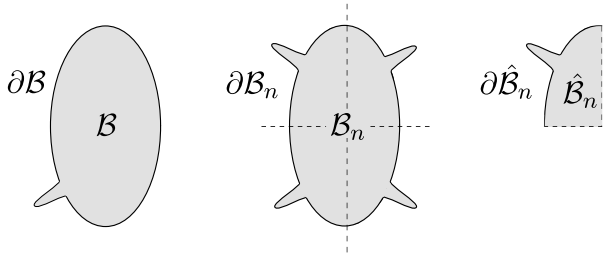

Figure 3.8: (left) Original manifold $\mathcal{B}$ with a boundary $\partial\mathcal{B}$; (center) n-fold cover $\mathcal{B}_n$ with a boundary $\partial\mathcal{B}_n$ for the case of $n = 4$, where the dotted line is used to represent the $\mathbb{Z}_n$ (in this case $\mathbb{Z}_4$) symmetry; (right)

It is this continuation of the boundary symmetry into the bulk which is a key step in the (LM) proof of the RT formula. However, since this thesis does not go into explicit QFT entropy calculations, we will not proceed further with more details about the proof.

The RT formula refers to the case of a static spacetime (and in the absence of quantum corrections). In the next section, we will provide a bit of a history on the generalizations of the RT formula. We will not go into any details, but we will explain the current version of the generalized entanglement entropy formula and how to use it.

3.4 Generalized Entanglement Entropy

Following the conjecture of the RT formula, there have been several generalizations it. Although it provided a simple geometric way of calculating the entanglement entropy, the RT

formula was only applicable to static spacetimes and could not be used for time-dependent spacetime solutions. Even though, as mentioned in Section 3.3, the RT formula can be used to calculate the entropy of the eternal black hole, this is not sufficient to study the information paradox, which deals with evaporating black holes, and hence non-static solutions.

A generalization of the RT formula that resolved this issue was done by Hubeny, Rangamani and Takayanagi (HRT) [51]. In the HRT prescription, the minimal area surface, which we will now refer to as χ, extending from the holographic boundary and into the bulk, is no longer defined on a constant time slice.

The next important generalization to the gravitational entanglement entropy was done by Faulkner, Lewkowycz and Maldacena (FLM) [52], who still focused on static spacetimes, but incorporated the contributions from quantum corrections. The new formula still contained the previous term proportional to the area $\mathcal{A}(\chi)$ of the minimal area surface, but also included a contribution from the entanglement entropy across the minimal surface χ due to the quantum fields in the bulk. Note, in the FLM proposal the area of the surface is extremized before the addition of the quantum corrections.

The final, and most recent, generalization to the gravitational entanglement entropy, was done by Engelhardt and Wall (EW) [53], who generalized the FLM proposal to non-static spacetimes. Hence, the final formula included both the incorporation of dynamics, and also of quantum corrections into the original RT formula. The formula is given by

$$S = \mathrm{Min}_{\chi}\Big[\mathrm{Ext}_{\chi}\Big\{\frac{\mathcal{A}(\chi)}{4G_N} + S_{\text{semi-cl}}(\Sigma_{\chi})\Big\}\Big] = \mathrm{Min}_{\chi}\Big[\mathrm{Ext}_{\chi} S_{\text{gen}}(\chi)\Big] \,, \tag{3.48}$$

where the surface χ is now referred to as a *quantum extremal surface* (QES), the Σ_{χ} is a region bounded by the QES and a cut-off surface (which depends on the situation considered) and $S_{\text{semi-cl}}(\Sigma_{\chi})$ is the von Neumann entropy of the quantum fields on Σ_{χ}. The formula works by first extremizing the generalized entropy $S_{\text{gen}}(\chi)$ respect to the position of the QES χ, in order to find its location. The resulting entropy is then minimized over all possible choices of χ. Note, a key difference between the EW and FLM a method is that in the EW formula, the area of the surface is extremized in relation to the whole entanglement entropy, including the quantum correction term. The formula also allows for disconnected regions Σ_{χ}, which can sometimes provide a global minimum of the generalized entropy.

In Chapter 5, where a specific black hole evaporation model will be discussed, this formula will be used to explain the evolution of the black hole entropy, as well as the evolution of the Hawking radiation entropy.

3.5 Conclusion

In this chapter, we reviewed some key features about the entanglement entropy. We reviewed entropies in quantum mechanics, in quantum field theories, and the subsequent generalization of gravitational entanglement entropy formula. The results from this chapter will be important in Chapter 5, where the thermodynamics of a particular black hole evaporation protocol will be studied.

4
Black holes in AdS

In this chapter, we use the theoretical background from Chapter 2 to study black holes in AdS. In Section 4.1, we motivate the reason for studying these black hole solutions, even though our Universe is not AdS. In Section 4.2, we compare the thermodynamic stability of the AdS black hole solution to black holes in an asymptotically flat spacetime. In Section 4.3, we explain the issues surrounding these AdS black holes, arising from, the nature of the AdS geometry and its reflective boundary conditions. We explain why large black holes do not evaporate in AdS, with all the Hawking radiation bouncing off the AdS boundary, and why making them smaller presents further issues. With that in mind, in Section 4.4, to resolve the problem with the boundary conditions, we show that changing these boundary conditions to allow absorption into the holographic boundary is not possible, since any particle that escapes the bulk will no longer have a description at the holographic boundary.

4.1 Why AdS?

Based on the fact that an extensive amount of experimental data from cosmology points towards evidence that the Universe is asymptotically de-Sitter (dS), it is not too far-fetched for members of the community to keep asking themselves why bother studying a Universe which is asymptotically AdS at all. The possible pure-to-mixed state evolution of an evaporating black hole pointed towards a discrepancy between the evaporation mechanism (leading to a thermal radiation in a mixed state) and the laws of quantum mechanics (requiring unitary time evolution). Either the Hawking radiation was not exactly thermal and had subtle correlations or quantum gravity was not a unitary theory.

The motivation for using AdS has to do with the development of the AdS/CFT correspondence, which settled the issue in favor of unitarity and conservation of information. The fact that a gravitational theory in AdS spacetime is dual to a quantum field theory, namely a CFT, that lives on its boundary, has strong implications for black holes in AdS. Since AdS black holes can be, equivalently, described by a quantum field theory, which is manifestly unitary, means that black hole evaporation must be a unitary process (at least for asymptotically

AdS spacetimes). This consequence of the duality shifted the general opinion on black hole evaporation, including famously that of Hawking [54], since it implied that the continuous monotonic increase in entropy of the Hawking radiation could not be the full story.

However, AdS black holes present certain challenges as well. In the following section we will review some key differences in the behaviour of black holes in asymptotically flat and asymptotically AdS spacetimes. We will explain why the current focus is on large, rather than small, AdS black holes, as well as why they make it difficult to study the information paradox.

4.2 Black hole evaporation in AdS

The Schwarzschild black hole, i.e. the black hole in an asymptotically flat spacetime, has a negative specific heat and a temperature given by

$$T = \frac{1}{8\pi M} \,, \tag{4.1}$$

as derived in Section 3.3.1. This shows that smaller black holes have higher temperatures. That is why this black hole solution is not thermodynamically stable. Small fluctuations that decrease the temperature outside the black hole will cause it to lose some extra energy to the outside. This will cause the black hole's mass to decrease, making its temperature rise, since $T \propto 1/M$. This will in turn cause the black hole to lose energy to the outside and get hotter again. The black hole will keep getting hotter and hotter until it has shrunk all the way down to zero. If we, instead, introduce a fluctuation of higher temperature outside the black hole, this will get absorbed by the black hole. The black hole's mass will increase and it's temperature will drop. Again, this is a runaway process, if we keep supplying energy to the black hole. The black hole will keep consuming the radiation and get infinitely large. That's why the asymptotically flat black hole is not thermodynamically stable. As we will see, the black hole in an asymptotically AdS spacetime, is much better-behaved!

Hawking's effort to make the solution stable involved putting the Schwarzschild black hole in a finite box of a positive heat capacity [11]. He found that that, provided the energy of the radiation in the box $E_{\text{Rad}} \leq M/4$, there can exist a stable solution, where the black hole is in thermodynamic equilibrium with the radiation. A nice derivation of this can be found in [55].

Although not physical, Hawking's model yielded a thermodynamically stable solution. A perhaps more natural model is placing the black hole in a "fancier" box, namely in an asymptotically AdS spacetime. As opposed to the asymptotically flat case, the asymptotically AdS black hole has a positive specific heat. The derivation of the temperature profile of AdS black holes follows the same approach as the Schwarzschild case derived in Section 3.3.1. We will again focus on the $d = 4$ case, in which case the AdS-Schwarzschild metric is given by

$$\mathrm{d}s^2_{\text{AdSS}} = -\Big(1 - \frac{2M}{r} + \frac{r^2}{\ell^2_{\text{AdS}}}\Big)\mathrm{d}t^2 + \Big(1 - \frac{2M}{r} + \frac{r^2}{\ell^2_{\text{AdS}}}\Big)^{-1}\mathrm{d}r^2 + r^2\mathrm{d}\Omega_2^2 \,. \tag{4.2}$$

In the limit of small r, the metric approaches the Schwarzschild solution, while for large r, it approaches the AdS metric. The horizon r_+ is given by the vanishing of the g_{00} component of the metric, which is the largest root of the three solutions to [55]

$$r_+^3 + \ell^2_{\text{AdS}} r_+ - M\ell^2_{\text{AdS}} = 0 \,. \tag{4.3}$$

To find the temperature of this black hole, one can either use the extrinsic curvature, or the Euclidean method, which will be used here. Performing a Wick rotation to Euclidean time via $t \to -i\tau$, and using the periodicity $\beta = T^{-1}$, the black hole temperature is given by

$$T = \frac{\ell_{\text{AdS}}^2 + 3r_+^2}{4\pi\ell_{\text{AdS}}^2 r_+} \,. \tag{4.4}$$

This is the temperature at which the black hole exists in stable thermodynamic equilibrium with the evaporated thermal radiation[56]. The temperature of the black hole can be written as a function of its mass M by using the relation between the radius of the event horizon r_+ and the mass in (4.3). This has been illustrated in Figure. 4.1, which shows that, unlike the Schwarzschild case (left), the temperature of the AdS black hole (right) no longer decreases monotonically as the black hole evaporates. In fact, the temperature has a minimum of $T_0 = \sqrt{3}/2\pi\ell_{\text{AdS}}$ at $r_0 = \ell_{\text{AdS}}/\sqrt{3}$, when the mass of the black hole is $M = 2\ell_{\text{AdS}}/3\sqrt{3}$. At temperatures $T < T_0$, there are no black hole solutions, but only Hawking radiation. At temperatures $T > T_0$, there are two black hole solutions. One of the solutions has a negative specific heat, namely the one that has a negative gradient ($\mathrm{d}T/\mathrm{d}M < 0$), which occurs when $M < M_0$. These smaller black holes, just as the Schwarzschild black hole, are thermodynamically unstable. The other solution has a positive specific heat, namely the one with the positive gradient ($\mathrm{d}T/\mathrm{d}M > 0$), which occurs when $M > M_0$. Hence these larger black holes, unlike the Schwarzschild black hole, are thermodynamically stable.

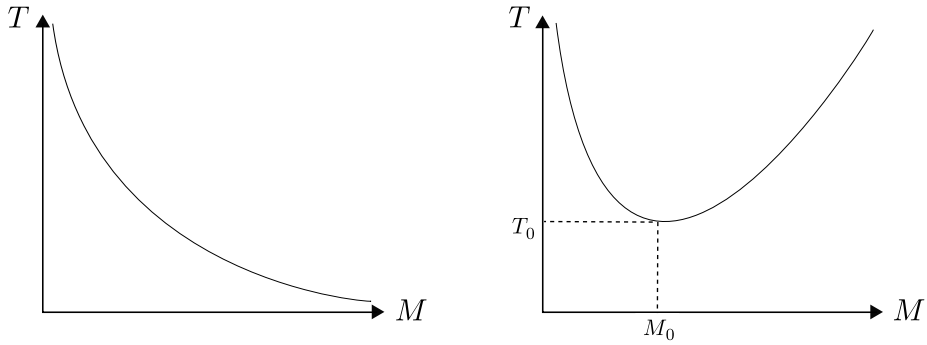

Figure 4.1: (left) The temperature of the Schwarzschild black hole decreases monotonically with its mass, demonstrating a thermodynamically unstable solution. (right) Small AdS black holes show the same thermodynamic instability as Schwarzschild black hole. However, large AdS black holes are thermodynamically stable solutions, as can be seen by their positive specific heat behaviour. Adapted from [55].

While they resolve the stability issue, large AdS black holes introduce another problem, namely their evaporation. Above a certain size, black holes in asymptotically AdS spacetime, do not evaporate since they reach a thermodynamic equilibrium before they have had the chance to emit all the Hawking radiation. This is due to the AdS reflective boundary conditions, which cause all radiation that reaches the boundary to reflect back into the black hole, hence preventing it from evaporating. This is not an issue for small AdS black holes which do manage to evaporate completely before reaching a thermodynamic equilibrium. The AdS reflective boundary conditions will be discussed in the next section.

4.3 Reflective Boundary Conditions

Even though the AdS boundary is infinitely far away, massless particles follow null geodesics, which take a finite affine parameter (proper time) to reach the AdS boundary from within the bulk [57]. One would compute this time from the AdS metric, and any choice of coordinates could work. Supposing there is no black hole, using global coordinates (2.6), null geodesics satisfy

$$\mathrm{d}s^2 = 0 = -\left(1+\frac{r^2}{\ell_{\mathrm{AdS}}^2}\right)\mathrm{d}t^2 + \left(1+\frac{r^2}{\ell_{\mathrm{AdS}}^2}\right)^{-1}\mathrm{d}r^2 + r^2\mathrm{d}\Omega_{d-1}^2 \tag{4.5}$$

Radial null geodesics would therefore satisfy

$$\mathrm{d}t^2 = \left(1+\frac{r^2}{\ell_{\mathrm{AdS}}^2}\right)^{-2}\mathrm{d}r^2 \,, \tag{4.6}$$

which can be integrated to find that the proper time for a photon to go from $r=0$ to $r=\infty$ is given by

$$\Delta t = \int_0^\infty \left(1+\frac{r^2}{\ell_{\mathrm{AdS}}^2}\right)^{-1}\mathrm{d}r = \frac{\pi}{2}\ell_{\mathrm{AdS}} \,, \tag{4.7}$$

which is finite. The finite amount of time it takes null geodesics to reach the boundary at infinity precisely the reason for reflective boundary conditions to be usually imposed at the AdS boundary. Since energy must be conserved, there could be no net flux of energy across the AdS boundary, so these waves must reflect back into the interior [58, 59]. In this sense, the spacetime acts as a box, as illustrated in Figure. 4.2.

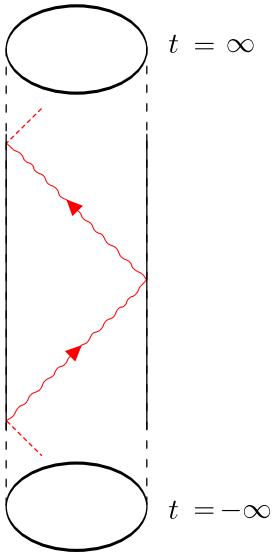

Figure 4.2: Null geodesics reach the AdS_3 boundary in a finite amount of time, where reflective boundary conditions are imposed to ensure energy conservation.

Since a large enough black hole in AdS is thermodynamically stable, and any Hawking radiation from it is reflected from the boundary back into the black hole, these black holes do not

evaporate, but rather bathe in their radiation. Considering that evaporation is a key aspect to the information paradox, being the reason it started in the first place, large black holes in AdS make it difficult to resolve it.

One might ask the obvious question, namely: Why not simply study small black holes in AdS, which would indeed be able to evaporate completely? These black holes are expected to behave similarly to black holes in asymptotically flat spacetime, since they both have negative heat capacity. This is because small black hole do not exist in lower dimensions [60]. As we will discuss in the next chapter, due to the non-renormalizability of $4d$ Einstein gravity, it is prefferable to work in lower dimensions.

Besides considering smaller AdS black holes, the other way to tackle the problem with their evaporation is to change the boundary conditions at the holographic boundary. This will be discussed in the next sections, where we will focus in the AdS_3/CFT_2 duality and check if it is possible to absorb a bulk field into the holographic boundary.

4.4 Absorbing Boundary Conditions

Following the discussion so far, it can be concluded that is difficult to study the information paradox for large black holes in AdS/CFT, since large black holes in AdS do not evaporate. To reinstate the information paradox, we need a protocol that would allow the Hawking radiation to escape the bulk and be absorbed somewhere else. One mechanism, and the one we will consider in this chapter, is allowing the Hawking radiation to be absorbed from the bulk into the conformal boundary. We will focus on the case of AdS_3/CFT_2 and use the duality to find out what a disappearing bulk mode means for the field operator on the boundary. To do this we will first study the bulk field and impose that it gets annihilated when it reaches the boundary at $t = 0$. We will then study its dual CFT operator in the conformal field theory and verify that the annihilation of the bulk field also causes the CFT operator to also get annihilated.

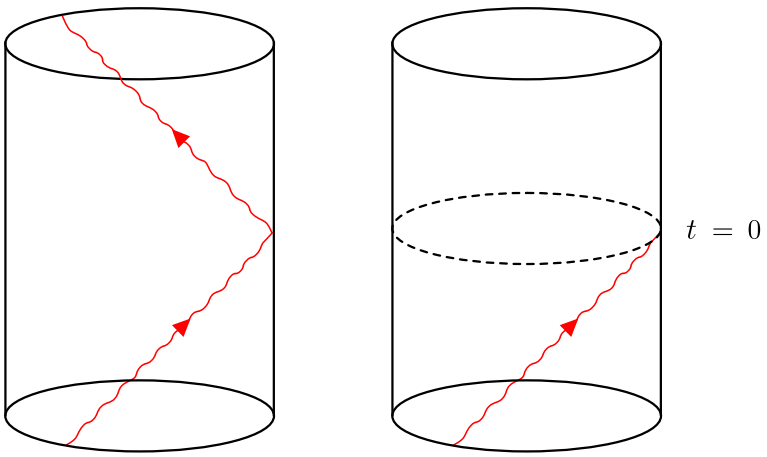

Figure 4.3: Removing the reflective boundary conditions at the AdS_3 boundary and imposing absorbing boundary conditions at $t = 0$.

4.4.1 Free Scalar Field Quantization in Global AdS

We will consider a scalar field theory in Lorentzian AdS_{d+1}, described by the action

$$S = \frac{1}{2}\int \mathrm{d}^{d+1}x\,\sqrt{-g}\,(g^{\mu\nu}\partial_\mu\phi\partial_\nu\phi + m^2\phi^2)\ . \tag{4.8}$$

We choose to work with the Lorentzian signature, since we derived in Section 2.1.2, that only the Lorentzian signature admits a normalizable mode solution. As explained in Section 2.3.2, this normalizable mode is identified as the boundary operator. In what follows we will use the metric in global coordinates, which covers the entirety of the bulk. It was defined in (2.7) and we will set $\ell_{\mathrm{AdS}} = 1$ for simplicity. To obtain the equation of motion (2.13) for ϕ, we vary the action with respect to ϕ and since $\sqrt{-g} = \tan^{d-1}\rho/\cos^2\rho$, the equation of motion for the scalar field becomes

$$-\cos^2\rho\,\partial_t^2\phi + \frac{\cos^2\rho}{\tan^{d-1}\rho}\partial_\rho(\tan^{d-1}\rho\,\partial_\rho\phi) + \frac{\cos^2\rho}{\sin^2\rho}\partial_\Omega^2\phi = m^2\phi\ . \tag{4.9}$$

To solve this equation of motion, we assume a separation of variables and a basis of the form

$$\phi_{E\ell\vec{m}}(t,\rho,\Omega) = \mathrm{e}^{-iEt}\psi_{E\ell}(\rho)Y_{\ell\vec{m}}(\Omega) \tag{4.10}$$

where $Y_{\ell\vec{m}}(\Omega)$ are the spherical harmonics on $\mathbb{S}^{d-1}$ and ℓ is the angular momentum. $Y_{\ell\vec{m}}(\Omega)$ are eigenfunctions of the Laplacian with eigenvalues $-\ell(\ell+d-2)$. The Laplacian acts on the spherical harmonics as

$$\nabla^2_{\mathbb{S}^{d-1}}Y_{\ell\vec{m}}(\Omega) = -\ell(\ell+d-2)Y_{\ell\vec{m}}(\Omega)\ . \tag{4.11}$$

Using the above separation of variables, we obtain an equation of motion for $\psi_{E\ell}(\rho)$, given by

$$\cos^2\rho\,\partial_\rho^2\psi + (d-1)\frac{\cos\rho}{\sin\rho}\partial_\rho\psi + \psi\left(E^2\cos^2\rho - \ell(\ell+d-2)\frac{\cos^2\rho}{\sin^2\rho} - \Delta(\Delta-d)\right) = 0\ , \tag{4.12}$$

where we have used that the mass of the scalar field can be related to the scaling dimension of the CFT operator via $m^2 = \Delta(\Delta-d)$. The above can be solved numerically to obtain two possible solutions for $\psi(\rho)$, but only one of them is regular at the origin $\rho = 0$ and it has the form [61]

$$\psi(\rho) = (\cos\rho)^{\Delta_+}(\sin\rho)^\ell\ {}_2F_1\left(\frac{\Delta_+ + \ell + E}{2}, \frac{\Delta_+ + \ell - E}{2}, \ell + \frac{d}{2}; \sin^2\rho\right)\ . \tag{4.13}$$

The hypergeometric function is a function of $\sin^2\rho$. To study the behaviour at the boundary $\rho \to \pi/2$, it is more convenient to express it in terms of $\cos^2\rho$. This can be achieved using the following identity for the hypergeometric function:

$$\begin{aligned}{}_2F_1(a,b,c;z) = {}& \frac{\Gamma(c)\Gamma(c-a-b)}{\Gamma(c-a)\Gamma(c-b)}\ {}_2F_1(a,b,a+b-c+1;1-z) \\ &+ \frac{\Gamma(c)\Gamma(a+b-c)}{\Gamma(a)\Gamma(b)}(1-z)^{c-a-b}\ {}_2F_1(c-a,c-b,1+c-a-b;1-z)\ .\end{aligned} \tag{4.14}$$

This allows us to write(4.13) as

$$\psi(\rho) = C^+\psi^+(\rho) + C^-\psi^-(\rho)\ , \tag{4.15}$$

where

$$\psi^{\pm}(\rho) = (\cos\rho)^{\Delta_\pm}(\sin\rho)^{\ell}\ {}_2F_1\left(\frac{\Delta_\pm+\ell+E}{2}, \frac{\Delta_\pm+\ell-E}{2}, \Delta_\pm+1-\frac{d}{2}; \cos^2\rho\right) \tag{4.16}$$

and we have defined

$$C^{\pm} = \frac{\Gamma(\ell+\frac{d}{2})\Gamma(\frac{d}{2}-\Delta_\pm)}{\Gamma(\frac{d-\Delta_\pm+\ell+E}{2})\Gamma(\frac{d-\Delta_\pm+\ell-E}{2})}. \tag{4.17}$$

Approaching the boundary at $\rho = \pi/2$, $\psi^{\pm}(\rho) \sim (\cos\rho)^{\Delta\pm}$ and it can be seen, following the same arguments as in Section 2.1.2, namely by substituting into the action and testing its regularity, that $\psi^{+}(\rho)$ is a normalizable solution, while $\psi^{-}(\rho)$ is a non-normalizable one. Hence, for the total solution (4.15) to be normalizable, we need to set the non-normalizable mode $\psi^{-}(\rho)$ to zero, which is achieved by imposing $C^{-} = 0$. This can done if a Gamma function in its denominator has a negative integer argument, which imposes a restriction on the allowed energies in the bulk modes. Namely, the allowed energy spectrum is

$$E = E_{nl} = \Delta_+ + 2n + \ell; \ \ n = 0, 1, \dots\ . \tag{4.18}$$

In terms of this quantized energy, the normalizable and non-normalizable solutions in (4.16) can be written in terms of Jacobi polynomials as[24]

$$\psi^{\pm}_{E\ell}(\rho) = (\cos\rho)^{\Delta_\pm}(\sin\rho)^{\ell}P_n^{(\ell+\frac{d}{2}-1, \frac{d}{2}-\Delta_\mp)}(\cos 2\rho)\ . \tag{4.19}$$

Now we can finally write the full general solution by using (4.10) and including both solutions for $\psi^{\pm}_{E\ell}(\rho)$ in (4.19). However, this will only give us the general single-particle solutions at the classical level. To describe the field, we need to expand it in terms of those solutions using creation and annihilation operators and summing over all possible mode energies and angular momenta. This results in the Heisenberg solution for the scalar field given by

$$\phi(t,\rho,\Omega) = \phi^{+}(t,\rho,\Omega) + \phi^{-}(t,\rho,\Omega)\ , \tag{4.20}$$

where

$$\phi^{+}(t,\rho,\Omega) = \sum_{n=0}^{\infty}\sum_{\ell\vec{m}} \mathrm{e}^{-iE_{n\ell}t}Y_{\ell\vec{m}}(\Omega)(\cos\rho)^{\Delta_+}(\sin\rho)^{\ell}P_n^{(\ell+\frac{d}{2}-1, \Delta_+-\frac{d}{2})}(\cos 2\rho)\, b_+ + \text{c.c.} \tag{4.21}$$

$$\phi^{-}(t,\rho,\Omega) = \sum_{n=0}^{\infty}\sum_{\ell\vec{m}} \mathrm{e}^{-iE_{n\ell}t}Y_{\ell\vec{m}}(\Omega)(\cos\rho)^{\Delta_-}(\sin\rho)^{\ell}P_n^{(\ell+\frac{d}{2}-1, \Delta_--\frac{d}{2})}(\cos 2\rho)\, b_- + \text{c.c.}\ , \tag{4.22}$$

are the full general normalizable and non-normalizable modes respectively, expanded in terms of their own sets of creation and annihilation operators, namely $\{b_+, b_+^\dagger\}$ for the normalizable mode and $\{b_-, b_-^\dagger\}$ for the non-normalizable mode [61].

Since we wish to work with $\mathrm{AdS}_3/\mathrm{CFT}_2$, the global coordinate metric (2.7) is just

$$\mathrm{d}s^2_{\mathrm{AdS}_3} = \frac{1}{\cos^2\rho}(-\mathrm{d}t^2 + \mathrm{d}\rho^2 + \sin^2\rho\,\mathrm{d}\theta^2)\ . \tag{4.23}$$

[24] One of the Gamma functions in (4.17), namely $\Gamma(\frac{d}{2}-\Delta_\pm) = \Gamma(\mp\nu)$, depends on whether $\nu > 1$ or $\nu < 1$ [23]. Here we have implicitly assumed the former case.

We wish to study what a massless scalar field corresponds to on the conformal boundary, so we will only consider the normalizable mode (4.21). We know from Section 2.3.2 that near the boundary, this normalizable mode is related to the conformal field theory operator. In the case we are considering $d = 2$, so $(\Delta_+, \Delta_-) = (2, 0)$ and the scalar field can be written as [62]

$$\phi(t, \rho, \theta) = \sum_{n=0}^{\infty} \sum_{\ell \vec{m}} \left(\phi_{E_{n\ell} \ell \vec{m}} b_{n\ell\vec{m}} + \phi^*_{E_{n\ell} \ell \vec{m}} b^\dagger_{n\ell\vec{m}} \right) , \tag{4.24}$$

where

$$\phi_{E_{n\ell} \ell \vec{m}} = \mathrm{e}^{-iE_{n\ell}t} Y_{\ell\vec{m}}(\theta) \cos^2\rho \sin^\ell \rho P_n^{(\ell,1)}(\cos 2\rho) . \tag{4.25}$$

The creation and annihilation operators in (4.24) act on the AdS bulk vacuum as

$$b_{n\ell\vec{m}} |0\rangle_{\text{Bulk}} = 0 \tag{4.26}$$

$$b^\dagger_{n\ell\vec{m}} |0\rangle_{\text{Bulk}} = |n\ell\vec{m}\rangle , \tag{4.27}$$

where $|n\ell\vec{m}\rangle$ is a generic single-particle state described by the quantum numbers $(n, \ell, \vec{m})$. Similarly, many-particle states can be constructed by acting on the vacuum state with the multiple creation operators such that a generic k-particle state can be written as

$$b^\dagger_{n_1 \ell_1 \vec{m}_1} \dots b^\dagger_{n_k \ell_k \vec{m}_k} |0\rangle_{\text{Bulk}} . \tag{4.28}$$

The creation/annihilation operators satisfy the following commutation relations

$$[b_{n\ell\vec{m}}, b^\dagger_{n'\ell'\vec{m}'}] = \delta_{nn'} \delta_{\ell\ell'} \delta_{\vec{m}\vec{m}'} , \tag{4.29}$$

which come from requiring that the solutions $\phi_{E\ell\vec{m}}$ to have a unit norm

$$\langle \phi_{E_{n\ell}\ell\vec{m}}, \phi_{E_{n'\ell'}\ell'\vec{m}'} \rangle = \delta_{nn'} \delta_{\ell\ell'} \delta_{\vec{m}\vec{m}'} . \tag{4.30}$$

In terms of the creation/annihilation operators, the bulk Hamiltonian can be written in the familiar form

$$H_{bulk} = \sum_{n=0}^{\infty} \sum_{\ell\vec{m}} E_{n\ell} \, b^\dagger_{n\ell\vec{m}} b_{n\ell\vec{m}} , \tag{4.31}$$

where $N_{n\ell\vec{m}} = b^\dagger_{n\ell\vec{m}} b_{n\ell\vec{m}}$ is the number operator, specifying the number of particles that can be described by the quantum numbers $(n, \ell, \vec{m})$. The bulk state is given by

$$\begin{aligned} \phi(t, \rho, \theta) |0\rangle_{\text{Bulk}} &= \sum_{n=0}^{\infty} \sum_{\ell\vec{m}} \phi^*_{E_{n\ell}\ell\vec{m}} \, b^\dagger_{n\ell\vec{m}} \, |0\rangle_{\text{Bulk}} \\ &= \sum_{n=0}^{\infty} \sum_{\ell\vec{m}} \mathrm{e}^{iE_{n\ell}t} Y^*_{\ell\vec{m}}(\theta) \cos^2\rho \sin^\ell\rho P_n^{(\ell,1)}(\cos 2\rho) \, b^\dagger_{n\ell\vec{m}} \, |0\rangle_{\text{Bulk}} , \end{aligned} \tag{4.32}$$

which represents a superposition of single particle states. However, what we are really interested in is the state near the boundary. The boundary value of the bulk field, which is related to the dual field theory operator, is given by

$$\phi_{\text{bdy}}(t, \theta) = \lim_{\rho \to \pi/2} \frac{\phi(t, \rho, \theta)}{\cos^2\rho} = \sum_{n=0}^{\infty} \sum_{\ell\vec{m}} \mathrm{e}^{iE_{n\ell}t} Y^*_{\ell\vec{m}}(\theta) P_n^{(\ell,1)}(-1) \, b^\dagger_{n\ell\vec{m}} , \tag{4.33}$$

in accordance with the extrapolate dictionary (2.74) in global coordinates.[25] We can use this to write the bulk state near the boundary $|\phi\rangle_{\rm bdy} = \phi_{\rm bdy}(t,\theta)|0\rangle_{\rm Bulk}$ as

$$|\phi\rangle_{\rm bdy} = \sum_{n=0}^{\infty}\sum_{\ell\vec{m}} \mathrm{e}^{iE_{n\ell}t} Y^*_{\ell\vec{m}}(\theta) P_n^{(\ell,1)}(-1)\, b^\dagger_{n\ell\vec{m}}\,|0\rangle_{\rm Bulk}\ . \tag{4.34}$$

Imposing absorbing boundary conditions requires a mechanism by which the bulk field vanishes at the boundary and hence the boundary state $|\phi\rangle_B$ is returned back to the bulk vacuum $|0\rangle_{\rm Bulk}$. To study such absorption into the conformal boundary, we first check what the bulk mode is dual to in the CFT theory.

4.4.2 Boundary Field Theory

To study the physics of the dual CFT boundary we first need the CFT metric. This can be obtained by using the bulk metric and approaching the boundary. There are multiple ways to do this, depending on the coordinates used, but in any case, one finds that the CFT lives on a conformally flat manifold. This can be obtained by approaching the boundary ($\rho = \pi/2$) at the same rate for all (t,θ) via $\rho \to \pi/2 - \epsilon f(t,\theta)$, where $f(t,\theta)$ is some general regulating function. The cut-off ϵ is small and we take $\epsilon \to 0$ at the end [26]. In this case, the metric (79) becomes

$$\begin{aligned} \mathrm{d}s^2_{\partial \mathrm{AdS}_3} &= \frac{1}{(\epsilon f)^2}\left(-\mathrm{d}t^2 + [1-(\epsilon f)^2]\mathrm{d}\theta^2\right) \\ &\approx \frac{1}{(\epsilon f)^2}\left(-\mathrm{d}t^2 + \mathrm{d}\theta^2\right)\ , \end{aligned} \tag{4.35}$$

where we have used that

$$\cos^2\rho = \cos^2\left(\frac{\pi}{2} - \epsilon f\right) \approx (\epsilon f)^2 - \frac{(\epsilon f)^4}{3} + \dots \tag{4.36}$$

$$\sin^2\rho = \sin^2\left(\frac{\pi}{2} - \epsilon f\right) \approx 1 - (\epsilon f)^2 + \frac{(\epsilon f)^4}{3} + \dots\ . \tag{4.37}$$

This is related to the flat Minkowski metric via a Weyl transformation and since null geodesics do not care about the Weyl factor $1/(\epsilon f)^2$ of the metric, we will take the CFT metric to be

$$\mathrm{d}s^2_{\mathrm{CFT}_2} = -\mathrm{d}t^2 + \mathrm{d}\theta^2\ . \tag{4.38}$$

Having picked a bulk scalar of a specific mass, the AdS/CFT duality imposes a restriction (2.72) on the CFT operator. We are considering a massless bulk scalar in AdS_3, so $m = 0$ and $d = 2$, which means that there are two possible scaling dimensions for the dual CFT_2 operator, namely $\Delta = 0$ and $\Delta = 2$. The $\Delta = 0$ has been studied in more detail in [63]. However, for a number of reasons explained in [64], the $\Delta = 0$ solution is undesirable. One of these reasons is that the $\Delta = 0$ scaling dimension saturates the unitarity bound. But most importantly, we already chose the $\Delta = 2$, since we chose to work with the normalizable mode solution. Hence, we will use the $\Delta = 2$ solution and pick the easiest form for our CFT_2 operator. As an example, we will choose to work with the free massless boson φ and pick the CFT operator

[25] Note that the (-1) in $P_n^{(\ell,1)}(-1)$ is an argument of the Jacobi polynomial.

with $\Delta = 2$ to be $\mathcal{O} = \partial^\mu\varphi\partial_\mu\varphi$.[26] The dynamics of the massless boson is described by the action

$$S = \frac{1}{2}g\int \mathrm{d}^2x\ \partial_\mu\varphi\partial^\mu\varphi\ , \tag{4.39}$$

where g is a normalization parameter and the metric is the flat metric (4.38) with coordinates $x^\mu = (t, \theta)$. Although we are ultimately interested in the result in the Lorentzian signature, it is much more convenient to work in the Euclidean signature. So we Wick rotate to the Euclidean time; i.e. $t \to -i\tau$ and use the coordinates τ, θ. It is further useful to introduce the complex coordinates $(w, \bar{w})$ on the cylinder, defined as

$$\begin{aligned} w &= \theta - i\tau\ , \\ \bar{w} &= \theta + i\theta\ , \end{aligned} \tag{4.40}$$

in terms of which the CFT metric becomes

$$\mathrm{d}s^2_{\mathrm{CFT}_2} = \mathrm{d}\tau^2 + \mathrm{d}\theta^2 = \mathrm{d}w\mathrm{d}\bar{w}\ . \tag{4.41}$$

As mentioned in Section 2.2.2, it is useful to work in terms of the coordinates on the complex plane, defined as

$$\begin{aligned} z &= \mathrm{e}^{iw} = \mathrm{e}^{\tau+i\theta} \\ \bar{z} &= \mathrm{e}^{i\bar{w}} = \mathrm{e}^{\tau-i\theta}\ , \end{aligned} \tag{4.42}$$

The CFT operator $\mathcal{O} = \partial^\mu\varphi\partial_\mu\varphi = \partial_\tau\varphi\partial_\tau\varphi + \partial_\theta\varphi\partial_\theta\varphi$ can be written in terms of the complex plane coordinates as

$$\mathcal{O}(z, \bar{z}) = 4\partial_z\varphi\partial_{\bar{z}}\varphi\ . \tag{4.43}$$

The AdS/CFT correspondence relates bulk fields to boundary primary operators. We need to verify that the above proposed CFT operator is indeed a primary operator. This can be done, as outlined in Section 2.2, by evaluating its OPE with the energy stress tensor. The holomorphic energy stress tensor for the theory under consideration (4.39) is [27]

$$T(z) = -2\pi g : \partial_z\varphi(z)\partial_z\varphi(z) :\ , \tag{4.44}$$

so the OPE can be evaluated as

$$\begin{aligned} &T(z)\mathcal{O}(w, \bar{w}) = \\ &= -8\pi g : \partial_z\varphi(z)\partial_z\varphi(z) : \partial_w\varphi(w)\partial_{\bar{w}}\varphi(\bar{w}) \\ &= -8\pi g\,\{: \partial_z\varphi(z)\partial_z\varphi(z)\partial_w\varphi(w)\partial_{\bar{w}}\varphi(\bar{w}) : + 2 : \partial_z\varphi(z)\partial_w\varphi(w) : \partial_z\overbrace{\varphi(z)\partial_{\bar{w}}\varphi}(\bar{w}) \\ &+ 2 : \partial_z\varphi(z)\partial_{\bar{w}}\varphi(\bar{w}) : \partial_z\overbrace{\varphi(z)\partial_w\varphi}(w) + 2\partial_z\overbrace{\varphi(z)\partial_w\varphi}(w)\partial_z\overbrace{\varphi(z)\partial_{\bar{w}}\varphi}(\bar{w})\} + \text{non-singular} \\ &= \frac{\mathcal{O}(w, \bar{w})}{(z-w)^2} + \frac{\partial_w\mathcal{O}(w, \bar{w})}{z-w}\ . \end{aligned} \tag{4.45}$$

[26] Note, that this is not the only available choice for an operator with the desired scaling dimension. Since the scalar field is dimensionless, one could have also picked, for example, the more "meaningful" operator $\mathcal{O} = \partial^\mu(\varphi^{42})\partial_\mu(\varphi^{42})$. However, it not only will not provide the answer to "the ultimate question of life, the Universe, and everything" [65], but will also complicate the calculations unnecessarily.

In computing the above expression, we have used Wick's theorem, defined as

$$\varphi_i \dots \varphi_n = :\varphi_i \dots \varphi_n: + \text{all contractions} , \tag{4.46}$$

as well as

$$\overbrace{\varphi(z)\varphi(w)} = -\frac{1}{4\pi g}\ln(z-w) \tag{4.47}$$

$$\overbrace{\varphi(z)\varphi(\bar{w})} = 0 , \tag{4.48}$$

which arise from the correlation function (2.60) More details about these calculations can be found in [44]. One can similarly compute the OPE with the antiholomorphic energy stress tensor $\bar{T}(\bar{z})$ to obtain

$$\bar{T}(\bar{z})\mathcal{O}(w,\bar{w}) = \frac{\mathcal{O}(w,\bar{w})}{(\bar{z}-\bar{w})^2} + \frac{\partial_{\bar{w}}\mathcal{O}(w,\bar{w})}{\bar{z}-\bar{w}} . \tag{4.49}$$

Comparing to (**??**), we can confirm that $\mathcal{O}(z,\bar{z}) = 4\partial_z\varphi\partial_{\bar{z}}\varphi$ is indeed a conformal primary operator with $h=1$ and $\bar{h}=1$. Hence, the scaling dimension of the operator is indeed $\Delta = 2$, as expected.

Now, using the mode expansion (2.64), we can write an expression for the operator in (4.43) in terms of the right- and left-mover ladder operators

$$\mathcal{O}(z,\bar{z}) = -\frac{1}{\pi g}\sum_n\sum_m a_n\bar{a}_m z^{-n-1}\bar{z}^{-m-1} . \tag{4.50}$$

The state-operator map introduced in Section 2.2.3 can be used to find an expression for the CFT state at $z,\bar{z}=0$, which gives

$$\begin{aligned} |\mathcal{O}\rangle &= \lim_{z,\bar{z}\to 0}\mathcal{O}(z,\bar{z})|0\rangle_{\text{CFT}} \\ &= -\frac{1}{\pi g}a_{-1}\bar{a}_{-1}|0\rangle_{\text{CFT}} , \end{aligned} \tag{4.51}$$

where (2.54) was used in the last step. This state represents a pair of left- and right-moving boundary excitations.

So far, we have found an operator $\mathcal{O}$ in the CFT_2 theory, which is dual to the massless field in the AdS_3 bulk. We have also found the state, which this CFT_2 operator corresponds to. However, note that the state is defined at $z,\bar{z}\to 0$, which is equivalent to $\tau\to-\infty$, namely $|\mathcal{O}\rangle = |\mathcal{O}\rangle_{\tau=-\infty}$. The boundary conditions that we will choose to impose on the bulk field is that it gets annihilated at $\tau=0$, as illustrated in Figure 4.3. To find out what the CFT_2 state $|\mathcal{O}\rangle_{\tau=-\infty}$ is at $\tau=0$ and what vanishing of the bulk field implies for $\mathcal{O}$ operator, we need to first evaluate the state $|\mathcal{O}\rangle_{\tau=-\infty}$ at $\tau=0$. This requires time-evolving the state in (4.51) by using the CFT Hamiltonian $H=\partial_\tau$. In radial quantization, the time evolution is governed by the dilatation operator and states live on circles of constant radius [28]. Hence, in radial quantization, the Hamiltonian $H=\partial_\tau$ becomes

$$H = L_0 + \bar{L}_0 , \tag{4.52}$$

where $L_0 = z\partial_z$ and $\bar{L}_0 = \bar{z}\partial_{\bar{z}}$ are the scaling generators (2.45) in complex plane coordinates. They act on the vacuum state as $L_0|0\rangle_{\text{CFT}} = 0$ and $\bar{L}_0|0\rangle_{\text{CFT}} = 0$ and so $H|0\rangle_{\text{CFT}} = 0$ as expected. The Hamiltonian and the ladder operators share the following commutation relations:

$$\begin{aligned}[H, a_{-m}] &= m a_{-m} \ , \\ [H, \bar{a}_{-m}] &= m \bar{a}_{-m} \ . \end{aligned} \tag{4.53}$$

Using the above commutation relations with $m = 1$, the time-evolved CFT state can be evaluated as

$$\begin{aligned}|\mathcal{O}\rangle_{\tau=0} &= \mathrm{e}^{H\Delta\tau}|\mathcal{O}\rangle \\ &= -\frac{1}{\pi g}\mathrm{e}^{H\Delta\tau} a_{-1}\bar{a}_{-1}|0\rangle_{\text{CFT}} \\ &= -\frac{1}{\pi g}\sum_n \frac{1}{n!}(H\Delta\tau)^n a_{-1}\bar{a}_{-1}|0\rangle_{\text{CFT}} \\ &= -\frac{1}{\pi g}\sum_n \frac{1}{n!}(\Delta\tau)^n a_{-1}(H+1)^n\bar{a}_{-1}|0\rangle_{\text{CFT}} \\ &= -\frac{1}{\pi g}\sum_n \frac{2^n}{n!}(\Delta\tau)^n a_{-1}\bar{a}_{-1}|0\rangle_{\text{CFT}} \\ &= -\frac{1}{\pi g}\mathrm{e}^{2\Delta\tau} a_{-1}\bar{a}_{-1}|0\rangle_{\text{CFT}} \ , \end{aligned} \tag{4.54}$$

where $\Delta\tau$ is the amount of time with which we have time-evolved the state. To verify this, it can be seen that when $\Delta\tau = 0$, there is no time evolution of the state and one recovers (4.51). The normalization $g = 1/4\pi$ and Wick-rotating back to Lorentzian time,

$$|\mathcal{O}\rangle_{t=0} = -4\mathrm{e}^{2i\Delta t} a_{-1}\bar{a}_{-1}|0\rangle_{\text{CFT}}. \tag{4.55}$$

Now we have the full description in the bulk, namely the bulk field, its boundary value and the bulk state at the boundary at $t = 0$. We also have the full description in the CFT, namely the CFT operator dual to the bulk, and the CFT state at $t = 0$. These results can now be used, to show whether absorption into the holographic boundary is possible by checking what a field leaving the bulk means for its dual operator. This will be explored in the next section.

4.4.3 Conformal boundary "absorption"?

We should recall that the reason we are looking at whether this absorption mechanism is possible is because we are looking for a way to change the boundary conditions at the AdS boundary to allow large black holes to evaporate. This section will use results from the previous section to check if absorption into the holographic boundary is indeed possible.

We will consider a bulk mode that has been propagating in the bulk from $t = -\infty$ and vanishes once it reaches the conformal boundary at $t = 0$, where it gets absorbed. This requires a function that would annihilate all of the single-particle states at the boundary. We will call this function F and impose that

$$F|\phi\rangle_{\text{bdy}} \stackrel{!}{=} |0\rangle_{\text{Bulk}} \ . \tag{4.56}$$

To further simplify matters, we will focus only on the s-wave, hence the $\ell = 0$ mode, in which case $E_{n\ell} = 2(1+n)$, so

$$|\phi\rangle_{\text{bdy}} = \sum_{n=0}^{\infty}(-1)^n \frac{(2)_n}{n!} \mathrm{e}^{2i(1+n)t}\, b_n^\dagger\, |0\rangle_{\text{Bulk}}\ , \tag{4.57}$$

where we have used that the Jacobi polynomial can be written in terms of the Pochhammer's symbol, defined as $(x)_n := \Gamma(x+n)/\Gamma(x)$. In this case, the function that annihilates (4.57) is given by

$$F = \sum_{n=0}^{\infty}(-1)^n \frac{n!}{(2)_n} \mathrm{e}^{-2i(1+n)t}\, b_n\ , \tag{4.58}$$

because $[b_n, b_{n'}^\dagger] = \delta_{nn'}$. For the simple case of a single bulk particle in the ground state ($n = 0$), the above simplifies to

$$|\phi\rangle_{\text{bdy}} = \mathrm{e}^{2it}\, b_0^\dagger\, |0\rangle_{\text{Bulk}} \tag{4.59}$$

$$F = \mathrm{e}^{-2it}\, b_0\ , \tag{4.60}$$

and this is the case we will focus on for now. We have found the operator that annihilates the bulk field at the boundary at $\tau = 0$. What we wish to examine now is how this operator acts on its duel CFT state at $\tau = 0$, found in (4.55), which gives

$$F|\mathcal{O}\rangle_{\tau=0} = \mathrm{e}^{-2it}\, b_0\big(-4\mathrm{e}^{2i\Delta t} a_{-1}\bar{a}_{-1}|0\rangle_{\text{CFT}}\big). \tag{4.61}$$

The first time-evolution factor of e^{-2it} came from the time-evolution of the bulk field, which was propagating from $t = -\infty$ until it was annihilated at $t = 0$. The second time-evolution factor of $\mathrm{e}^{2i\Delta t}$ came from the time-evolution of the CFT state, which was also time-evolved from $t = -\infty$ to $t = 0$. Hence, the two exponentials cancel out and we obtain

$$F|\mathcal{O}\rangle_{\tau=0} = -4\, b_0\, a_{-1}\bar{a}_{-1}|0\rangle_{\text{CFT}}. \tag{4.62}$$

Since the boundary limit of the bulk field is identified as the CFT operator, according to the AdS/CFT dictionary, then the function F that annihilates the boundary value of the bulk field, must also annihilate its dual, and hence bring the CFT state at $\tau = 0$ to the vacuum CFT state; i.e. we need to impose that $F|\mathcal{O}\rangle_{\tau=0} \overset{!}{=} |0\rangle_{\text{CFT}}$. This is indeed satisfied if [27]

$$b_0^\dagger = -\frac{1}{4} a_{-1}\bar{a}_{-1}\ . \tag{4.63}$$

Hence, a bulk particle is dual to a left- and right-moving particle at the CFT boundary.[28] This agrees (up to a normalization) to a result by [63]. The result in (4.63) implies that any process, which leads to the annihilation of the bulk particle, would certainly lead to the annihilation of its dual CFT operator. Due to the direct proportionality between the bulk and boundary ladder operators, an absorption into the holographic boundary, which would imply bringing the bulk state to the bulk vacuum state (since the bulk field will no longer be in the

[27] One can easily verify this by substituting $a_{-1}\bar{a}_{-1} = -4b_0^\dagger$ into (4.62), which can be used to show that $b_0 b_0^\dagger|0\rangle_{\text{CFT}} = (b_0^\dagger b_0 + 1)|0\rangle_{\text{CFT}} = |0\rangle_{\text{CFT}}$.

[28] Recall from Section 2.2.4 that the operators a_{-1} and $\bar{a}_{-1}$ are not lowering operators, but raising operators.

bulk) would inevitable lead to the left- and right-moving excitations in the CFT also being brought to the CFT vacuum. Equivalently, higher excitations on the holographic boundary would correspond to a higher number of particle states in the bulk.

However, in the above computation, we picked the simplified case (4.59) of a single bulk particle in the ground state. This should also be applicable to the more generic case of (4.57). Using the AdS/CFT dictionary as before, for the function F in (4.58) to also bring the CFT state $|0\rangle_{\text{CFT}}$ to the CFT vacuum state, would require identifying

$$F = \sum_{n=0}^{\infty} (-1)^{-n} \frac{(2)_n}{n!} \mathrm{e}^{2i(1+n)t}\, b_n^\dagger = \frac{1}{4} a_{-1} \bar{a}_{-1} \,, \tag{4.64}$$

which can be seen as the superposition of single-particle states in the bulk being dual to a left- and right-moving particle at the CFT boundary.

In this section we saw that we cannot have a mechanism where the radiation gets absorbed from the AdS_3 bulk into the CFT_2 dual conformal boundary, since the two descriptions are dual to each other and the a field disappearing from the bulk will have its dual also disappear from the holographic boundary. It is precisely because of this dual description that one expect that this result can be generalized to the case of $\text{AdS}_{d+1}/\text{CFT}_d$ and show that the AdS_{d+1} radiation cannot be absorbed into the CFT_d boundary.

4.5 Conclusion

In this chapter we studied AdS black holes. We began by explaining why studying black holes in AdS is a great tool for resolving the Information paradox, namely due to the AdS/CFT correspondence which guarantees that black hole evaporation in AdS must be a unitary process, since its dual description is inherently unitary.

We then explained how large black holes in AdS, unlike black holes in an asymptotically flat spacetime, are thermodynamically stable. We explained how the usual AdS reflective boundary conditions do not allow these large AdS black holes to evaporate, since they reach a thermodynamic equilibrium before they have emitted all of their Hawking radiation. Although this is not an issue for small AdS black holes, which are thermodynamically unstable like the Schwarzschild black hole, these smaller black holes do not exist in smaller dimensions. The only way to resolve the issue with the evaporation of large AdS black holes without changing their size, is to change the boundary conditions at the holographic boundary to allow all the Hawking radiation to escape the bulk, way before the black holes falling into a thermodynamic equilibrium.

However, using results from Chapter 2, we showed that allowing the Hawking radiation to escape the bulk and be absorbed into the holographic CFT boundary is not possible, due to the AdS/CFT duality, since both descriptions are dual to each other, and any Hawking radiation leaving the bulk would result in its dual description on the holographic CFT boundary also disappearing.

However, recent work [18] has proposed that the radiation can be absorbed into an auxiliary CFT, namely a bath CFT system, described by CFT_{d+1} if we were to "attach" it to the AdS_{d+1} bulk and introduce the appropriate transparent boundary conditions. Describing this mechanism, and showing it allows black hole evaporation, will be the topic of the next chapter.

5

Coupling black holes to a bath

In the previous chapter we found that we cannot model absorption into the holographic boundary, since the AdS/CFT duality provides a description of the same physics, even though one is computed in the bulk, while the other one is computed on the holographic boundary. Hence, a field disappearing from the AdS bulk description will also disappear in its dual CFT description. Instead, there have been many other proposals for resolving the large black hole evaporation issue, based on changing the AdS boundary conditions, as well as coupling the bulk to an auxiliary system which can collect the Hawking radiation [66, 67, 68, 69].

In this chapter, we review one such recent model in the context of JT gravity [18], which proposes the attachment of an auxiliary bath to the AdS boundary, making one-sided black hole evaporation into the bath possible. In Section 5.1, we begin by reviewing some important aspects of JT gravity, including why one would use it, in the first place, to study black holes, and the black hole information paradox in particular. The semiclassical description of JT gravity, which incorporates effects from quantum matter and can be used to study Hawking radiation, is also reviewed. In Section 5.2, we show how coupling one side (of the double-sided black hole) to the bath achieves the evaporation protocol. The discussion in Chapter 3 on the generalized gravitational entanglement entropy is then used to explain how this proposed black hole evaporation model produces a unitary Page for both the evaporating black hole and the emitted Hawking radiation, hence leading to a possible resolution to the Information paradox. In Section 5.3, we look for a way to describe this one-sided black hole evaporation model in the dual theory, by using a toy-model for the boundary theory, namely working in the TFD formalism. We model the bath in the gravity theory as an operator in the dual theory, and we find such an operation which successfully reproduces all the expected results in the dual theory. However, this operation is shown to be non-unitary and we argue that a unitary bath operation may not be possible, at least with the way the bath is described to act on the bulk. As will be explained, this does not exclude the possibility for a global unitary bath operation, although the way that the bath is coupled to the bulk might have to be different. We also show that the one-sided evaporation can be modeled via an LOCC protocol, which uses the bath as a way to transfer classical information.

5.1 Review of JT Gravity

5.1.1 Why JT?

The issue with the non-renormalizability of (3+1)-dimensional Einstein's gravity has motivated the study of lower-dimensional gravity models. However, this still gives rise to some issues, including finding a suitable model to study. For example, the plain (1+1)-dimensional Einstein gravity action for some manifold $\mathcal{M}_2$ (in Euclidean signature) is given by

$$I[g] = -\frac{1}{16\pi G_N}\int_{\mathcal{M}_2} \mathrm{d}^d x\, \sqrt{g}R - \frac{1}{8\pi G_N}\int_{\partial\mathcal{M}_2} \mathrm{d}x\, \sqrt{h}\, K\,, \tag{5.1}$$

where the second term is the GHY boundary term, that needs to be added if the manifold has a boundary $\partial\mathcal{M}_2$.

When $d = 2$, this action is purely *topological*. There are several ways to see this. One way would be to see that when $d = 2$, the action $I[g] = \chi(\mathcal{M}_2)/4G_N$, where $\chi(\mathcal{M}_2)$ is the so-called *Euler characteristic*, which is a topological invariant and hence does not give rise to any dynamics. A way to see this is to consider the Einstein equations; i.e. $G_{\mu\nu} = R_{\mu\nu} - \frac{1}{2}g_{\mu\nu}R$, which for the case $d = 2$ become $R_{\mu\nu} = \frac{1}{2}g_{\mu\nu}R$ (due to general symmetries of the curvature tensor), so $G_{\mu\nu} = 0$ [70]. This is simply the vacuum solution. Furthermore, if the action is coupled to a matter action; i.e. $I = I[g] + I_{\mathrm{m}}$, one can compute the energy stress tensor via $T^{\mathrm{m}}_{\mu\nu} = -\frac{2}{\sqrt{g}}\frac{\delta I_m}{\delta g^{\mu\nu}}$. Since $T^{\mathrm{m}}_{\mu\nu} = G_{\mu\nu}/8\pi G_N$ and we established that symmetries lead to $G_{\mu\nu} = 0$, then $T_{\mu\nu} = 0$ [71]. The vanishing of the energy stress tensor implies there is no energy flow. Hence, this model cannot be used to study dynamical systems such as black hole formation or evaporation and will be of no obvious use when trying to resolve the information paradox.

Another motivation for the need of a different model is in the context of AdS/CFT. In the case of the $\mathcal{M}_2$ manifold being the AdS_2 spacetime, it can be described by its dual holographic CFT_1 theory, also known as *conformal quantum mechanics*. This is a (0+1)-dimensional theory, and since for any CFT_d, the stress energy tensor is traceless; i.e. $T^{\mu}_{\ \mu} = 0$, and the only component of the energy stress tensor in CFT_1 is $T^{t}_{\ t}$, then $T_{tt} = 0$. But this is precisely the Hamiltonian of the theory. Hence, the theory has zero energy and can describe only zero-energy states. To introduce dynamics into the picture, one can consider coupling the Ricci scalar R to a scalar field ϕ, known as the *dilaton*.

Another way to motivate the addition of this extra degree of freedom is to look at the number N_{dof} of gravitational degrees of freedom, which is given by $N_{\mathrm{dof}} = d(d-3)/2$ and hence becomes meaningless when $d = 2$, in which case $N_{\mathrm{dof}} = -1$. To bring more sense into this, we add another degree of freedom by introducing the dilaton field.
In what follows, we will follows closely the JT gravity review in [72].

A very general form of the $d = 2$ dilaton-gravity action takes the form

$$I[g,\phi] = -\frac{1}{16\pi G_N}\int_{\mathcal{M}_2} \mathrm{d}^2 x\, \sqrt{g}\,(\phi R + U(\phi)) + \dots\,, \tag{5.2}$$

where $U(\phi)$ is the dilaton potential. *Jackiw–Teitelboim* (JT) gravity, first introduced by Jackiw [73] and Teitelboim [74], refers to the special case where the dilaton potential takes the form $U(\phi) = -\Lambda\phi$, where Λ is the cosmological constant. Hence, the JT action is given by

$$I^{\Lambda}_{\mathrm{JT}}[g,\phi] = -\frac{1}{16\pi G_N}\int_{\mathcal{M}_2} \mathrm{d}^2 x\, \sqrt{g}\,\phi\,(R - \Lambda) + \dots\,, \tag{5.3}$$

where for a physical classical solution, we require that the effective Newton's constant $G_{\text{eff}}(x) = G_N/\phi(x) > 0$, since the gravitational constant should remain positive everywhere.

This dilaton-gravity model was later examined for AdS spacetimes by Almheiri and Polchinski [75], and is known as the *Almheiri-Polchinski* (AP) model. In the case of AdS spacetime, the cosmological constant $\Lambda = -2/\ell_{\text{AdS}}^2 < 0$. For convenience one can choose $\ell_{\text{AdS}} = 1$, in which case the action becomes

$$I_{\text{JT}}[g,\phi] = -\frac{1}{16\pi G_N}\int_{\mathcal{M}_2} \mathrm{d}^2x\,\sqrt{g}\,\phi\,(R+2) - \frac{1}{8\pi G_N}\int_{\partial\mathcal{M}_2}\mathrm{d}x\,\sqrt{h}\,\phi\,(K-1)\ , \tag{5.4}$$

where we have included the GHY term and the "-1" term is needed for the action to be well-defined at the boundary. It is important to also add the topological contribution, given by $I[g] = -\phi_0\chi(\mathcal{M}_2)/4G_N$ in (5.1), where ϕ_0 is a constant contribution to the dilaton, so the full action can be written as

$$\begin{aligned} I[g,\phi] = &-\frac{\phi_0}{16\pi G_N}\int_{\mathcal{M}_2}\mathrm{d}^2x\,\sqrt{g}\,R - \frac{\phi_0}{8\pi G_N}\int_{\partial\mathcal{M}_2}\mathrm{d}x\,\sqrt{h}\,K \\ &-\frac{1}{16\pi G_N}\int_{\mathcal{M}_2}\mathrm{d}^2x\,\sqrt{g}\,\phi\,(R+2) - \frac{1}{8\pi G_N}\int_{\partial\mathcal{M}_2}\mathrm{d}x\,\sqrt{h}\,\phi\,(K-1) + I_{\text{m}}[g]\ , \end{aligned} \tag{5.5}$$

where we have also included a matter action $I_{\text{m}}[g]$ if we want to couple JT gravity to matter, such that $I_{\text{m}}[g]$ couples only to the metric and not to the dilaton field. Note, adding the topological part of the action can be thought of as a result of shifting the dilaton field in (5.4) as $\phi(x) \to \phi_0 + \phi(x)$.

Of course, if the theory does not admit a black hole solution, it will be of no use. But as we will see soon from the equations of motion of (5.5), JT gravity indeed does have a black hole solution.

5.1.2 Equations of motion

The classical equations of motion for the metric and the dilaton field can be evaluated by varying the action (5.5). In what follows we will work in the Lorentzian signature. Setting $\delta I[g,\phi]/\delta\phi = 0$ imposes $R = -2$, which in $d = 2$ is sufficient to find that the metric is the AdS_2 metric, up to a coordinate transformation, which would correspond to just a different AdS patch.

To verify this, it is convenient to work in the *conformal gauge* (which can always be reached by an appropriate coordinate transformation) and write the metric in terms of some coordinates (x_+, x_-) as

$$\mathrm{d}s^2 = -\mathrm{e}^{2w(x_+,x_-)}\mathrm{d}x_+\mathrm{d}x_-\ , \tag{5.6}$$

where the Weyl factor $\mathrm{e}^{2w(x_+,x_-)}$ is still unspecified. Solving for the Ricci scalar of this metric yields

$$R = 8\mathrm{e}^{-2w}\partial_{x_+}\partial_{x_-}w\ . \tag{5.7}$$

Imposing $R = -2$ gives that $\mathrm{e}^{2w} = -4\partial_{x_+}\partial_{x_-}w$, which is just the *Liouville's* equation with a solution given by

$$\mathrm{e}^{2w(x_+,x_-)} = \frac{4}{(x_+ - x_-)^2} \,. \tag{5.8}$$

The coordinates $\{x_\pm\}$ are precisely the AdS_2 *lightcone* coordinates. One can arrive at the more familiar AdS_2 Poincaré patch coordinates (t, z) via $x_\pm = t \pm z$, which yields

$$\mathrm{d}s^2 = -\frac{4\mathrm{d}x_+\mathrm{d}x_-}{(x_+ - x_-)^2} = \frac{-\mathrm{d}t^2 + \mathrm{d}z^2}{z^2} \,. \tag{5.9}$$

The asymptotic boundary, where the holographic boundary dual theory lives, is timelike and located at $x_+ = x_- = t$, where t is the proper time in the boundary dual theory and will be referred to as the *boundary proper time*.
To study the dilaton dynamics requires varying the action with respect to the metric and setting $\delta I[g, \phi]/\delta g^{\mu\nu} = 0$, which yields the following equation of motion for the dilaton field

$$\nabla_\mu\nabla_\nu\phi - g_{\mu\nu}\nabla^2\phi + g_{\mu\nu}\phi = -8\pi G_N T_{\mu\nu} \,, \tag{5.10}$$

where $T_{\mu\nu}$ appears from varying the matter action with respect with the metric; i.e. $\delta I_\mathrm{m}/\delta g^{\mu\nu}$. Using that $\nabla^2\phi = (\sqrt{-g})^{-1}\partial_\mu\left(\sqrt{-g}g^{\mu\nu}\partial_\nu\phi\right)$, together with form of the conformal gauge in (5.6), and using (5.8)), then (5.10) can be written in terms of the lightcone coordinates (x_+, x_-) as [72, 69, 18]

$$8\pi G_N\, T_{x_+x_+} = -\mathrm{e}^{2w}\partial_{x_+}(\mathrm{e}^{-2w}\partial_{x_+}\phi) = -\frac{1}{(x_+ - x_-)^2}\partial_{x_+}\left((x_+ - x_-)^2\,\partial_{x_+}\phi\right) \tag{5.11}$$

$$8\pi G_N\, T_{x_-x_-} = -\mathrm{e}^{2w}\partial_{x_-}(\mathrm{e}^{-2w}\partial_{x_-}\phi) = -\frac{1}{(x_+ - x_-)^2}\partial_{x_-}\left((x_+ - x_-)^2\,\partial_{x_-}\phi\right) \tag{5.12}$$

$$16\pi G_N\, T_{x_+x_-} = 2\partial_{x_+}\partial_{x_-}\phi + \mathrm{e}^{2w}\phi = 2\partial_{x_+}\partial_{x_-}\phi + \frac{4}{(x_+ - x_-)^2}\phi \,. \tag{5.13}$$

However, (5.8) is not the only solution to the equation of motion for the metric. As mentioned before, in the $d = 2$ case, the constant curvature constraint $R = -2$ fixes the metric to be AdS_2, up to topology [76]. Hence, there are other coordinates $\{X_\pm\}$, which can be reached via an appropriate coordinate transformation $x_\pm \to X_\pm(x_\pm)$, in terms of which the metric can also be written in the usual 'Poincaré' form[29]. In fact, the most general solution to Liouville's equation is given by

$$\mathrm{e}^{2w(x_+,x_-)} = \frac{4\partial_{x_+}X_+(x_+)\partial_{x_-}X_-(x_-)}{[X_+(x_+) - X_-(x_-)]^2} \,, \tag{5.14}$$

where $X_+(x_+)$ and $X_-(x_-)$ are a set of chiral functions[30] of the respective lightcone coordinates, in terms of which the metric (5.6) can be written as

$$\mathrm{d}s^2 = -\frac{4\partial_{x_+}X_+(x_+)\partial_{x_-}X_-(x_-)}{[X_+(x_+) - X_-(x_-)]^2}\mathrm{d}x_+\mathrm{d}x_- = -\frac{4\mathrm{d}X_+(x_+)\mathrm{d}X_-(x_-)}{(X_+(x_+) - X_-(x_-))^2} \,. \tag{5.15}$$

[29]

[30]The chirality of these functions arises from requiring that the metric is asymptotically AdS_2, as will be seen later when discussing boundary dynamics.

Again, this can be written in the usual 'Poincaré' form, as illustrated in Figure 5.1, via $X_\pm = T \pm Z$

$$\mathrm{d}s^2 = \frac{-\mathrm{d}T^2 + \mathrm{d}Z^2}{Z^2} \,. \tag{5.16}$$

In these coordinates, the asymptotic boundary is at $X_+ = X_- = T$, but T, often referred to as the *Poincaré time* or the *dynamical boundary time*, should not be confused with the boundary proper time t.

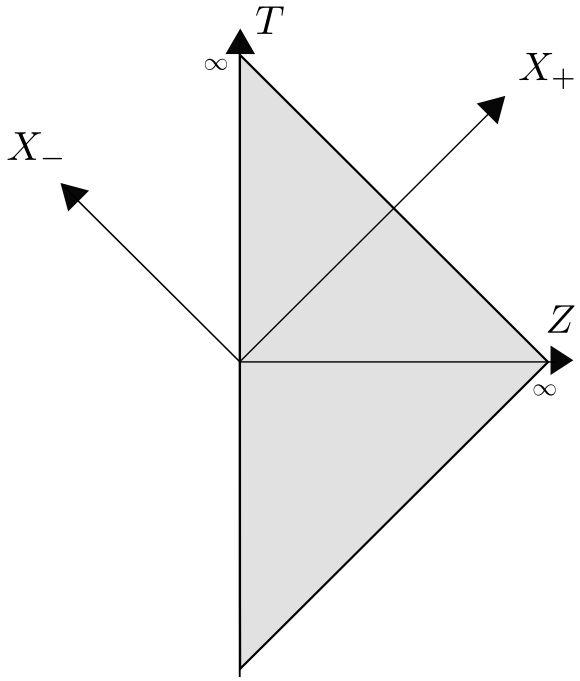

Figure 5.1: The Poincaré patch for AdS_2 and the lightcone coordinates $X_\pm$, adapted from [72].

An vital feature of JT gravity for the study of the information paradox is that it admits black hole solutions in the first place. Black holes can be dynamically formed by throwing in matter from the boundary. To see this, one needs to solve the dilaton equations of motion. A particular example is the vacuum solution, defined by $T_{\mu\nu} = 0$, in which case, $T_{X_+X_+} = T_{X_-X_-} = T_{X_+X_-} = 0$. The most general solution for the dilaton field is then given by [75]

$$\phi(x_+, x_-) = \frac{a + b(X_+ + X_-) + cX_+X_-}{X_+ - X_-} \,, \tag{5.17}$$

where a, b, c are integration constants. This is obtained by integrating (5.11) and (5.12) and imposing (5.13). The parameter b is not physically meaningful and can be set to zero by using the isometry of the AdS_2 metric, which can be used to rewrite the vacuum dilaton solution as [75]

$$\phi(x_+, x_-) = \frac{a - \mu X_+(x_+)X_-(x_-)}{X_+(x_+) - X_-(x_-)} \,. \tag{5.18}$$

Note that this solution diverges at the $X_+ = X_- = T$ boundary, as illustrated in Figure 5.2.

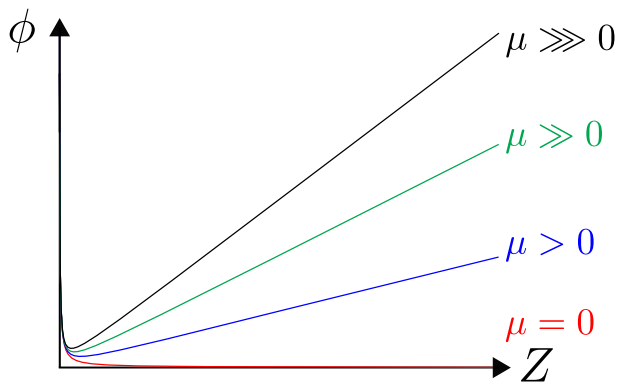

Figure 5.2: The dilaton profile is plotted for different values of μ at a constant $T = 0$ slice, showing that it diverges at the holographic boundary $Z = 0$.

One can also consider the dilaton solution with matter; i.e. $T_{\mu\nu} \neq 0$. For simplicity, we will consider the case of the matter being a CFT_2, in which case, $T_{X_+X_-} = 0$, because of the tracelessness condition for any CFT.[31] Taking into account that $T_{X_+X_+}$ and $T_{X_-X_-}$ are non-zero, and using the dilaton equations of motion (5.11-5.13), the dilaton solution is given by

$$\phi(x_+, x_-) = \frac{a - \mu X_+(x_+)X_-(x_-)}{X_+(x_+) - X_-(x_-)} - \frac{8\pi G_N}{X_+(x_+) - X_-(x_-)} (I_+ + I_-) \ , \tag{5.19}$$

where

$$I_+(x_+) = \int_{X_+}^{\infty} \mathrm{d}s \, (s - X_+)(s - X_-) T_{X_+X_+}(s) \tag{5.20}$$

$$I_-(x_-) = \int_{-\infty}^{X_-} \mathrm{d}s \, (s - X_+)(s - X_-) T_{X_-X_-}(s) \tag{5.21}$$

and $T_{x_\pm x_\pm} \mathrm{d}x_\pm^2 = T_{X_\pm X_\pm} \mathrm{d}X_\pm^2$. As revealed already, a black hole can be formed in JT gravity my throwing in matter from the boundary. To prove this, one can consider starting with the vacuum solution (5.18) and throwing an infalling energy pulse with $E > 0$ given by $T_{X_-X_-}(X_-) = E\delta(X_-)$ (and $T_{X_+X_+}(X_+) = 0$), which describes a pulse entirely along the $X_- = 0$ curve.

[31] Ignoring quantum anomaly contributions, $T^\mu_\mu = 0 = g^{\mu\nu} T_{\mu\nu} = 2g^{X_+X_-} T_{X_+X_-}$, so $T_{X_+X_-} = 0$.

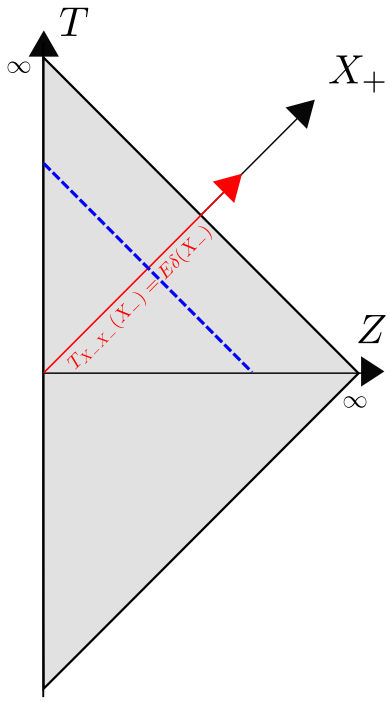

Figure 5.3: An inward positive-energy pulse (red) sent from the boundary, that can be used to create a black hole in the bulk. The black hole horizon of the newly formed black hole is shown in blue; Adapted from [72].

In this case, $I_+ = 0$ and $I_- = EX_+X_-\theta(X_-)$, so the dilaton solution in (5.19) becomes

$$\phi(x_+, x_-) = \frac{a - 8\pi G_N E X_+(x_+) X_-(x_-)\theta(X_-)}{X_+(x_+) - X_-(x_-)} \,, \tag{5.22}$$

where we have used the relationship between the delta function and the Heaviside step function $\theta(x) = \int_{-\infty}^{x} \mathrm{d}s\, \delta(s)$. Comparing this to the vacuum solution (5.18), one can identify the parameter $\mu = 8\pi G_N E$. This is the dilaton profile around a static black hole solution, formed as a response of an inward-falling matter pulse from the boundary, where the parameter μ is related to the mass of a black hole, which is identified as $M = E$.[75]. In particular, through the substitution

$$X_\pm(x_\pm) = \sqrt{\frac{a}{\mu}} \tanh\left(\sqrt{\frac{\mu}{a}} x_\pm\right) \tag{5.23}$$

the metric (5.15) can be written in the form

$$\mathrm{d}s^2 = -\frac{\mu}{a} \frac{4}{\sinh^2\left(\sqrt{\frac{\mu}{a}}(x_+ - x_-)\right)} \mathrm{d}x_+ \mathrm{d}x_- = \frac{4\mu}{a} \frac{-\mathrm{d}t^2 + \mathrm{d}z^2}{\sinh^2\left(\sqrt{\frac{\mu}{a}} 2z\right)} \,. \tag{5.24}$$

This is the so-called *black hole patch* (or *black hole exterior coordinates*) and the corresponding dilaton profile (5.22) becomes

$$\phi(x_+, x_-) = \sqrt{\mu a} \coth\left(\sqrt{\frac{\mu}{a}}(x_+ - x_-)\right) = \sqrt{\mu a} \coth\left(\sqrt{\frac{\mu}{a}} 2z\right) \,. \tag{5.25}$$

The black hole patch is contained within the Poincaré patch, as illustrated in Figure 5.3, as the black hole patch, as defined in (5.23), only cover the range $-\sqrt{\frac{a}{\mu}} < X_\pm < \sqrt{\frac{a}{\mu}}$. The black hole horizon in these coordinates is located at $z = \infty$.

One can further motivate that the metric (5.24) corresponds to a black hole solution via the further substitution $r = 2\sqrt{\mu/a}\coth\left(2\sqrt{\mu/a}z\right)$, in which case the metric can be written in the more familiar Schwarzschild-like form as

$$\mathrm{d}s^2 = -\left(r^2 - \frac{4\mu}{a}\right)\mathrm{d}t^2 + \left(r^2 - \frac{4\mu}{a}\right)^{-1}\mathrm{d}r^2 \,. \tag{5.26}$$

This solution has a horizon at $r = 2\sqrt{\mu/a}$.[32]The metric (5.24) and the dilaton solution (5.25) are both periodic in imaginary time with a period $\beta = \pi\sqrt{a/\mu}$. This can be used to find the Hawking temperature of the black hole via

$$T_0 = \beta^{-1} = \frac{1}{\pi}\sqrt{\frac{\mu}{a}} = \frac{1}{\pi}\sqrt{\frac{8\pi G_N E}{a}} \,, \tag{5.27}$$

which is the expected scaling with temperature of the energy of a near-extremal RN black hole [78]. As $E \to 0$, the Hawking temperature of the black hole $T_0 \to 0$ [79]. The presence of black hole solutions to the JT gravity action is what makes JT gravity a good contender to study the black hole information paradox.

5.1.3 Boundary dynamics

Due to the divergent behavior of the metric (and dilaton) at the holographic boundary, it is often convenient to express JT gravity in terms of the so-called 'boundary particle' dynamics, which is a reparameterization between the Poincaré coordinates near the boundary and the proper coordinates on the boundary. In particular, this simplifies to a reparameterization between the Poincaré time near the boundary T and the boundary proper time t. This is achieved via the appropriate boundary conditions and we demand that the spacetime is asymptotically AdS_2, such that in the limit $z \to 0$,

$$\mathrm{d}s^2 = \frac{-\mathrm{d}t^2 + \mathrm{d}z^2}{z^2} + \dots \,, \tag{5.28}$$

where $\{\dots\}$ represents terms subleading in the limit $z \to 0$. It can be shown that in order to preserve this asymptotic behavior, one needs to impose that at the boundary: (1) $\partial_{x_+} X_- = \partial_{x_-} X_+ = 0$, which leads to the chirality constraint and (2) $X_+(x_+, x_-) = X_-(x_+, x_-)$, which implies $X_+(x_+) = X_-(x_-)$.[72] Imposing that the holographic boundary $x_+ = x_- = t$ coincides with the AdS boundary $X_+(x_+) = X_-(x_-)$ implies that $X_+(t) = X_-(t) = T(t)$, where the Poincaré time (or the dynamical boundary time) $T(t)$ is a function of the boundary proper time t[69].

[32]This solution clearly resembles the BTZ black hole solution, with the exception that the BTZ black hole is a solution in a (2+1)-dimensional gravity theory. One can perform a dimensional reduction of a (2+1)-dimensional Einstein's gravity with a negative cosmological constant to obtain a solution similar to the (1+1)-dimensional JT gravity solution in (5.26), which is shown to correspond to the (t, r) section of the BTZ black hole; i.e. with the same causal structure [77].

However, the metric (5.28) diverges at the holographic boundary ($z = 0$) and needs to be regularized in order to extract the effective boundary dynamics. This is done by introducing a small distance $z = \frac{x_+ - x_-}{2} \approx \epsilon$ from the holographic boundary at $x_+ = x_- = t$, as illustrated in Figure 5.4 (left), and hence regularizing the boundary by moving it slightly inwards from $z = 0$ to $z = \epsilon$ via

$$\begin{aligned} x_+ &= t + z \to t + \epsilon \\ x_- &= t - z \to t - \epsilon \, . \end{aligned} \tag{5.29}$$

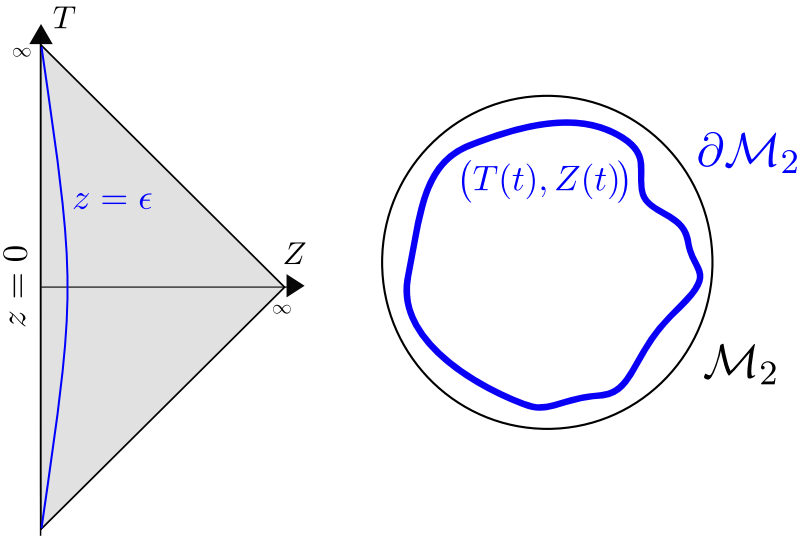

Figure 5.4: (left) The Poincaré patch with the location of cut-off surface. (right) Euclidean boundary disc with location of cut-off, where the holographic boundary $(T(t), Z(t))$ is parameterized in terms of the boundary time t adapted from [80].

The coordinates $X_\pm(x_\pm)$ on the new boundary; i.e. where $x_\pm = t \pm \epsilon$, can be translated into new (regularized) Poincaré time and radial coordinates (F, Z) via $X_\pm = F \pm Z$, such that

$$F(t) = \frac{1}{2}(X_+(t+\epsilon) + X_-(t-\epsilon)) = X_+(t) + \mathcal{O}(\epsilon^2) \approx X_+(t) \tag{5.30}$$

$$Z(t) = \frac{1}{2}(X_+(t+\epsilon) - X_-(t-\epsilon)) = \epsilon X'_+(t) + \mathcal{O}(\epsilon^2) = \epsilon F'(t) + \mathcal{O}(\epsilon^2) \approx \epsilon F'(t) \, . \tag{5.31}$$

The regularized boundary dynamics, illustrated in Figure 5.4 (right), is hence determined only in terms of the function $F(t)$ via the Poincaré coordinates $(T = F(t), Z = \epsilon F'(t))$, which are now parameterized in terms of the boundary proper time t, so the metric can be written as

$$\mathrm{d}s^2 = \frac{-\mathrm{d}T(t)^2 + \mathrm{d}Z(t)^2}{Z(t)^2} \, . \tag{5.32}$$

We saw that the function $T = F(t)$ is a diffeomorphism giving the bulk Poincaré time T near the boundary in terms of boundary proper time t. More generally, this diffeomorphism determines $X_\pm$ in terms of the lightcone coordinates $x_\pm$ via $X_+ = F(x_+)$ and $X_- = F(x_-)$,

and one can use this to rewrite the bulk AdS metric (5.15) as[33]

$$\mathrm{d}s^2 = -\frac{4F'(x_+)F'(x_-)}{(F(x_+)-F(x_-))^2}\mathrm{d}x_+\mathrm{d}x_- \tag{5.33}$$

where the cut-off is located at $\epsilon = \frac{x_+ - x_-}{2}$.

Using the 'boundary particle' description, one can compute the holographic energy-stress tensor [69], which in the (0+1)-dimensional case is just the total energy (ADM energy) in the spacetime. It can be written in terms of the reparameterization $F(t)$ using the Schwarzian derivative as

$$E = -\frac{a}{16\pi G_N}\{F(t), t\}\ , \tag{5.34}$$

where the Schwarzian derivative is defined as

$$\{F(t), t\} \equiv \frac{F'''}{F'} - \frac{3}{2}\left(\frac{F''}{F'}\right)^2\ . \tag{5.35}$$

Having defined the ADM energy of the spacetime, it is only natural to have to impose a conservation of the energy within some boundary. This can be written in terms of the net flux of energy moving across the holographic boundary in terms of the proper (dual theory) coordinates $\{x_\pm\}$, which yields the energy balance equation

$$\begin{aligned}\frac{\mathrm{d}E(t)}{\mathrm{d}t} &= \Big[T_{x_-x_-}(t) - T_{x_+x_+}(t)\Big]\Big|_{\partial\mathcal{M}_2} \\ &= \Big[\left(\frac{\mathrm{d}X_-(x_-)}{\mathrm{d}x_-}\right)^2 T_{X_-X_-}(t) - \left(\frac{\mathrm{d}X_+(x_+)}{\mathrm{d}x_+}\right)^2 T_{X_+X_+}(t)\Big]\Big|_{\partial\mathcal{M}_2} \\ &= F'(t)^2\Big[(T_{X_-X_-}(t) - T_{X_+X_+}(t))\Big]\Big|_{\partial\mathcal{M}_2}\ ,\end{aligned} \tag{5.36}$$

where we have used the reparameterization $X_\pm = F(x_\pm)$ to write the expression in terms of the energy stress tensor in the Poincaré patch coordinates $\{X_\pm\}$.

We have seen in this section that JT gravity admits black hole solutions and soon it will be used as a model to address the issue with the evaporation of large black holes in AdS, by adding an auxiliary system to absorb the radiation.

The energy conservation equation (5.36) will be used to calculate the change in energy as a result of Hawking radiation. However, since it is a quantum mechanical result, involving quantum matter, the classical JT gravity discussed so far is not sufficient to describe it. Hence, in what follows, we will review the semi-classical regime, where quantum effects of the CFT matter sector are taken into account, namely the trace anomaly of the stress-energy tensor.

5.1.4 Semi-classical regime

It has been shown that there exists a direct relationship between the conformal anomaly, which governs quantum effects in the CFT matter sector, and the appearance of Hawking radiation.

[33] We can see this from (5.30) and (5.31), since $T = F(t) = X_+$ implies that $X_+ = X_- = T$. This means that $\frac{\mathrm{d}F(t)}{\mathrm{d}t} = \frac{\mathrm{d}X_+}{\mathrm{d}t} = \frac{\mathrm{d}X_-}{\mathrm{d}t}$ and $\frac{\mathrm{d}F(t)}{\mathrm{d}z} = \frac{\mathrm{d}X_+}{\mathrm{d}z} = \frac{\mathrm{d}X_-}{\mathrm{d}z}$. Hence, $\frac{\mathrm{d}X_\pm}{\mathrm{d}x_\pm} = \frac{\mathrm{d}F(x_\pm)}{\mathrm{d}x_\pm}$, so $X_\pm = F(x_\pm)$.

The JT gravity discussed until now was purely classical, which was sufficient to study the classical equations of motion, governing the black hole solution and the dilaton dynamics. However, a crucial ingredient in the study of Hawking radiation is the effect of *backreaction*, namely the effect of quantum matter (such as Hawking radiation) on the classical geometry. The backreaction of the Hawking radiation on the geometry has an important implication on black hole thermodynamics, namely, it helps explain why the first law of black hole dynamics is identified as the first law of thermodynamics. The classical derivation works only after identifying a relation between the Hawking temperature and the extrinsic curvature of the event horizon, which raises the conceptual question of how Hawking radiation is aware of the event horizon geometry at all [81]. This is addressed in the semiclassical regime, which takes into account the effect of backreaction and helps understand why the temperature of the Hawking radiation is identified as the temperature of the black hole.

In this semiclassical regime, one considers quantum effects (such as the existence of Hawking radiation) to study quantum matter while still remaining in the classical gravity regime. For this to be plausible, the classical gravitational effects need to dominate the quantum effects of the quantum matter, which is a valid approximation for large black holes.[34]The semiclassical regime approximation is valid if the central charge of the CFT is $c \gg 1$, with $c \to$ in the classical limit [81].

Promoting the classical matter sources to be quantum mechanical has an effect on the energy stress tensor, namely $T_{\mu\nu} \to \langle T_{\mu\nu} \rangle$, so allowing for the backreaction, the net energy flow across the holographic boundary (5.36) becomes

$$\frac{\mathrm{d}E(t)}{\mathrm{d}t} = \langle T_{x_-x_-}(t) \rangle \big|_{\partial \mathcal{M}_2} - \langle T_{x_+x_+}(t) \rangle \big|_{\partial \mathcal{M}_2} \, . \tag{5.37}$$

The Einstein equations $G_{\mu\nu} = 8\pi G_N T_{\mu\nu}$ become $G_{\mu\nu} = 8\pi G_N \langle T_{\mu\nu} \rangle$. Using the conformal anomaly $\langle T^{\mu}{}_{\mu} \rangle = -{}^{cR}/_{24\pi}$, together with the conformal gauge Ricci scalar in (5.7), given by $R = 8\mathrm{e}^{-2w} \partial_{x_+} \partial_{x_-} w$, leads to

$$\langle T_{x_+x_-} \rangle = -\frac{c}{12\pi} \partial_{x_+} \partial_{x_-} w \, , \tag{5.38}$$

where we have used the conformal gauge where the only non-zero components of the metric are $g_{uv} = g_{vu} = -{}^{\mathrm{e}^{2w}}/_2$. To find the other components of the stress-energy tensor, one can use (5.38) and substitute it into the equations of motion (5.11-5.13). It has been shown [72, 75, 69] that imposing conservation of the energy-stress tensor; i.e. $\nabla_\mu T^{\mu\nu} = 0$, yields that its components acquire some additional contributions and take the form

$$\langle T_{x_+x_+} \rangle = -\frac{c}{12\pi} ((\partial_{x_+} w)^2 - \partial^2_{x_+} w) + \langle : T_{x_+x_+} : \rangle \tag{5.39}$$

$$\langle T_{x_-x_-} \rangle = -\frac{c}{12\pi} ((\partial_{x_-} w)^2 - \partial^2_{x_-} w) + \langle : T_{x_-x_-} : \rangle \tag{5.40}$$

where the additional contributions, namely $\langle T_{x_\pm x_\pm} \rangle$ are normal-ordered components, also often referred to as *operational*. Being normal-ordered means that these contributions are frame-dependent (i.e. measured by local observers), since the normal-ordering is always with respect to a certain vacuum, according to

$$: T_{x_+x_+} : = T_{x_+x_+} - \langle 0_{x_+} | T_{x_+x_+} | 0_{x_+} \rangle \tag{5.41}$$

$$: T_{x_-x_-} : = T_{x_-x_-} - \langle 0_{x_-} | T_{x_-x_-} | 0_{x_-} \rangle \, . \tag{5.42}$$

[34]To be more precise, this is valid as long as the black hole is not Planck-scale sized.

Due to the conformal anomaly, they transform between different frames $\{x_\pm\}$ and $\{X_\pm(x_\pm)\}$ according to

$$:T_{x_+x_+}: = \left(\frac{\mathrm{d}X_+}{\mathrm{d}x_+}\right)^2 :T_{X_+X_+}: -\frac{c}{24\pi}\{X_+, x_+\} \tag{5.43}$$

$$:T_{x_-x_-}: = \left(\frac{\mathrm{d}X_-}{\mathrm{d}x_-}\right)^2 :T_{X_-X_-}: -\frac{c}{24\pi}\{X_-, x_-\}\ . \tag{5.44}$$

From (5.33), one can write the conformal factor in terms of the reparameterization $X_\pm = F(x_\pm)$ as

$$\mathrm{e}^{2w(x_+,x_-)} = -4\frac{\mathrm{d}F(x_+)}{\mathrm{d}x_+}\frac{\mathrm{d}F(x_-)}{\mathrm{d}x_-}\frac{1}{(F(x_+)-F(x_-))^2}\ , \tag{5.45}$$

which when differentiated with respect to the holographic boundary coordinates $x_\pm$ yields

$$\begin{aligned}(\partial_{x_+}w)^2 - \partial_{x_+}^2 w &= -\frac{1}{2}\{F(x_+), x_+\}\\ (\partial_{x_-}w)^2 - \partial_{x_-}^2 w &= -\frac{1}{2}\{F(x_-), x_-\}\ .\end{aligned} \tag{5.46}$$

The reason this is important is that when evaluated at the boundary, where $x_+ = x_- = t$, these expressions become equal, so substituting them into (5.39) and (5.40) gives

$$\begin{aligned}\langle T_{x_-x_-}(t)\rangle\big|_{\partial\mathcal{M}_2} &= \frac{c}{24\pi}\{F(t), t\} + \langle :T_{x_-x_-}(t):\rangle\big|_{\partial\mathcal{M}_2}\\ \langle T_{x_+x_+}(t)\rangle\big|_{\partial\mathcal{M}_2} &= \frac{c}{24\pi}\{F(t), t\} + \langle :T_{x_+x_+}(t):\rangle\big|_{\partial\mathcal{M}_2}\ ,\end{aligned} \tag{5.47}$$

which shows that the energy conservation equation (5.37), when evaluated at the boundary, can be written purely in terms of the normal-ordered contributions, such that

$$\frac{\mathrm{d}E(t)}{\mathrm{d}t} = \langle T_{x_-x_-}(t)\rangle\big|_{\partial\mathcal{M}_2} - \langle T_{x_+x_+}(t)\rangle\big|_{\partial\mathcal{M}_2} = \langle :T_{x_-x_-}(t):\rangle\big|_{\partial\mathcal{M}_2} - \langle :T_{x_+x_+}(t):\rangle\big|_{\partial\mathcal{M}_2}\ . \tag{5.48}$$

This energy conservation equation provides an expression for the energy flow across the holographic boundary (as seen from the first equality), which is equivalent to the energy conservation measured locally, by a local observer, at the holographic boundary (as seen from the second equality). Together with the expression for the ADM energy in terms of the boundary reparameterization, defined in (5.34), these will be the key results in the computation of black hole evaporation. This will be seen in the next section, where the black hole is coupled to an auxiliary bath.

5.2 Coupling the black hole to a bath

5.2.1 Setup

In this section we review the model proposed in [18] which allows large black holes in AdS to evaporate. We will show how this is computed for one-sided black hole evaporation by

coupling the right black hole exterior to an auxiliary bath which is allowed to absorb the Hawking radiation.

The model is that of a 2-dimensional JT gravity coupled to 2-dimensional CFT; i.e. gravity coupled to matter in the special case (chosen for simplicity) where the matter is a CFT. The action describing the theory is given by

$$I = I_{\rm JT}[g,\phi] + I_{\rm CFT}[g]\,, \tag{5.49}$$

where $I_{\rm CFT}[g]$ is a general CFT which couples directly to the metric, but not to the dilaton.[35] This is equivalent to the action we considered in (**??**), with the additional constraint that the matter sector is a conformal field theory, as discussed in the example in the previous section. The JT gravity action is given by (5.5) and in the Euclidean signature,

$$\begin{aligned} I_{\rm JT}[g,\varphi] = &-\frac{\phi_0}{8\pi G_N}\left[\frac{1}{2}\int_{\mathcal{M}_2} \mathrm{d}^2x\,\sqrt{-g}\,R + \int_{\partial\mathcal{M}_2}\mathrm{d}x\,\sqrt{-h}\,K\right] \\ &-\frac{1}{8\pi G_N}\left[\frac{1}{2}\int_{\mathcal{M}_2}\mathrm{d}^2x\,\sqrt{-g}\,\phi(R+2) + \phi_b\int_{\partial\mathcal{M}_2}\mathrm{d}x\,\sqrt{-h}\,(K-1)\right]\,, \end{aligned} \tag{5.50}$$

where, as before, $\varphi = \phi_0 + \phi$ is the dilaton, which has a constant contribution of ϕ_0 and a dynamical contribution ϕ. The dilaton has a boundary value of $\varphi_b = \phi_0 + \phi_b$, where ϕ_b is the boundary limit of ϕ and assuming it is constant, it has been written outside of the integral above. Again, the first bracket in (5.50) is purely topological and equal to $2\pi\chi(\mathcal{M}_2)$, where $\chi(\mathcal{M}_2) = 2-2g-b$ is the Euler characteristic of $\mathcal{M}_2$, which depends on the genus g and the number of boundaries b. Hence, φ_0 controls the topological expansion of the theory. It is in the second bracket of (5.50) where all the dynamics ocurs.

As we saw in the previous section, the AdS_2 boundary is located at $X_+ = X_- = T$ (or $Z = 0$) and both the metric (5.15) and the dilaton (5.19) diverge at the boundary. Hence, boundary conditions need to be specified in order to regulate these divergences.

Metric: A boundary condition is imposed on the metric requiring that it is asymptotically AdS_2; i.e. approaching the boundary at $Z = 0$,

$$\mathrm{d}s^2 = \frac{-\mathrm{d}T^2 + \mathrm{d}Z^2}{Z^2} \tag{5.51}$$

However, as discussed in the previous section, in order to regulate the divergence at $Z = 0$, one can cut the geometry along some boundary curve $(T(t), Z(t))$, parameterized in terms of the boundary proper time t via $T = F(t)$, which is diffeomorphism giving Poincaré time T in terms of boundary proper time t.[36] The metric (5.51)) can then be written in terms of the proper boundary time as

$$\mathrm{d}s^2 = \frac{-\mathrm{d}T(t)^2 + \mathrm{d}Z(t)^2}{Z(t)^2} = \left(-\frac{\mathrm{d}T(t)^2}{\mathrm{d}t^2} + \frac{\mathrm{d}Z(t)^2}{\mathrm{d}t^2}\right)\frac{\mathrm{d}t^2}{Z(t^2)} = \frac{-T'(t)+Z'(t)}{Z(t)}\mathrm{d}t^2 \tag{5.52}$$

[35] Note that $I_{\rm CFT}[g]$ is a general CFT_2 in the AdS_2 bulk (i.e. with the same dimensionality as the bulk) and it should not be confused with the boundary dual theory, which is a CFT_1 (i.e. with one less dimension compared to the bulk). Also, the action (5.50) is a bulk gravitational action and has boundary terms because the manifold has a boundary. These boundary terms should also not be confused with the holographic dual CFT_1 description living on the boundary.

[36] To compare notation with [75], their (x_+, x_-) correspond to the (X_+, X_-), their (y_+, y_-) correspond to the (x_+, x_-) and their $t = f(u)$ corresponds to $T = F(t)$ here.

Using the boundary conditions discussed in the previous section, namely $Z(t) = \epsilon T'(t)$, where ϵ is a cut-off distance from the boundary, the induced metric on the boundary satisfies the following cut-off condition

$$\mathrm{d}s^2\big|_{\partial\mathcal{M}_2} = \left(-\frac{1}{\epsilon^2} + \mathcal{O}(\epsilon^0)\right)\mathrm{d}t^2 \approx -\frac{\mathrm{d}t^2}{\epsilon^2}\ , \tag{5.53}$$

and the only component of the metric is

$$g\big|_{\partial\mathcal{M}_2} = g_{tt}\big|_{\partial\mathcal{M}_2} \sim -\frac{1}{\epsilon^2}\ , \tag{5.54}$$

which is the time-time component of the metric near the boundary along the physical boundary time t.

Dilaton: The dilaton solution blows up at the boundary, as seen in (5.19). To regulate this divergence, a boundary condition is imposed on the dilaton, such that

$$\phi\Big|_{\partial\mathcal{M}_2} = \phi_b \sim \frac{a}{2\epsilon} = \frac{\bar{\phi}_r}{\epsilon}\ , \tag{5.55}$$

where $\bar{\phi}_r$ is the renormalized value of the dilaton. From this boundary condition, it can be seen that the model considers the case of a large dilaton value at the boundary.

These are the standard Dirichlet-Dirichlet boundary conditions, where the dilaton and the boundary metric are fixed (and when the cosmological constant in JT gravity is set to be negative). However, this is not the only possible choice of boundary conditions and the different choices are classified in [82].

One can use this renormalized dilaton value to rewrite the dilaton profile (5.22) as

$$\phi = \frac{2\bar{\phi}_r}{X_+ - X_-}\left(1 - \frac{4\pi G_N E}{\bar{\phi}_r}X_+X_-\right)\ , \tag{5.56}$$

which we saw is the dilaton profile for the black hole solution. Using the result for the black hole energy in (5.27), the dilaton solution (5.56) can be written as [18]

$$\phi = 2\bar{\phi}_r\frac{1 - (\pi T_0)^2 X_+X_-}{X_+ - X_-}\ . \tag{5.57}$$

In the previous section, the temperature of the black hole was found from the periodicity of the metric, in terms of its energy (mass), which came from the parameter μ in the vacuum dilaton solution. This result is closely intertwined with the ADM energy of the spacetime, which was simply stated in 5.34, but can be easily verified for this case. The ADM energy can be written in terms of the renormalized dilaton such that

$$E = -\frac{\bar{\phi}_r}{8\pi G_N}\{F(t), t\}\ . \tag{5.58}$$

One can check that using the black hole exterior coordinates in (5.23) and substituting the periodicity of the black hole solution obtained in (5.27), the static black hole reparameterization can be written as $F(t) = {}^1\!/_{\pi T_0}\tanh(\pi T_0 t)$. Using the renormalized value of the dilaton

($a = 2\bar{\phi}_r$), this can be used to find that the energy (or mass) of the black hole (i.e. the energy of the pulse used to create it), is related to the black hole temperature T_0 via

$$E = -\frac{\bar{\phi}_r}{8\pi G_N}\left\{\frac{1}{\pi T_0}\tanh\left(\pi T_0 t\right), t\right\} = \frac{\pi\bar{\phi}_r T_0^2}{4G_N} =: E_0 \ , \tag{5.59}$$

where we have defined E_0 to be the energy of the eternal black hole solution of temperature T_0. This result recovers the black hole energy-temperature result (5.27) from the previous section. [37] Note, the reason this black hole solution is called *static* is precisely because its energy is constant (since E_0 is not time-dependent), and hence, it does not evaporate. Even though the Schwarzian derivative parameters are time-dependent, the Schwarzian derivative itself is not; i.e. $\partial_t\{F(t), t\} = \partial_t(-2\pi^2 T_0^2) = 0$.[38]

As seen before, with this reparameterization one can write the metric and dilaton in terms of the black hole exterior coordinates as done in (5.24) and (5.25) respectively. Using the renormalized value of the dilaton and the black hole energy-temperature relation, these can be written as

$$\mathrm{d}s^2 = -\frac{4\pi^2 T_0^2}{\sinh^2\left(\pi T_0(x_+ - x_-)\right)}\mathrm{d}x_+\mathrm{d}x_- = 4\pi^2 T_0^2\frac{-\mathrm{d}t^2 + \mathrm{d}z^2}{\sinh^2\left(2\pi T_0 z\right)} \tag{5.60}$$

$$\phi = 2\pi T_0\bar{\phi}_r\coth\left(\pi T_0(x_+ - x_-)\right) = 2\pi T_0\bar{\phi}_r\coth\left(2\pi T_0 z\right) \ , \tag{5.61}$$

where the coordinates $x_\pm$ cover the exterior of the black hole. This black hole has two exterior regions, namely the right exterior region and the left exterior region, as illustrated in Figure 5.6.

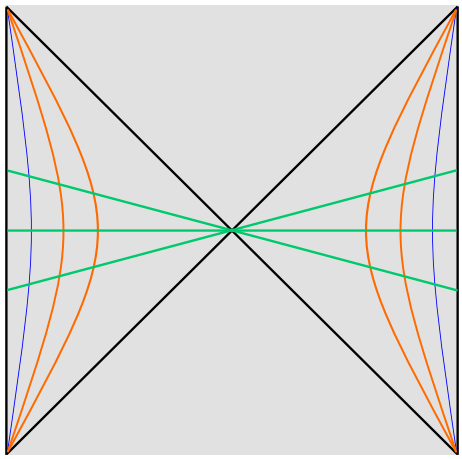

Figure 5.5: Double-sided black hole with locations of horizons (black), cut-offs (blue), constant t-lines (green) and constant z-lines (i.e. constant dilaton lines) (orange).

Figure 5.5 shows the locations of the cut-offs, but most importantly, the constant time slices, which show that time moving up in the right exterior, moves down in the left exterior.

[37] This result will be important later for computing the thermal entropy within the system.

[38] The reason for paying special attention to this is because it will be important when looking at the no-static black hole case, namely the evaporating black hole solution. In that case, the energy becomes time-dependent and has a time-dependent Schwarzian derivative; i.e. $\partial_t\{F(t), t\} \neq 0$, because the reparameterization, also commonly refered to as the *gluing function*, is different.

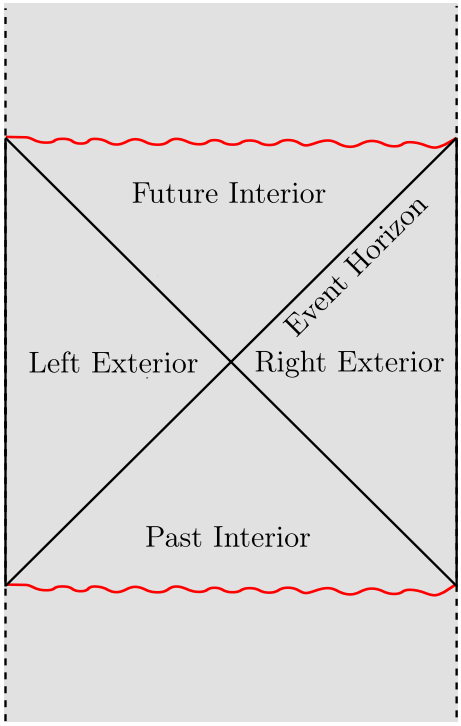

Figure 5.6: The AdS black hole has two exterior regions, called the right exterior region and the left exterior region.

In this thesis, the focus is on the one-sided black hole evaporation. In particular, we will be focusing only on the evaporation of the right black hole exterior, by coupling the bath to the boundary of the right exterior region. However, since the model we will be discussing imposes energy conservation by transferring the emitted Hawking radiation back into the bulk and the left black hole exterior region, we really need to have transparent boundary conditions along both the right and left holographic boundaries.

5.2.2 Eternal black hole in a bath

Since AdS spacetime acts as a box which reflects back the emitted Hawking radiation, coupling it to an external auxiliary system which can collect the Hawking radiation is analogous to removing this box and hence allowing the Hawking radiation to escape. The way this has been achieved in [75] is by coupling the right-ride R of the (one-sided) eternal black hole to a so-called bath B. The bath is chosen to be a CFT_2 theory, analogous to the matter CFT_2 in the bulk [39], with the exception that the bath is chosen to live in a flat spacetime.

[39] The bath CFT_2 should not be confused with the the AdS_2 dual theory, which is a CFT_1 living on the boundary.

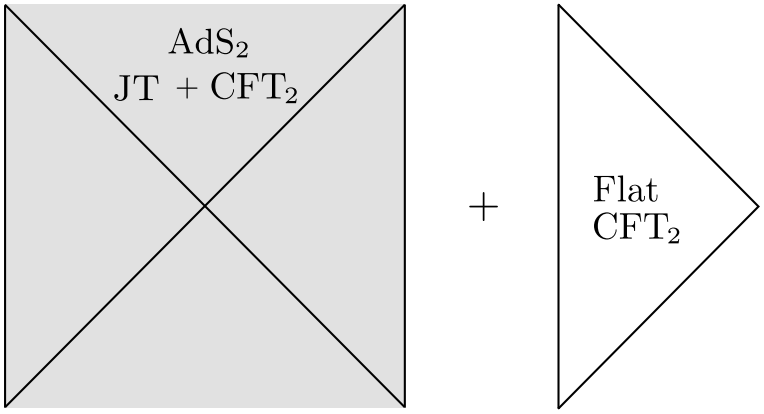

Figure 5.7: Coupling the right exterior of the eternal black hole to an auxiliary flat bath system, with tha same CFT theory as the CFT theory in the bulk region.

The bulk is still described by the AdS_2 metric

$$ds^2_{\text{Bulk}} = \frac{-dT^2 + dZ^2}{Z^2} = \frac{-4dX_+dX_-}{(X_+ - X_-)^2} , \tag{5.62}$$

which we saw, with the appropriate reparameterization $X_\pm = F(x_\pm)$, namely $F(t) = {}^1/_{\pi T_0} \tanh(\pi T_0 t)$, can be written in terms of the black hole exterior coordinates as

$$ds^2_{\text{Bulk}} = 4\pi^2 T_0^2 \frac{-dt^2 + dz^2}{\sinh^2(2\pi T_0 z)} = -4\pi^2 T_0^2 \frac{dx_+dx_-}{\sinh^2(2\pi T_0 z)} . \tag{5.63}$$

The reason for bringing up the black hole exterior coordinates is that these coordinates cover only the region outside the black hole and, importantly, extend naturally to the coordinates in the flat bath spacetime, which is described by

$$ds^2_{\text{Bath}} = \frac{-dt^2 + dz^2}{\epsilon^2} = -\frac{dx_+dx_-}{\epsilon^2} . \tag{5.64}$$

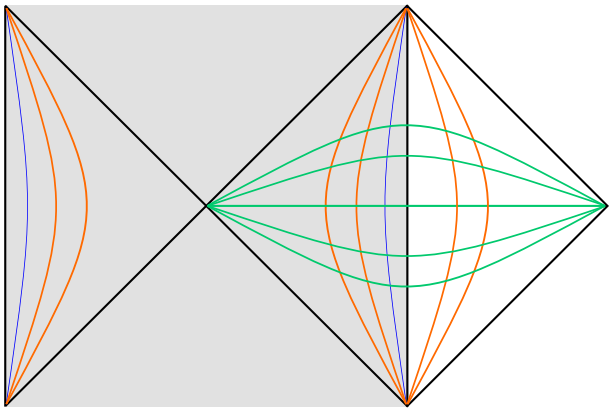

Figure 5.8: Constant t-lines (green) and constant z-lines (i.e. constant dilaton lines) (orange) get naturally extended into the bath spacetime, since the black hole exterior coordinates are extended into the bath spacetime.

So far the black hole solution discussed represented a static black hole solution (up to a reparameterization), solved by a constant Schwarzian $\{F(t), t\} = -2\pi^2 T_0^2$ as seen from (5.59).

Coupling this near-extremal black hole to the auxiliary bath, successfully incorporates evaporation into the model, due to an important consequence of the coupling, namely the subsequent injection of positive energy into the black hole, as shown in Figure. 6.13. This positive energy shockwave is required in order to prevent the wormhole connecting the two black holes from becoming traversable, as demanded by general relativity. The initial shockwave is also required for considerations of causality. In the absence of the positive energy impulse, it would be possible for something that was initially behind the horizon to escape to infinity once the black hole is coupled to the bath. The inward shockwave causes a change in the location of the event horizon, which resolves this issue. Adding the positive-energy shockwave means that the black hole is no longer static and does allow evaporation. Quantifying this process will be the central theme of the rest of this section, which will rely greatly on the concepts discussed in section 6.1.4.

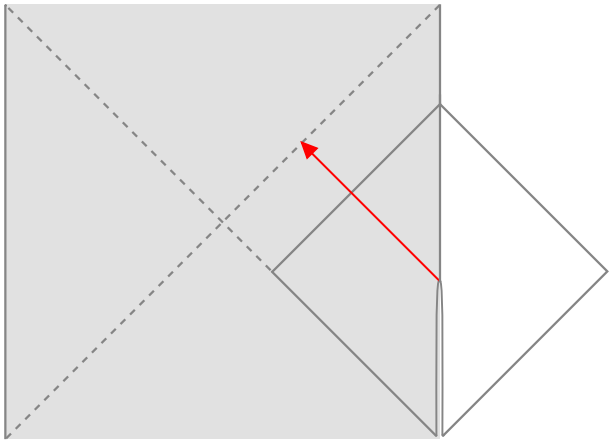

Figure 5.9: The black hole with coupling at $t = 0$ and inward shock and change in the location of the horizon from its initial location (dotted line) to its final location (solid line). Note that at this point we have not yet imposed transparent boundary conditions, so the AdS_2 boundary is still reflective.

It should be noted that black hole evaporation in JT was already studied way before the proposal of implementing absorption of the Hawking radiation via the auxiliary bath, from simply assuming the injection of the positive-energy pulse and some (unspecified) absorption mechanism at the boundary [69]. This is the approach that will be used here too. Along the way, we will also compare the results to those where the absorption was achieved specifically via the bath, hence also deriving the evaporation result in [18].

For completeness, we will further assume that the initial state (before the pulse) was just the Poincaré patch vacuum (extremal black hole) solution. The addition of the shockwave contributes to the energy conservation equation (5.37), namely [83]

$$\frac{\mathrm{d}E(t)}{\mathrm{d}t} = E_S\delta(t) + \langle T_{x_-x_-}(t)\rangle\big|_{\partial\mathcal{M}_2} - \langle T_{x_+x_+}(t)\rangle\big|_{\partial\mathcal{M}_2} \,, \tag{5.65}$$

where E_S denotes the energy of the shock, which goes inwards from the holographic boundary. The same example was depicted in Figure. 6.3, where the inward-falling pulse was used to create the black hole solution. We will split the derivation into 3 parts, starting from the solution before the pulse, and then moving on to study the solution after the pulse, both with and without reflecting boundary conditions.

$\boldsymbol{t < 0}$: Before the pulse, the solution is a vacuum solution describing an extremal black hole. Since extremal black holes have a temperature of absolute zero, meaning that they emit no Hawking radiation and remain stable, nothing goes in or out of the holographic boundary. Hence, $\langle T_{x_+x_+}(t)\rangle\big|_{\partial\mathcal{M}_2} = \langle T_{x_-x_-}(t)\rangle\big|_{\partial\mathcal{M}_2} = 0$, and using (5.65) gives $\mathrm{d}E/\mathrm{d}t = \langle T_{x_-x_-}(t)\rangle\big|_{\partial\mathcal{M}_2} - \langle T_{x_+x_+}(t)\rangle\big|_{\partial\mathcal{M}_2} = 0$, as expected. Using (5.34), this can also be written as $\partial_t\{F(t),t\} = 0$. Furthermore, a local observer at the holographic boundary of the static black hole solution would simply measure the Poincaré vacuum, so the normal-ordered components of the energy-stress tensor vanish as well, such that $\langle : T_{x_+x_+}(t) : \rangle\big|_{\partial\mathcal{M}_2} = \langle : T_{x_-x_-}(t) : \rangle\big|_{\partial\mathcal{M}_2} = 0$. Hence, using the result from (5.47), further implies that $\{F(t),t\} = 0$. The equations that are left to solve are therefore

$$\{F(t),t\} = 0 \qquad \text{and} \qquad \partial_t\{F(t),t\} = 0\,, \tag{5.66}$$

which are solved by $F(t) = t$.

The inward positive-energy pulse causes the extremal black hole solution to become a non-extremal solution. These black holes do not have an absolute zero temperature and do emit Hawking radiation. However, simply allowing the black hole to emit Hawking radiation is not sufficient to allow the black hole to actually evaporate, since the boundary conditions at the holographic boundary also need to be changed. In what follows, we will focus on the more trivial case and we assume the boundary is still reflective, so all radiation bounces off the boundary and falls back into the black hole. In this case, the black hole eventually reaches a thermal equilibrium with its surroundings. This case is equivalent to coupling the black hole to a bath, such that the black hole and bath are at the same temperature, and hence in a thermodynamic equilibrium [84]. Although it may seem obvious, from the point of thermodynamics, that this will not lead to actual evaporation, we will now show this more rigorously.

It should be noted that even though it does not actually evaporate (due to the Hawking radiation reflecting off the boundary back into the black hole), the non-extremal black hole in thermal equilibrium keeps emitting Hawking quanta, though with no net evaporation, since Hawking radiation keeps moving back and forth between the black hole and the AdS boundary (or equivalently, between the black hole and the (bath).

$\boldsymbol{t > 0}$ **+ Reflective boundary conditions** : After the pulse has been sent, the matter is still described by the Poincaré vacuum and since nothing else is being sent in or out of the spacetime, $\langle T_{x_+x_+}(t)\rangle\big|_{\partial\mathcal{M}_2} = \langle T_{x_-x_-}(t)\rangle\big|_{\partial\mathcal{M}_2} = 0$. The net energy $E \propto \{F(t),t\}$ in the bulk spacetime will keep being constant; i.e. $\partial_t\{F(t),t\} = 0$, but due to the additional energy of the pulse, the total energy in the spacetime is now E_S. Therefore, to find the new reparametrization, one needs to solve

$$\{F(t),t\} \propto E_S \qquad \text{and} \qquad \partial_t\{F(t),t\} = 0\,, \tag{5.67}$$

which gives a reparameterization, which is the same as that of the static black hole solution discussed in (5.59). That is because, just like this black hole, the black hole discussed in (5.59) was precisely one formed from sending an inward pulse of energy from the boundary.

Since the holographic boundary has reflecting boundary conditions, all the incoming energy that a local observer would measure at the boundary will be balanced by the energy that they would measure to be going backwards into the black hole after being reflected at the boundary. Hence, the local observer would still not measure any influx of energy; i.e. $\langle : T_{x_+x_+}(t) : \rangle\big|_{\partial\mathcal{M}_2} =$

$\langle : T_{x_-x_-}(t) : \rangle\big|_{\partial\mathcal{M}_2}$. However, the observer would no longer measure a vacuum at the boundary; i.e. $\langle : T_{x_\pm x_\pm}(t) : \rangle\big|_{\partial\mathcal{M}_2} \neq 0$, since the black hole is no longer extremal and does emit Hawking radiation. In fact, due to $\langle T_{x_+x_+}(t)\rangle\big|_{\partial\mathcal{M}_2} = \langle T_{x_-x_-}(t)\rangle\big|_{\partial\mathcal{M}_2} = 0$, their measurement will be governed by the conformal anomaly, according to (5.47), which yields

$$\langle : T_{x_+x_+}(t) : \rangle\big|_{\partial\mathcal{M}_2} = \langle : T_{x_-x_-}(t) : \rangle\big|_{\partial\mathcal{M}_2} = -\frac{c}{24\pi}\{F(t), t\} \tag{5.68}$$

As viewed from the black hole, i.e. using the black hole frame reparameterization (5.23), this gives

$$\langle : T_{x_+x_+}(t) : \rangle\big|_{\partial\mathcal{M}_2} = \langle : T_{x_-x_-}(t) : \rangle\big|_{\partial\mathcal{M}_2} = \frac{c\pi}{12\beta^2} \ . \tag{5.69}$$

This is known as the *Unruh heat bath*.[40]To emphasize again, even though the black hole is emitting Hawking radiation, it is not evaporating because of the reflective boundary conditions. To make the black hole actually evaporate would require introducing transparent boundary conditions for the Hawking radiation.

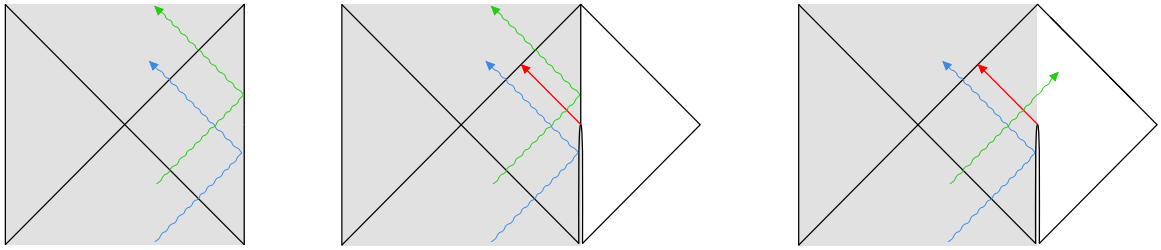

Figure 5.10: (left) The static two-sided black hole with reflective boundary conditions; (center) coupling the one-sided black hole to a bath with reflective boundary conditions; (right) coupling the one-sided black hole to a bath with transparent boundary conditions.

5.2.3 Evaporating black hole in a bath

To have an evaporating solution requires a mechanism that takes away the Hawking radiation. Removing the reflecting boundary conditions, and imposing absorbing boundary conditions for the matter fields, allows the black hole to evaporate. The case we are interested in the one where the absorption is achieved via the coupling to an auxiliary bath, again accompanied with an inward flux of energy. Before deriving the evaporation, which is almost identical to the one derived above, we should explain what these absorbing (or equivalently transparent) boundary conditions really mean for the black hole-bath system.

The transparent boundary conditions are imposed at the boundary between the right exterior region of the black hole and the flat bath. Since the bulk solution considered is a black hole solution, and hence a vacuum solution, the stress-energy tensor in the right exterior region vanishes; i.e. $\langle T_{x_\pm x_\pm}\rangle_{\mathrm{AdS}_2} = 0$. To model absorption by the bath requires imposing transparent

[40]This result is equivalent to the result in [84], where an eternal black hole was coupled to a bath of the same temperature, and radiation was allowed to flow between the black hole and bath. In the same way as discussed in the example here, there is no actual evaporation of the black hole and the gravitational system reaches a thermodynamic equilibrium, with the black hole bathing in its radiation.

boundary conditions and determining the stress-energy tensor in the flat bath region. This is achieved via a Weyl transformation of the right black hole exterior from an AdS_2 spacetime to a flat spacetime. This transformation causes the, otherwise vanishing energy stress tensor for the right exterior, to pick up a contribution from the conformal anomaly according to (5.44) and (5.44), which means that $\langle T_{x_\pm x_\pm}\rangle_{\text{Flat}} \neq 0$. The resulting non-zero energy-stress tensor in the now flat region is able to freely flow into the flat bath region and is hence identified as the energy stress tensor in the bath. Another way of looking at this is that this non-zero stress-energy tensor in the bath is the stress-energy tensor needed to support the eternal black hole, which has a vanishing stress-energy tensor in AdS_2. So, the energy in the black hole region determines the energy in the bath region. If the temperature of the bath is lower than the temperature of the black hole, positive stress energy will leave the black hole until they system has reached a thermodynamic equilibrium.

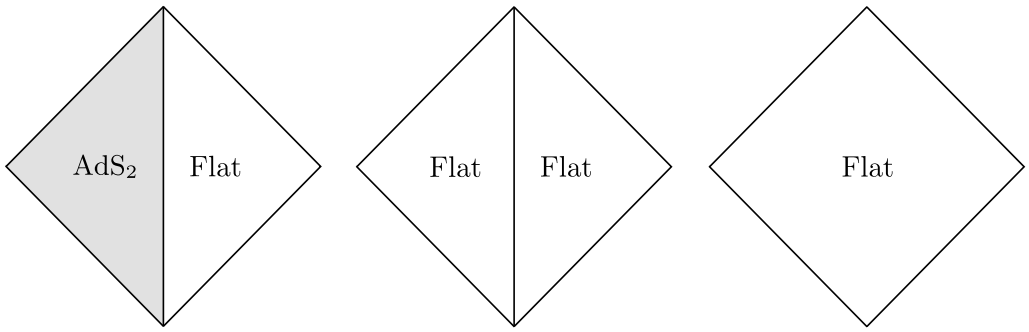

Figure 5.11: Transparent boundary conditions are achieved by first performing a Weyl transformation of the right exterior AdS_2 spacetime to a flat spacetime, and then identifying the stress-energy tensor in this spacetime as the stress-energy tensor in the bath.

$t > 0$ + Transparent boundary conditions : Before the bath model was proposed, it was already shown that the black hole evaporates in the case of a general transparent boundary, without specifying where the Hawking radiation went after the evaporation [69]. Without specifying the precise absorption method, one can imagine an observer at the holographic boundary, collecting all the Hawking radiation that reaches it. From the perspective of this boundary "collector", assuming they are perfectly efficient at their job, no Hawking radiation is going back into the black hole, so the normal ordered inward component of the stress-energy tensor vanishes; i.e. $\langle : T_{x_- x_-} : \rangle\big|_{\partial\mathcal{M}_2} = 0$. While the outward component $\langle T_{x_+x_+}\rangle\big|_{\partial\mathcal{M}_2} = 0$, now we need to take into account the inward pulse, which means that $\langle T_{x_-x_-}\rangle\big|_{\partial\mathcal{M}_2} \neq 0$. Hence, from (5.47),

$$\langle : T_{x_+x_+} : \rangle\big|_{\partial\mathcal{M}_2} = -\frac{c}{24\pi}\{F(t),t\} \qquad \text{and} \qquad \langle T_{x_-x_-}\rangle\big|_{\partial\mathcal{M}_2} = \frac{c}{24\pi}\{F(t),t\}\ , \tag{5.70}$$

which, when substituted into the energy conservation equation (5.48), yields

$$\frac{\mathrm{d}E}{\mathrm{d}t} = \frac{c}{24\pi}\{F(t),t\}\ . \tag{5.71}$$

From the other energy equation (5.58), by differentiating, one can write another energy conservation equation, namely

$$\frac{\mathrm{d}E}{\mathrm{d}t} = -\frac{\bar{\phi}_r}{8\pi G_N}\partial_t\{F(t),t\}\ . \tag{5.72}$$

Combining both energy conservation conditions yields the differential equation

$$-\frac{\bar{\phi}_r}{8\pi G_N}\partial_t\{F(t),t\} = \frac{c}{24\pi}\{F(t),t\}\ , \tag{5.73}$$

which, when solved, yields an energy decay profile, given by

$$E(t) = E_S \mathrm{e}^{-\frac{cG_N}{3\bar{\phi}_r}t}\ . \tag{5.74}$$

This energy decay is analogous to a decay in the mass of the black hole, hence describing an evaporating black hole solution. To re-emphasize, this black hole evaporation was achieved by forming a black hole by means of throwing a pulse of energy from the holographic boundary into the bulk and imposing transparent boundary conditions, without specifying where the Hawking radiation went.

The aim is now to incorporate the bath into this result, and hence derive the result in [18]. To do this, we need to first impose that the initial state was not the Poincaré vacuum state, but an already formed static black hole of some energy E_0. Then we need to use that the addition of the bath also leads to an inwards positive-energy pulse E_S. The last difference between the model discussed here and the one in [18] is that the bath absorbs the Hawking radiation, rather than some unspecified perfect "collector" living at the holographic boundary, though this last detail does not affect the evaporation calculation. Incorporating these changes into the result (5.74) is simple and results into an energy decay given by

$$E(t) = E_0\theta(-t) + (E_0+E_S)\theta(t)\mathrm{e}^{-\frac{cG_N}{3\bar{\phi}_r}t}\ , \tag{5.75}$$

where E_0 is the energy (mass) of the initial black hole, defined in (5.59), before the coupling to the bath. The black hole is then coupled to the bath at $t = 0$, via the additional pulse injection, leading to a solution of total energy $E_0 + E_S$, which decays at the same rate as in (5.59). Hence, this model starts with a black hole of some energy E_0, and after the injection of the positive energy pulse E_S, it evaporates until it reaches its original energy.

For the evaporation-via-bath model in (5.75), reparameterization $F(t)$ before the pulse is simply the one for the black hole solution, given by $F(t) = {}^1\!/_{\pi T_0}\tanh(\pi T_0 t)$, which we found was the solution to the constant Schwarzian $\{F(t),t\} = -2\pi^2 T_0^2$. However, after the pulse, the total energy is $E_0 + E_S =: E_1$ with temperature T_1, evolving according to the exponential decay in (5.75), so the Schwarzian becomes $\{F(t),t\} = -2\pi^2 T_1^2 \mathrm{e}^{-\frac{cG_N}{3\bar{\phi}_r}t}$. This can be solved to find that the new reparameterization after the pulse is given in terms of the modified Bessel functions [18]

$$F(t) = \frac{1}{\pi T_1}\frac{I_0(\frac{2\pi T_1}{k})K_0(\frac{2\pi T_1}{k}\mathrm{e}^{-\frac{kt}{2}}) - I_0(\frac{2\pi T_1}{k}\mathrm{e}^{-\frac{kt}{2}})K_0(\frac{2\pi T_1}{k})}{I_0(\frac{2\pi T_1}{k}\mathrm{e}^{-\frac{kt}{2}})K_1(\frac{2\pi T_1}{k}) + I_1(\frac{2\pi T_1}{k})K_0(\frac{2\pi T_1}{k}\mathrm{e}^{-\frac{kt}{2}})}\ , \tag{5.76}$$

where $k := cG_N/3\bar{\phi}_r$ was defined for convenience.

In this section, we have shown that, via an injection of a positive-energy pulse (such as by coupling to the auxiliary bath), and by imposing transparent boundary conditions are the holographic boundary, black holes evaporate at an exponential rate. However, just because the large AdS black hole evaporation issue has been resolved, that does not mean that Information paradox has been resolved. In the next section, we review some aspects of black hole thermodynamics and explain how a unitary Page curve was achieved for the black hole evaporation model.

5.2.4 Thermodynamics: Review

The bath evaporation model, just as any other proposed evaporation model, needs to be unitary if it is to resolve the information paradox successfully, so we need to be able to recover unitary evolution of both the black hole and the Hawking radiation individually. This section will provide a review of the way the entanglement entropy is calculated, but will not go into too much detail.

Calculating the gravitational entanglement entropy
Before calculating any entropies for the black hole bath evaporation model, one should begin with studying entropy in JT gravity for a simpler model, such as the eternal black hole, whose temperature was calculated in (5.59). Using the second law of thermodynamics, relating the change in entropy to the amount of heat transfer (familiarly written as $\Delta S(\beta) = \delta Q/T$), the entropy of the eternal black hole system can be found from

$$\frac{\mathrm{d}S(\beta)}{\mathrm{d}E} = \frac{1}{T} = \sqrt{\frac{\pi\bar{\phi}_r}{4G_N E}}\,, \tag{5.77}$$

which can be integrated and gives an expression for the thermodynamic entropy, given by

$$S(\beta) = \sqrt{\frac{\pi\bar{\phi}_r}{4G_N}}\int \mathrm{d}E\ \frac{1}{\sqrt{E}} = S_0 + \sqrt{\frac{\pi\bar{\phi}_r E}{G_N}} = S_0 + \frac{\pi\bar{\phi}_r}{2G_N}T\,. \tag{5.78}$$

It can be shown that this thermal entropy matches the Bekenstein-Hawking black hole entropy

$$S_{\mathrm{BH}} = \frac{\mathcal{A}}{4G_{\mathrm{eff}}(x)} = \frac{\phi_0 + \phi_{\mathrm{h}}}{4G_N}\,. \tag{5.79}$$

One way to motivate why the last equality in (5.80) is true is by using that the volume of S^{d-2} is $V_{S^{d-2}} = 2\pi^{\frac{d-2}{2}}/\Gamma(\frac{d-1}{2})$. This leads to the area of the event horizon being $\mathcal{A} = 1$ for the $d = 2$ case. The effective Newton's constant is related to the value of the dilaton, as explained in Section 5.1.1 and this is evaluated at the location of the horizon ($z \to \infty$), where $\phi(z)|_{z\to\infty} = \phi_{\mathrm{h}}$[72]. The reason this is evaluated at the event horizon can be seen from the RT entropy formula. As discussed in Chapter 3, for the AdS black hole, the surface which minimizes the entropy, is the event horizon itself. It has been shown that the RT formula for the JT black hole yields

$$S = \mathrm{Min}_z \frac{\phi_0 + \phi(z)}{4G_N}\,, \tag{5.80}$$

which is minimized at the location of the event horizon where $z \to \infty$.

A more formal way to derive (5.80) is to use the definition of the thermal entropy in terms of the thermal partition function (3.15), and then follow the same approach as in Section 3.3.1 for finding the entropy of the Euclidean Schwarzschild solution. To do this, we need to use the Euclidean JT gravity action in 5.50 and evaluate it on-shell. The on-shell JT action in $d = 2$

with coordinates $x \in \{t, z\}$ is given by

$$\begin{aligned} I_{\rm JT}[g,\varphi]\big|_{\rm on-shell} &= -\frac{\phi_0}{8\pi G_N}\left[\frac{1}{2}\int_{\mathcal{M}_2} \mathrm{d}^2x\,\sqrt{-g}\,R + \int_{\partial\mathcal{M}_2}\mathrm{d}x\,\sqrt{-h}\,K\right]\Big|_{\rm on-shell} \\ &\quad - \frac{1}{8\pi G_N}\left[\frac{1}{2}\int_{\mathcal{M}_2} \mathrm{d}^2x\,\sqrt{-g}\,\phi(R+2) + \phi_b\int_{\partial\mathcal{M}_2}\mathrm{d}x\,\sqrt{-h}\,(K-1)\right]\Big|_{\rm on-shell} \\ &= -\frac{\phi_0}{8\pi G_N}(2\pi) - \frac{\phi_b}{8\pi G_N}\int_{\partial\mathcal{M}_2}\mathrm{d}t\,\sqrt{g_{tt}}\,(K-1)\Big|_{\rm on-shell} \\ &= -\frac{\phi_0}{4G_N} - \frac{\bar{\phi}_r}{8\pi G_N\epsilon}\Big(\beta\frac{1}{\epsilon}\frac{4\pi^2\epsilon^2}{2\beta^2}\Big) \\ &= -\frac{\phi_0}{4G_N} - \frac{\bar{\phi}_r}{4G_N}\frac{\pi}{\beta}\,, \end{aligned} \tag{5.81}$$

where we have used that the first square bracket on the first line is simply related to the Euler characteristic and it evaluates to 2π, and the first term on the second square bracket goes to zero, since $R = -2$ on-shell. We have also used the boundary conditions, (5.54) and (5.55), and that the extrinsic curvature at the boundary $\partial\mathcal{M}_2$ (at $z = \epsilon$) can be evaluated to give $K = {}^{4\pi^2\epsilon^2}/_{2\beta^2}$.[41] The on-shell JT action $I_{\rm JT}[g,\varphi]\big|_{\rm on-shell}$ is really the action evaluated for the eternal black hole solution at temperature β^{-1}; i.e. I_{JT}[Eternal Black hole (β)].

Hence, the thermal entropy can be evaluated by using the saddle point approximation (3.35), which gives[42]

$$\begin{aligned} S(\beta) &= (1-\beta\partial_\beta)\log Z \\ &\approx -(1-\beta\partial_\beta)\,I_{\rm JT}[g,\varphi]\Big|_{\rm on-shell} \\ &= (1-\beta\partial_\beta)\Big(\frac{\phi_0}{4G_N} + \frac{\bar{\phi}_r}{4G_N}\frac{\pi}{\beta}\Big) \\ &= \frac{1}{4G_N}\Big(\phi_0 + \bar{\phi}_r\frac{2\pi}{\beta}\Big) \\ &= \frac{\phi_0+\phi_{\rm h}}{4G_N}\,. \end{aligned} \tag{5.82}$$

Comparing this to the Bekenstein-Hawking entropy, we can see that the area of the event horizon in $d = 2$ JT gravity is given by the dilaton value at the horizon. It was claimed above that this entropy can be related to the thermal entropy in (5.78). This can be easily shown by substituting the expression for dilaton profile of the eternal black hole (5.56) into the RT formula (5.80).

[41] This can be (more easily) evaluated using that the extrinsic curvature at the boundary can be written in terms of the way we choose to parameterize the boundary curve. This has been derived in Section 2.3.4 in [72] and the result is that $K = 1 + \epsilon^2\{F(t), t\} + \mathcal{O}(\epsilon^4)$. Substituting the reparametrization for the black hole solution, namely $F(t) = {}^1/_{\pi T_0}\tanh(\pi T_0 t)$ gives that $K = {}^{4\pi^2\epsilon^2}/_{2\beta^2}$.

[42] To avoid confusion, in what follows, $\bar{\phi}_r \neq \phi_{\rm h}$. $\bar{\phi}_r$ is the renormalized value of the dilaton at the holographic boundary, while $\phi_{\rm h}$ is the value of the dilaton at the black hole event horizon. The latter can be evaluated from the black hole dilaton profile in (5.61) by taking the limit $z \to \infty$, where the black hole horizon is, which gives that $\phi_{\rm h} = 2\pi\bar{\phi}_r/\beta$.

As introduced in Chapter 3, the gravitational fine-grained entropy contains a von Neumann entropy contribution. The formula is given by

$$\begin{aligned} S &= \text{Min}_\chi\Big[\text{Ext}_\chi\Big\{\frac{\mathcal{A}(\chi)}{4G_N} + S_{\text{semi-cl}}(\Sigma_\chi)\Big\}\Big] \\ &= \text{Min}_\chi\Big[\text{Ext}_\chi\Big\{\frac{\phi_0 + \phi(\chi)}{4G_N} + S_{\text{semi-cl}}(\Sigma_\chi)\Big\}\Big] \,, \end{aligned} \tag{5.83}$$

where χ is the codimension-2 QES, Σ_χ is the region bounded by the QES and the cut-off surface (located at the AdS_2 boundary) and $S_{\text{semi-cl}}(\Sigma_\chi)$ is the von Neumann entropy of the quantum fields on Σ_χ. The formula works by first extremizing with respect to the position of the QES χ in order to find its location. The resulting entropy is then minimized over all possible choices of χ. This method has been used to reproduce a Page curve for the black hole [18] and a Page for the Hawking radiation [85]. The outline of the approach will be reviewed for completeness, though without showing any details of the calculation.

The matter sector in both the bulk and the bath is the same CFT_2 theory. For a CFT_2 with a flat metric, the von Neumann entropy of a region A (with a complement $B = \bar{A}$) was introduced in (3.25). For an interval between the points w_1 and w_2, it is given by [86]

$$\begin{aligned} S_A &= \frac{c}{3}\log\frac{|w_1 - w_2|}{\sqrt{\epsilon_1\epsilon_2}} \\ &= \frac{c}{6}\log\frac{(w_1^+ - w_2^+)(w_1^- - w_2^-)}{\sqrt{\epsilon_1^+\epsilon_1^-\epsilon_2^+\epsilon_2^-}} \,, \end{aligned} \tag{5.84}$$

where in the second line we have used the lightcone coordinates (w^+, w^-) and the ϵ_1 and ϵ_2 are the UV cut-offs at the interface between A and B as shown in Figure. 5.12 below.

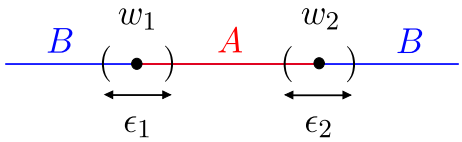

Figure 5.12: An interval A and its complement B, with the locations of the cut-offs ϵ_1 and ϵ_2 at the interfaces between them, namely w_1 and w_2.

Note that if the CFT_2 interval is such that the end-points are no longer described by a flat metric, then there is a contribution from the conformal factor needed to transform the metric to the flat CFT_2 metric, in order to use (5.84). To be more precise, if the CFT_2 metric is not flat, but given by $ds = -\Omega^{-2}dw^+dw^-$, then the von Neumann entropy of a region A between the interval $\{w_1^+, w_1^-\}$ and $\{w_2^+, w_2^-\}$ is given by

$$S_A = \frac{c}{6}\log\frac{(w_1^+ - w_2^+)(w_1^- - w_2^-)}{\sqrt{\epsilon_1^+\epsilon_1^-\epsilon_2^+\epsilon_2^-}\Omega(w_1)\Omega(w_2)} \,, \tag{5.85}$$

where $\Omega(w_1)$ and $\Omega(w_2)$ are the conformal factors needed to transform the metrics at the end-points (w_1 and w_2 respectively) to the flat metric. If the interval being considered is such that the two endpoints are in different space-times, hence described by different metrics, the conformal factors that the metrics receive, namely $\Omega(w_1)$ and $\Omega(w_2)$, will be different. This has been illustrated in Figure 5.13 below, showing two different (unspecified) spacetime metrics, and the middle interval has one endpoint in each.

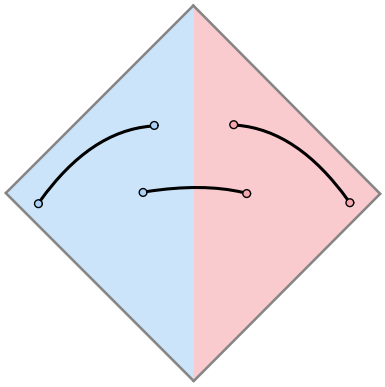

Figure 5.13: A spacetime with two distinct regions (blue and red), which are described by different metrics (not necessarily flat), but have the same CFT_2 matter sector. The three intervals (black lines), each have a different von Neumann entropy (5.85), since their endpoints are at different locations and hence the conformal factors $\Omega(w_1)$ and $\Omega(w_2)$ will be different. The left interval has its endpoint in the same spacetime, so the $\Omega(w_1)$ and $\Omega(w_2)$ will be the same. The same applies for the right interval. However, the middle interval has each endpoint in a different spacetime, so $\Omega(w_1)$ and $\Omega(w_2)$ will be different.

This is important when calculating the entropy of the Hawking radiation, in which case the entanglement entropy is calculated across an interval with one end-point in the AdS_2 bulk and the other in the flat bath region.

One could then pick intervals in the bulk, the bath or across both regions, and calculate the von Neumann entropy across the intervals in each case. The locations of the quantum extremal surfaces are then found by extremizing the generalized entropy. Minimizing across all possible χ then gives the entanglement entropy in the region.

Using this approach, it has been found that the black hole entropy has contributions from two sets of quantum extremal surfaces, both located in the bulk, while the entanglement entropy of the Hawking radiation has not only quantum extremal surfaces in the bath (where the Hawking radiation is collected), but also quantum extremal surfaces behind the horizon of the black hole, which also extremize the entropy of the radiation. These quantum extremal surfaces will be discussed in more detail in what follows.

Entropy of the evaporating black hole

Despite not having derived the locations of the quantum extremal surfaces, in this section we will use them to motivate the entropy evolution without having to mathematically calculate it. We will follow closely the review in [87] and refer to the gravitational entanglement entropy formula

$$S = \text{Min}_\chi\Big[\text{Ext}_\chi\Big\{\frac{\mathcal{A}(\chi)}{4G_N} + S_{\text{semi-cl}}(\Sigma_\chi)\Big\}\Big]\,. \tag{5.86}$$

After the black hole has formed from the initial inward shock of energy E_0, it has some initial entropy $S_{\text{BH}}(E_0)$. This is the eternal black hole solution, which has not yet began to evaporate, so at this early time, no Hawking radiation escapes the black hole region. There are no quantum extremal surfaces and the region Σ_χ extends all the way down to the bifurcate horizon, where χ has zero size. Hence, this surface is commonly referred to as the *vanishing surface*. The bifurcate horizon is illustrated in Figure 5.14 as a green circle. Note that the

bifurcate horizon in question is the original one (drawn with a dashed line); i.e. before the spacetime has been coupled to the bath, which introduces the inward positive-energy shock and hence causes the location of the event horizon to move outwards (drawn with a solid line). Since the vanishing surface has a vanishing area, then all contribution to the entanglement entropy comes from the von Neumann entropy of the quantum fields on Σ_χ. Note that if we were to consider a black hole which formed from the gravitational collapse of matter that was initially in a pure state, then the von Neumann contribution will also vanish at this early time. However, the black hole we are considering has a non-zero initial entropy entropy $S(E_0 + E_S)$. This has been illustrated by the dotted line in Figure 5.17, which is located at some $S > 0$.

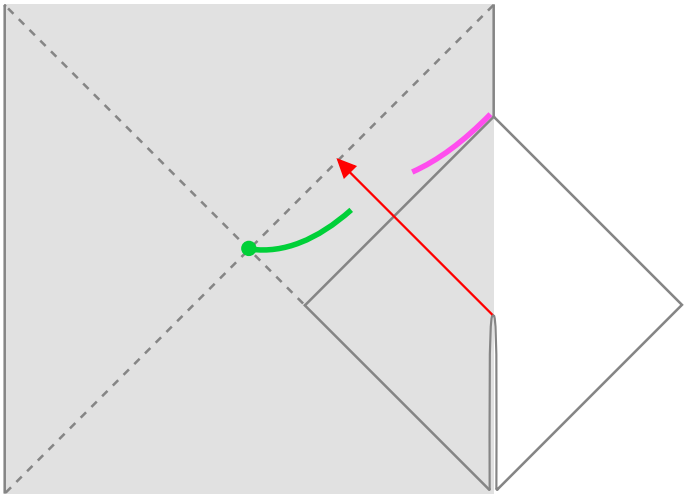

Figure 5.14: Location of the quantum extremal surfaces, adapted from [18], where the green line is the vanishing QES and the pink line is the non-vanishing QES. The green dot is at the location of the initial bifurcate horizon. The initial and final location of the event horizon are indicated by a dashed and solid line respectively. Due to the close proximity of the vanishing QES to the original bifurcate horizon, it can be expected that the area contribution to the entanglement entropy from this QES will be very little. This will not be the case for the non-vanishing surface, whose area contribution to the entanglement entropy will be large.

The coupling to the bath introduces a pulse of energy E_S causes a sharp increase in the black hole entropy, which becomes $S_{\text{BH}}(E_0 + E_S)$. Following this inward pulse, the black hole starts evaporating. It has been illustrated in Figure 5.14, that the location of the QES χ changes, forming a locus of quantum extremal surfaces (drawn in green) still very close to the bifurcate horizon. This locus of quantum extremal surfaces is often referred to as the *early time branch*. This causes the region Σ_χ to evolve such that it moves up, as shown in Figure 5.15 (left), where the Σ_χ regions at different times are drawn as black lines starting from the AdS_2 boundary.

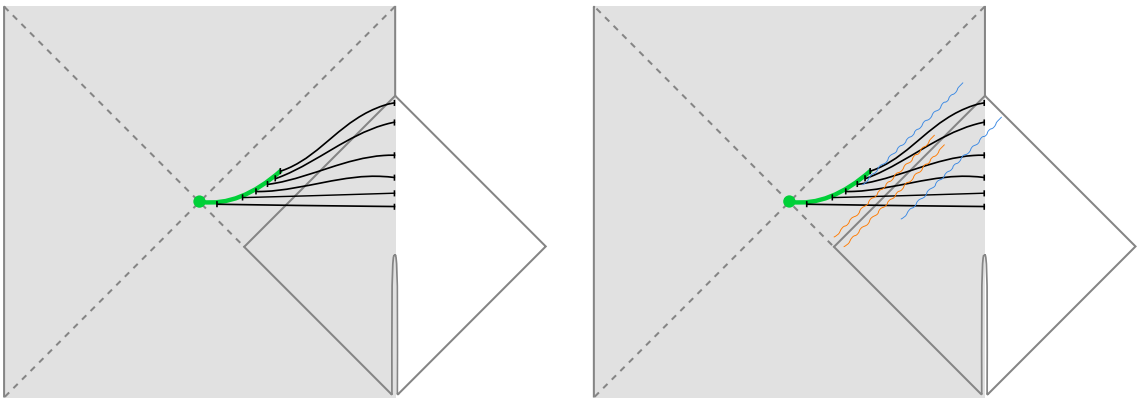

Figure 5.15: (left) The locus of vanishing quantum extremal surfaces (green line) and the respective extremal surfaces Σ_χ (black lines), each of which has one of their endpoints on the quantum extremal surface χ, and the other located at the AdS_2 boundary. With time, the extremal surfaces Σ_χ move upwards, with the right endpoint moving up the AdS_2 boundary. (right) Entangled Hawking pairs of the same color cross different extremal surfaces Σ_χ, showing that the late time extremal surfaces capture mostly the region inside the horizon, and hence contribute to an increasing entanglement entropy over time.

As the black hole evaporates, the entropy of the black hole increases, since the pile-up of unpaired Hawking modes across the Σ_χ region causes its von Neumann entropy to increase. This has been illustrated in Figure 5.15 (right), where the entangled Hawking modes have the same color. It can be seen that at earlier times, when Σ_χ covers a bigger region outside the horizon, there will be less unpaired Hawking modes, and hence a lower increase in $S_{\text{semi-cl}}(\Sigma_\chi)$. As the location of χ moves up, so does the Σ_χ region. At later times, the endpoint of Σ_χ moves up the AdS_2 boundary but also gets closer to the event horizon, so it covers less of the region outside the event horizon. This means that there are more unpaired Hawking modes contributing to the black hole entropy. This has been illustrated in Figure 5.15 (right), where both entangled modes of the blue Hawking pair contribute to the von Neumann entropy of the early Σ_χ, while only one of them (namely the one that goes into the black hole) crosses the later Σ_χ. Hence, as the black hole evaporates, the contribution from this QES causes the black hole entropy to keep growing. This has been illustrated in Figure 5.17, where the green line represents the increase in the black hole entropy due to the QES discussed above. It should be noted that Figure 5.17 also shows an initial drop in the black hole entropy. This is because once the black hole starts evaporating, it takes some time until it recovers the information about the emitted Hawking modes. This time is known as the *scrambling time*, t_{scr} [88].

As illustrated in Figure 5.17, the increase in the black hole entropy due to the increasing von Neumann entropy of the outgoing radiation (drawn in green), eventually surpasses the thermodynamic entropy of the black hole (drawn in black), which decreases due to the decrease in the area of the event horizon. As discussed in the Introduction, for the evaporation to be unitary, it needs to follow the Page curve, which is bounded from above by the thermodynamic entropy. Hence, there needs to be a process which lowers the black hole entropy.

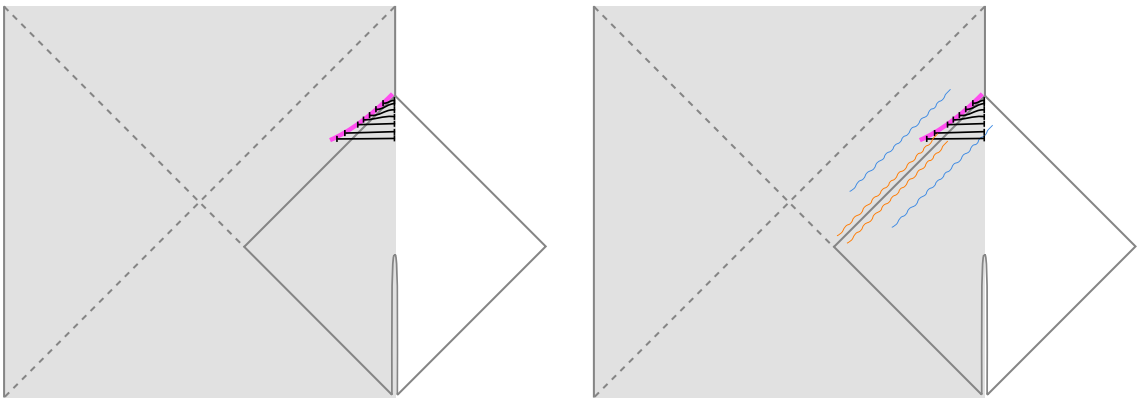

Figure 5.16: (left) The locus of non-vanishing quantum extremal surfaces (pink line), located very close to the event horizon, and the respective extremal surfaces Σ_χ (black lines), each of which has one of their endpoints on the quantum extremal surface χ, and the other located at the AdS_2 boundary. With time, the extremal surfaces Σ_χ move upwards, with the right endpoint moving up the AdS_2 boundary. (right) Entangled Hawking pairs of the same color cross different extremal surfaces Σ_χ, showing that the late time extremal surfaces capture barely any Hawking modes and the contribution from the non-vanishing surfaces to the gravitational entanglement entropy is dominated by the area term, hence causing the entanglement entropy to decrease.

This is resolved by the appearance of another QES, referred to as the *non-vanishing surface*, which appears soon after the black hole starts evaporating. Its location is also time-dependent, and the locus of these quantum extremal surfaces, often referred to as the *late time branch*, is very close to the event horizon, as illustrated in Figure 5.14 by the pink line. As it evolves, the Σ_χ also move up, with their endpoint along the AdS_2 boundary, as illustrated in Figure 5.16 (left). Although the generalized entropy now gets a contribution from both the area term (since now the QES is not at the bifurcate horizon) and the von Neumann entropy across Σ_χ, the contribution is greatly dominated by the area term. This can be explained with the aid of Figure 5.16 (right), which shows that due to the proximity to the event horizon, the regions Σ_χ do not capture many Hawking modes, especially at later times. Hence, the contribution from this QES simply follows the evolution of the thermodynamic black hole entropy and decreases as the black hole evaporates, as illustrated in Figure 5.17 by the pink line.

Since the gravitational entropy formula requires taking the minimum over all quantum extremal surfaces, the entropy does indeed follow a Page curve as illustrated in Figure 5.17 by the blue line. There are two quantum extremal surfaces to consider. The entropy increases at early times, since the contribution from the vanishing surface (green) is smallest. However, at some later time, namely the Page time, the contribution from the non-vanishing surface (pink) is smaller, so the entropy starts decreasing.

Although the entropy of the black hole has been shown to follow the Page curve, this is not sufficient to resolve the information paradox, which is concerned with the entropy of the Hawking radiation. Hence, one needs to show that the entropy of the radiation also follows a Page curve. This will be discussed next.

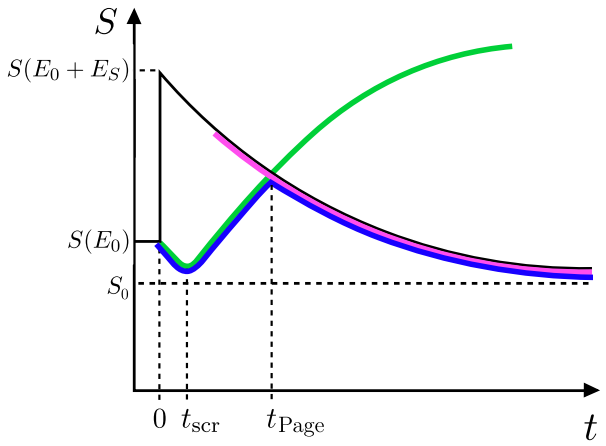

Figure 5.17: The contribution to the gravitational entanglement entropy from the vanishing QES (green), from the non-vanishing QES (pink) and the thermodynamic black hole entropy (black). It can be seen that the gravitational entanglement entropy of the non-vanishing QES, being dominated by the area of the event horizon, closely follows the evolution of the thermodynamic black hole entropy. A Page curve (blue) is achieved by minimizing the gravitational entropy over all quantum extremal surfaces. At early times the entropy is minimized by the vanishing QES, while at later times it is minimized by the non-vanishing QES. Figure adapted from [89].

Entropy of the Hawking radiation

The Hawking radiation is absorbed into the flat bath region. Even though there is no black hole present in this spacetime, and the gravitational effects are very small beyond the AdS_2 boundary cut-off, the generalized entanglement entropy can still be used. However, although the regions Σ_χ considered so far were all connected, this is not a necessary condition for the formula. As will be explained in this section, for the case of the entropy of the Hawking radiation, it is a disconnected region which minimizes the generalized entropy. This disconnected region consists of two intervals. One of the intervals, called Σ_{Rad}, is in the flat bath region, starting from the AdS_2 boundary, as illustrated in Figure 5.18 (left), where the endpoint of this region is shown to move up along the AdS_2 boundary as time evolves. The other interval, called Σ_{Island}, is a region behind the black hole horizon, such that one of its endpoints is at the original bifurcate horizon, while the other one is very close to the final horizon.[43] As illustrated in Figure 5.18 (right), the endpoint of this region is close to the final horizon and also moves up with time. This region, known as the *Island*, becomes important at late times. Since the gravitational entropy will include contributions from two disconnected regions, Σ_{Rad} and Σ_{Island}, it needs to be modified such that the region Σ is the union of the two disconnected surfaces, which gives the so-called *Island formula*

$$S_{\text{Rad}} = \text{Min}_\chi\left[\text{Ext}_\chi\left\{\frac{\mathcal{A}(\chi)}{4G_N} + S_{\text{semi-cl}}(\Sigma_{\text{Rad}} \cup \Sigma_{\text{Island}})\right\}\right] . \tag{5.87}$$

We will begin by discussing how the radiation entropy evolves without the Island contribution.

[43] Note that any number of islands is allowed in the computation, including no islands.

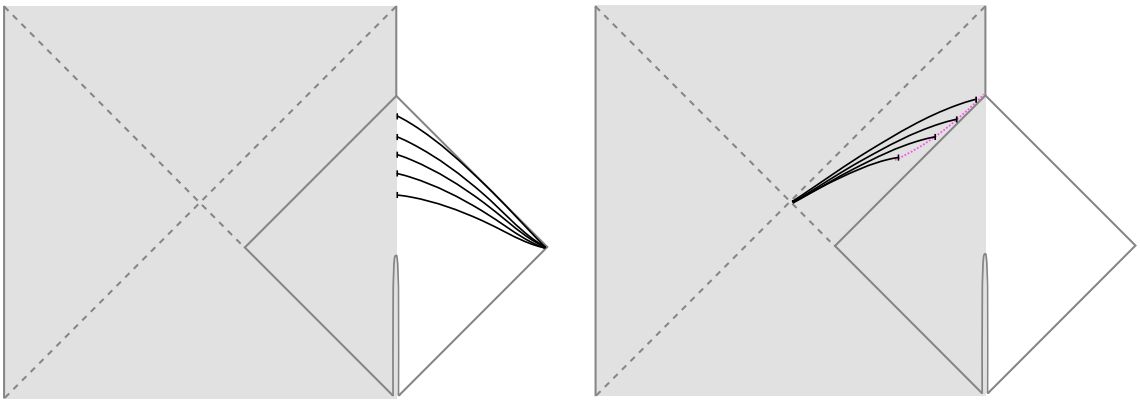

Figure 5.18: (left) The regions Σ_{Rad} in the bath region, which have one of their endpoints on the AdS_2 boundary. With time, these extremal surfaces evolve to move up, with the endpoint moving up along the AdS_2 boundary. (right) The regions Σ_{Rad}, each of which starts at the bifurcate horizon and ends at a region very close to the event horizon (pink dashed line). These regions evolve such that the bifurcate end point does not move, but their other endpoint gets closer to the event horizon.

As time evolves, the endpoint of Σ_{Rad} moves up along the AdS_2 boundary. As illustrated in Figure 5.19 (left), the early regions capture less Hawking modes than the later ones. This can be demonstrated with the purple Hawking mode, which only crosses the later regions, and not the early ones. Hence, without the Island contribution, the entropy of the Hawking radiation in the bath increases with time. This has been illustrated by the orange curve in Figure 5.20.

However, the contribution from Σ_{Rad} is not always the global minimum of the generalized entropy and one needs to take into account the contribution from an island which forms soon after the black hole has formed, and also extremizes the entropy. The island causes a decrease in the entropy because for any time slice, the Hawking modes captured by the Σ_{Rad} region have their entanglement partner captured by the Σ_{Island} region. Hence, the incorporation of the island causes the Hawking modes which contributed earlier (i.e. without the island) to become purified. Instead of looking at $\Sigma_{\text{Rad}} \cup \Sigma_{\text{Island}}$, another way of explaining the entanglement evolution of the union between the island and radiation regions is to look at the complement region. One can see from Figure 5.19 (right) that the complement region of $\Sigma_{\text{Rad}} \cup \Sigma_{\text{Island}}$ gives the same contribution as that from the non-vanishing QES in Figure 5.16 (left), namely starting very close to the horizon and ending on the AdS_2 boundary. Hence, the entanglement entropy of the region $\Sigma_{\text{Rad}} \cup \Sigma_{\text{Island}}$ decreases with time, as illustrated in Figure 5.20 by the red curve.

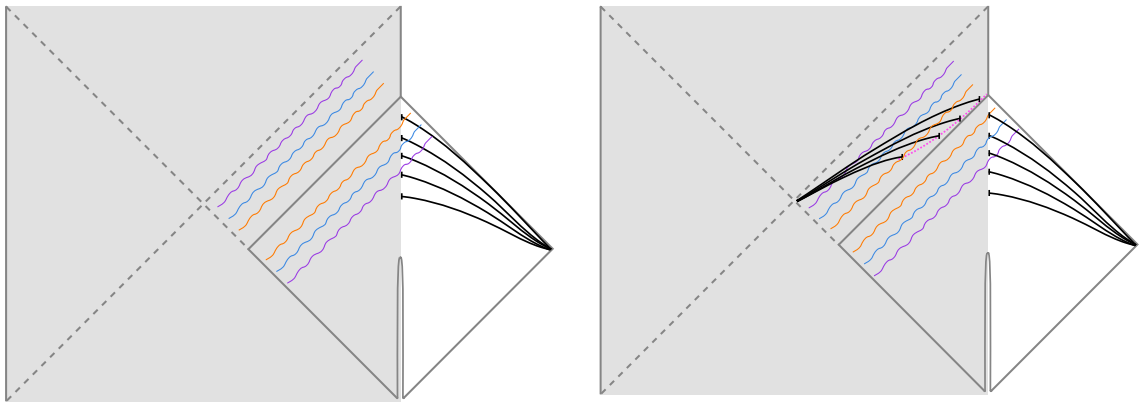

Figure 5.19: (left) Entangled Hawking pairs of the same color cross different Σ_{Rad} regions, which contribute towards an increase in the entanglement entropy, since more unpaired Hawking modes cross the regions at later times. (right) The disconnected region $\Sigma_{\text{Rad}} \cup \Sigma_{\text{Island}}$, which contributes towards a decrease in the entanglement entropy, since the island purifies most of the Hawking modes that are collected by the Σ_{Rad} region. The complement of the Σ_{Rad} is the region between the AdS_2 boundary and the near-horizon region endpoint of the island region (pink dashed line).

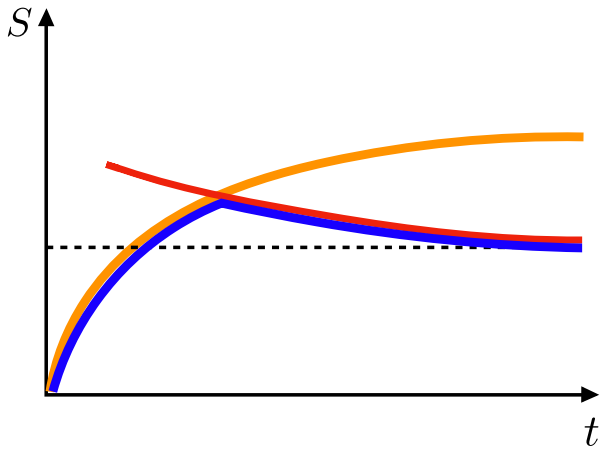

Figure 5.20: An increasing contribution to the gravitational entanglement entropy of the radiation due to the radiation region Σ_{Rad} (orange) and a decreasing contribution from the disconnected region $\Sigma_{\text{Rad}} \cup \Sigma_{\text{Island}}$ containing the island contribution. Since the gravitational entanglement entropy requires minimizing over all surfaces, a Page curve is achieved, by considering only Σ_{Rad} at early times and only $\Sigma_{\text{Rad}} \cup \Sigma_{\text{Island}}$ at later times [89].

This section reviewed how a Page curve was achieved for both the evaporating black hole and the Hawking radiation, indicating that the proposed evaporation model is unitary. Thinking back on how it was the AdS/CFT conjecture which motivated that AdS black holes should evolve unitarily due to their dual being described by a quantum field theory, which is a unitary theory, it makes sense that the dual description of the evaporation model discussed so far should have a dual description which also evolves unitarily. This will be discussed in the next section, where a toy model will be used for the dual of the black hole evaporation.

5.3 One-sided evaporation of the eternal black hole in the dual theory

The black hole bath evaporation model [18] was shown to be unitary via entropy calculations in the gravity theory, i.e. without examining how the dual CFT_1 theory evolves. Transparent boundary conditions were imposed at the AdS boundary, in contrast to the usual reflective AdS boundary conditions, which were required for energy conservation. However, the issue with energy conservation has now returned, since the auxiliary bath spacetime has absorbed energy from the bulk. The bath model employs energy conservation by imposing that after the evaporation of the one-sided black hole in the right exterior into the bath, all the collected radiation is transferred back into the bulk, into the left black hole exterior. In this section, we will study this process in the dual theory and try to find out if this transfer of radiation can be achieved unitarily. Although JT gravity is dual to an SYK model at the boundary, in this section we will employ a simplified toy model which uses the dual of the eternal black hole solution, namely the *thermofield double state* (TFD) [90].

5.3.1 Review of the TFD formalism

It has been shown that the eternal black hole in AdS is dual to a thermofield double state on the boundary [90], which is an entangled state of two copies of the CFT theory, which will be labeled as $\mathrm{CFT_L}$ and $\mathrm{CFT_R}$. The state on the boundary before coupling to the bath (i.e. while the black hole is still eternal) is hence

$$|\mathrm{TFD}\rangle = \frac{1}{\sqrt{Z}} \sum_{i=0}^{\infty} \mathrm{e}^{-\frac{\beta}{2}E_i} \, |i\rangle_L \otimes |i\rangle_R \,, \qquad Z = \sum_{i=0}^{\infty} \mathrm{e}^{-\beta E_i} \tag{5.88}$$

where $|i\rangle_L$ are the energy eigenstates of a single copy of the CFT living on the boundary of the AdS, namely the CFT_L, and Z is the thermal partition function. The set $\{|i\rangle_L\}$ forms an orthonormal basis spanning $\mathcal{H}_L$ and the set $\{|i\rangle_R\}$ forms an orthonormal basis spanning $\mathcal{H}_R$, which can be arbitrary, but have been chosen to represent the energy eigenstates of the theory.

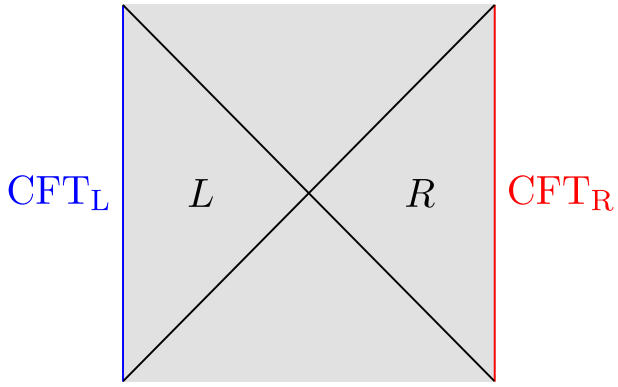

Figure 5.21: The eternal AdS_2 black hole is dual to two entangled copies of CFT_1, labeled as CFT_L and CFT_R.

The density matrix for the TFD state is hence

$$\rho_{LR} = |\text{TFD}\rangle\langle\text{TFD}| = \frac{1}{Z}\sum_{i=0}^{\infty}\sum_{j=0}^{\infty} \mathrm{e}^{-\frac{\beta}{2}(E_i+E_j)}\Big(|i\rangle_{LL}\langle j| \otimes |i\rangle_{RR}\langle j|\Big) \tag{5.89}$$

such that the reduced density matrices of the subsystems, obtained via a partial trace of (5.89), are

$$\rho_L = \mathrm{Tr}_R\rho_{LR} = \frac{1}{Z}\sum_{i=0}^{\infty}\sum_{j=0}^{\infty} \mathrm{e}^{-\frac{\beta}{2}(E_i+E_j)}\ |i\rangle_{LL}\langle j|\ \mathrm{Tr}\Big[|i\rangle_{RR}\langle j|\Big] = \frac{1}{Z}\sum_{i=0}^{\infty}\mathrm{e}^{-\beta E_i}\ |i\rangle_{LL}\langle i| \tag{5.90}$$

$$\rho_R = \mathrm{Tr}_L\rho_{LR} = \frac{1}{Z}\sum_{i=0}^{\infty}\sum_{j=0}^{\infty} \mathrm{e}^{-\frac{\beta}{2}(E_i+E_j)}\ \mathrm{Tr}\Big[|i\rangle_{LL}\langle j|\Big]\ |i\rangle_{RR}\langle j| = \frac{1}{Z}\sum_{i=0}^{\infty}\mathrm{e}^{-\beta E_i}\ |i\rangle_{RR}\langle i|\ , \tag{5.91}$$

where we have used that $\mathrm{Tr}[|i\rangle\langle j|] = \langle i|j\rangle = \delta_{ij}$. The Hamiltonian, also sometimes called modular Hamiltonian, satisfies $H_L|i\rangle_L = E_i|i\rangle_L$ and $H_R|i\rangle_R = E_i|i\rangle_R$, so the reduced density matrices can be written as the more familiar Gibbs states

$$\rho_L = \frac{1}{Z}\sum_{i=0}^{\infty}\mathrm{e}^{-\beta E_i}\ |i\rangle_{LL}\langle i| = \frac{\mathrm{e}^{-\beta H_L}}{Z}\sum_{i=0}^{\infty}|i\rangle_{LL}\langle i| = \frac{1}{Z}\mathrm{e}^{-\beta H_L} \tag{5.92}$$

$$\rho_R = \frac{1}{Z}\sum_{i=0}^{\infty}\mathrm{e}^{-\beta E_i}\ |i\rangle_{RR}\langle i| = \frac{\mathrm{e}^{-\beta H_R}}{Z}\sum_{i=0}^{\infty}|i\rangle_{LL}\langle i| = \frac{1}{Z}\mathrm{e}^{-\beta H_R}\ , \tag{5.93}$$

where we have used that $\sum_i |i\rangle\langle i| = I$. The TFD state is a pure state, so the von Neumann entropy $S(\rho_{LR}) = 0$. A further property of a pure bipartite state is that the entropy of any of the subsystems is the same; i.e. $S(\rho_L) = S(\rho_R)$, and the entanglement entropy is given by $S(\rho_R) = S(\rho_L)$. This can be evaluated using the definition (3.6) of von Neumann entropy, but since the reduced density matrix is diagonal (hence in a Schmidt decomposition), it is easier to use the eigenvalues and the definition (3.9) of the Shannon entropy. This yields

$$\begin{aligned} S(\rho_R) &= -\mathrm{Tr}[\rho_R \log \rho_R] \\ &= -\sum_{i=0}^{\infty}\lambda_i(\rho_R)\log\lambda_i(\rho_R) \\ &= -\sum_{i=0}^{\infty}\frac{\mathrm{e}^{\beta E_i}}{Z}\log\frac{\mathrm{e}^{\beta E_i}}{Z} \\ &= \frac{1}{Z}\sum_{i=0}^{\infty}\mathrm{e}^{\beta E_i}\left(\beta E_i + \log Z\right) \end{aligned} \tag{5.94}$$

where $\lambda_i(\rho_R)$ are the eigenvalues of ρ_R and we have used that $\log\rho_R = \sum_{i=0}^{\infty}\log\lambda_i(\rho_R)\ |i\rangle_{RR}\langle i|$.[44] Evaluating the entanglement entropy using ρ_L would yield the same result, by definition, but it is also obvious from (5.90), since both reduced density matrices have the same eigenvalues.

Having reviewed the TFD state, the goal of the next section will be to model the one-sided evaporation of the eternal black hole, which is dual to the TFD. Recall the result from Chapter

[44] This comes from the more general property that a function of a Hermitian operator with a decomposition $\rho = \sum_i \lambda_i(\rho)\ |i\rangle\langle i|$ takes the form $f(\rho) = \sum_i f(\lambda_i(\rho))\ |i\rangle\langle i|$.

2, where we found that absorption from the bulk into the holographic boundary is not possible due to the two descriptions being equivalent, and hence describing the same physics, hence the need for the auxiliary bath. In the next section we wish to incorporate this bath into the evolution of the TFD state, expected from the black hole evaporation into the bath.

To avoid having to write $\mathrm{CFT}_{L/R}$ every time, since the discussion will be primarily about the dual theory, we will refer to the $\mathrm{CFT}_{L/R}$ subsystems as simply the L/R subsystems.

5.3.2 On a quest for a unitary evaporation toy model

The paper [18] goes into great detail as to how the one-sided evaporation is achieved on the gravitational side of the theory, while also mentioning what should be expected in the dual theory. The evaporation in the dual theory is claimed to begin with the R and L subsystems in a pure entangled TFD state and result in another pure state, where the ADM energy in the right exterior is lower than that in the left exterior, with smaller entanglement between the R and L subsystems. In this section, we will establish the evolution in the dual theory, based closely on these claims, and argue if this can be achieved unitarily. We need to emphasize that we will NOT be looking for an operator that transfers the radiation from the right exterior into the bath, and then from the bath into the left exterior, while acting on the WHOLE (AdS bulk + bath) system. Instead, we will try to model the bath itself as an operator that transfers the radiation from the right to the left exterior. The reasoning behind this choice will be explained in the following section.

Mimicking the claimed one-sided evaporation protocol

Coupling the eternal black hole to the bath at $t = 0$ can be modeled as

$$|\psi\rangle_{t=0} = \Big\{ \frac{1}{\sqrt{Z}} \sum_{i=0}^{\infty} \mathrm{e}^{-\frac{\beta}{2}E_i} \, |i\rangle_L \otimes |i\rangle_R \Big\} \otimes |\Omega\rangle_B \, , \tag{5.95}$$

where $|\Omega\rangle_B$ represents the vacuum state of the bath. The bath is attached to the right exterior, so the radiation will move from the right exterior to the bath. The energy of the state $|i\rangle_R$ will decrease and the bath will no longer be in the vacuum state $|\Omega\rangle_B$. The bath is then decoupled from the right exterior and attached to left exterior, so the radiation is then transferred to the left exterior. Even though there is an effective radiation transfer from right to the left exterior, there is no direct interaction between these two entangled subsystems, which are still connected via a non-traversable wormhole. The claims in [18] are that the final state will have the following properties:

1. A pure state;
2. Lower energy in the right than the left exterior (with the state of the quantum fields on the left exterior being more excited than those on the right exterior), and lower than the initial energy in the right exterior;
3. Smaller entanglement between the two subsystems.

These claims are naturally expected from unitary one-sided evaporation of the black hole. If the process is unitary, Claim 1 is obviously satisfied, since the von Neumann entropy is invariant under unitary evolution. Claim 2 also makes sense, since the transfer of radiation

from the right to the left exterior will definitely lower the energy in the right exterior, while lowering the energy in the left one. Although the reason for the entanglement entropy change in Claim 3 may not be as obvious in the dual theory, it can be motivated by events in the bulk. The two boundary theories are entangled, and being dual to a double-sided black hole in the bulk, they are connected via a wormhole. As a result of the one-sided evaporation of the black hole, the geometry of the spacetime, and hence of the wormhole, must have changed, hence changing the entanglement between the boundary theories. It should be noted that this is also expected from a double-sided evaporation; i.e. the simultaneous evaporation of both exterior regions, since this will also cause the wormhole to shrink, hence lowering the corresponding entanglement entropy between the boundary regions.

In our quest for a unitary evaporation model in the dual theory, we will look for one which reproduces these claims.

Note: One way to approach the question about unitarity in the dual theory is to search for an operator that would achieve the unitary one-sided evaporation by acting on the whole initial system, including the bulk and the bath, described by the state $|\psi\rangle_{t=0}$ in (5.95). Such an operator would need to act on the initial state in such a way, that the final state has higher energy in the L subsystem (since the left exterior has absorbed all the radiation) and there is a vacuum state in both the R subsystem (which is the completely evaporated right exterior) and the bath (since all the radiation has been transferred from the bath to L).

However, instead of an operator that acts on the whole (AdS bulk + bath) system, we will model the action of the bath as an operator acting on the AdS bulk, and hence search for such a bath operator that achieves the one-sided evaporation unitarily. The reason why we choose to model the bath as this operator (rather than looking for an operator that acts of the whole bulk and bath system) is motivated by the reason these models study black hole evaporation in AdS in the first place. It is useful to recall that this reason was due to the AdS/CFT correspondence, which guarantees that AdS black holes must evolve unitarily, due to their dual description being a conformal field theory, which is inherently unitary. However, having coupled the bulk to the bath, which is an additional gravitational system, the gravity side of the correspondence has been altered. Of course, one might argue that since the bath is described by a flat spacetime, it should not affect to the "AdS" part of the AdS/CFT duality. However, even though the exact metric of the bath should not make a difference to the evaporation protocol,[45]

[45]To explain this, it is helpful to recall the transparent boundary conditions between the bulk and the bath, which allowed the black hole evaporation into the bath. They were achieved by the following steps: First, a Weyl transformation was performed on the AdS bulk, transforming it to a flat spacetime. This caused the originally vanishing AdS stress-energy tensor (since the black hole is a vacuum solution) to pick up a contribution, hence resulting in a flat bulk spacetime with a non-vanishing stress-energy tensor. It was this stress-energy tensor that was identified as the stress-energy tensor in the bath, allowing energy flow from the flat bulk to the flat bath. Since this choice for the bath stress-energy tensor was achieved by performing a Weyl transformation that maps the bulk and bath to the same metric, one could have, identically, just used an AdS bath and identified the vanishing stress-energy tensor in the AdS bulk as the stress-energy tensor in the AdS bath. However, even though an AdS bath would also achieve the evaporation, this solution to the issue with large black hole evaporation in AdS is a bit trivial. It would be equivalent to simply considering a small black hole in AdS, since the addition of an AdS bath would enlarge the AdS space, effectively making the black hole smaller. This is not the approach in [18], where the effective size of the black hole is not changed (since the size of the AdS bulk is not changed), and the issue is fixed by changing the boundary conditions. Another way to think about why the metric in the bath does not affect the evaporation protocol, is to remember that the evaporation protocol, as previously established in [69], and discussed in Sections 5.2.2 and 5.2.3, did not specify where the radiation was absorbed, except that it was collected at the holographic boundary. This

since the total spacetime is now no longer simply AdS, unitary evolution of the whole (AdS bulk + bath) system is not necessarily guaranteed by the AdS/CFT correspondence (since the dual description is not necessarily simply a CFT). Hence, to summarize, it is a unitary evolution in the AdS bulk that is guaranteed by the AdS/CFT correspondence, rather than unitary evolution of the whole (AdS bulk + bath). Therefore, in our search for a unitary dual description of the one-sided black hole evaporation, we will not focus on the whole (AdS bulk + bath) system, but rather on just the AdS bulk theory, which should definitely be unitary, since its dual is definitely a CFT theory.

Indeed, as discussed in Section 5.2.4, the black hole evolution in the bulk was shown to be unitary, as illustrated by the black hole Page curve in Figure... And since all computation for this black hole evolution took place in the bulk, with all quantum extremal surfaces contributing to the black hole entropy being in the bulk, one should expect that the dual to this one-sided evaporation evolves unitarily too. The aim for the rest of this section is to model the evolution in this dual theory (which we will describe with the TFD), and check if it is unitary indeed, as one should expect. Note that this is not necessarily true for the dual description of the evolution of the Hawking radiation, which although was argued to be unitary in the gravity theory (since it also resulted in a Page curve for the Hawking radiation), the gravity theory used for the calculation was not just the AdS, but the whole (AdS bulk + bath), since the entropy of the Hawking radiation contained contributions from extremal surfaces in the bath region.

Hence, the question we wish to address is: Can the action of the bath on the TFD state, be used to model the dual of the one-sided black hole evaporation unitarily, while also satisfying the three claims about the final state? Based on Claim 2, the energy in the right exterior is lowered, while the energy in the left exterior is raised. This can be modeled via lowering the excitations of the energy eigenstates in R, while increasing the excitations of those in L. The reason for this was discussed in Section 4.4, where we found that the raising operator in the AdS_3 bulk can be related to the excitation operators in the dual CFT_2 theory. Although we have not derived this specifically for the AdS_2/CFT_1 duality, we will assume that this still holds true. So any radiation that has entered the left exterior will be dual to higher excitations in the Lsubsystem (the CFT_L theory). Conversely, the radiation leaving the right exterior will be dual to lower excitations in the the R subsystem (the CFT_R theory. An intuitive choice for such a protocol is to use the ladder operators $\{\hat{a}_{L/R}, \hat{a}^\dagger_{L/R}\}$ of the CFT theory. The energy eigenstates can be constructed from the creation operators acting on the CFT vacuum state, which is annihilated via the lowering operators; i.e. $a_{L/R}|0\rangle = 0$. To be more precise, the ladder operators raise and lower the excitation of the energy eigenstates according to

$$\hat{a}_{L/R}|i\rangle = C_{i,-}|i-1\rangle_{L/R} \tag{5.96}$$

$$\hat{a}^\dagger_{L/R}|i\rangle = C_{i,+}|i+1\rangle_{L/R}\ , \tag{5.97}$$

where $C_{i,\pm}$ are constants that depend on the quantum numbers i, required to ensure the ladder operators do not commute.[46]The total TFD Hamiltonian depends on the individual

model, however, did not transfer the collected radiation back into the bulk.

[46]The precise form of these functions depends on the theory in use. Although the theory is a CFT, the dimensionality of the theory has not been specified here, and this would have implications on the $C_{i,\pm}$ functions.

Hamiltonians of the subsystems, namely $H = H_R - H_L$, such that

$$\begin{aligned} H_L &= E\,\hat{a}_L^\dagger \hat{a}_L \\ H_R &= E\,\hat{a}_R^\dagger \hat{a}_R\,, \end{aligned} \tag{5.98}$$

where the reason both subsystems have the same energy (and temperature) is a property of the TFD formalism, in which the subsystems are not interacting with each other. [47]

Using the ladder operators, an operator that would achieve the desired lowering of excitations in R, while raising the excitation in L is the operator

$$\hat{\mathcal{A}} = \hat{a}_L^\dagger \otimes \hat{a}_R\,, \tag{5.99}$$

where for now we focus on the simplest case, in which there is a single excitation exchange between the subsystems. The $\hat{\mathcal{A}}$ operator should not be confused with the number operator which appears in the Hamiltonian and is defined as

$$\hat{N}_{L/R} = \hat{a}_{L/R}^\dagger \hat{a}_{L/R}\,, \tag{5.100}$$

where $\hat{N}_L$ and $\hat{N}_R$ count the number of particles in the L and R subsystems respectively, such that $\hat{N}_{L/R}|i\rangle_{L/R} = n_{L/R}|i\rangle_{L/R}$. Acting on the TFD state with the $\hat{\mathcal{A}}$ operator yields the state

$$\hat{\mathcal{A}}|\mathrm{TFD}\rangle = \frac{1}{\sqrt{Z}}\sum_{i=0}^{\infty} \mathrm{e}^{-\frac{\beta}{2}E_i}\left(\hat{a}_L^\dagger \otimes \hat{a}_R\right)\left(|i\rangle_L \otimes |i\rangle_R\right) = \frac{1}{\sqrt{Z}}\sum_{i=1}^{\infty} \mathrm{e}^{-\frac{\beta}{2}E_i} C_{i,+}C_{i,-}|i+1\rangle_L \otimes |i-1\rangle_R \tag{5.101}$$

where the sum over energy eigenstates now begins at $i = 1$, since the lowest energy eigenstate must be the vacuum state $|0\rangle$. However, the operator $\hat{\mathcal{A}}$ is not unitary; i.e. $\hat{\mathcal{A}}\hat{\mathcal{A}}^\dagger = \hat{\mathcal{A}}^\dagger\hat{\mathcal{A}} \neq I$, since the ladder operators are not Hermitian. This means that modeling the evaporation in this way will not be unitary, and hence not reversable.

The same final state can be achieved by acting on the TFD with another operator, which we define by

$$\hat{\mathcal{O}}_{(1)} = \sum_{i=0}^{\infty}\sum_{j=1}^{\infty} |i+1\rangle_{LL}\langle i| \otimes |j-1\rangle_{RR}\langle j|\,, \tag{5.102}$$

where one of the sums in the definition of the operator starts from $j = 1$ because the lowest energy eigenstate is always the vacuum state $|0\rangle$; i.e. $|j-1\rangle_R$ does not make sense if $j = 0$. The operator acts on the TFD state such that

$$\begin{aligned} \hat{\mathcal{O}}_{(1)}|\mathrm{TFD}\rangle &= \frac{1}{\sqrt{Z}}\sum_{i=0}^{\infty}\sum_{j=1}^{\infty}\sum_{k=0}^{\infty} \mathrm{e}^{-\frac{\beta}{2}E_k}\left(|i+1\rangle_{LL}\langle i| \otimes |j-1\rangle_{RR}\langle j|\right)\left(|k\rangle_L \otimes |k\rangle_R\right) \\ &= \frac{1}{\sqrt{Z}}\sum_{i=0}^{\infty}\sum_{j=1}^{\infty}\sum_{k=0}^{\infty} \mathrm{e}^{-\frac{\beta}{2}E_k}\,|i+1\rangle_{LL}\langle i|k\rangle_L \otimes |j-1\rangle_{RR}\langle j|k\rangle_R \\ &= \frac{1}{\sqrt{Z}}\sum_{i=1}^{\infty} \mathrm{e}^{-\frac{\beta}{2}E_i}\,|i+1\rangle_L \otimes\, |i-1\rangle_R\,. \end{aligned} \tag{5.103}$$

[47] Since the two subsystems are entangled, they are connected via a wormhole. The interaction restriction comes from the requirement that the wormhole is non-traversable. Allowing interaction between the two boundaries makes the wormhole traversable [91]. This will be discussed more later on.

Note that, unlike the ladder operators, which contributed additional factors, depending on the specific theory, when acting on the energy eigenstates, this operator is independent on any specific properties of the theory, and does not contribute any additional factors when acting on the energy eigenstates. The density matrix of this new state is given by

$$\rho^{(1)}_{LR} = \hat{\mathcal{O}}_{(1)}|\text{TFD}\rangle\langle\text{TFD}|\hat{\mathcal{O}}^{\dagger}_{(1)} = \frac{1}{Z_{(1)}}\sum_{i=1}^{\infty}\sum_{j=1}^{\infty}\mathrm{e}^{-\frac{\beta}{2}(E_i+E_j)}\Big(|i+1\rangle_{LL}\langle j+1|\otimes|i-1\rangle_{RR}\langle j-1|\Big)\,, \tag{5.104}$$

where to have a properly normalized quantum state; i.e. one that satisfies $\text{Tr}[\rho^{(1)}_{LR}] = 1$, we have re-defined the partition function, such that $Z_{(1)} = \sum_{i=1}\mathrm{e}^{-\beta E_i}$. When compared to the partition function of the TFD state in (5.88), one can notice that the new partition function is smaller, since it no longer has a contribution from the ground state energy E_0. This decrease in the value of the thermal partition function demonstrates a decrease in the number of available microstates and will naturally have implications on the thermodynamic properties of the system, some of which will be explored later. It can be seen from the density matrix that the new L subsystem seems to have higher excitations than it did in the TFD state. On the other hand, the new R subsystem seems to have lower excitations than it did in the TFD state. This will be more clear when looking at the reduced density matrices later.

Besides lowering the excitation in R and raising the excitation in L, Claim 1 for the final state in the dual theory is that it should be a pure state. One can verify that $\rho^{(1)}_{LR}$ is indeed a pure state by calculating the purity, defined as $\text{Tr}[(\rho^{(1)}_{LR})^2]$. For a pure state ρ, by definition $\rho^2 = \rho$, so $\text{Tr}[\rho^2] = \text{Tr}[\rho] = 1$, while for a mixed one, $\text{Tr}[\rho^2] < 1$. Indeed, this can be shown to be true via

$$\begin{aligned}
&\text{Tr}[(\rho^{(1)}_{LR})^2] = \\
&= \text{Tr}\Big[\frac{1}{Z^2_{(1)}}\sum_{i=1}^{\infty}\sum_{j=1}^{\infty}\sum_{k=1}^{\infty}\sum_{l=1}^{\infty}\mathrm{e}^{-\frac{\beta}{2}(E_i+E_j+E_k+E_l)}\Big(|i+1\rangle_L\otimes|i-1\rangle_R\Big) \\
&\qquad\qquad\Big({}_L\langle j+1|\otimes{}_R\langle j-1|\Big)\Big(|k+1\rangle_L\otimes|k-1\rangle_R\Big)\Big({}_L\langle l+1|\otimes{}_R\langle l-1|\Big)\Big] \\
&= \frac{1}{Z^2_{(1)}}\text{Tr}\Big[\sum_{i=1}^{\infty}\sum_{j=1}^{\infty}\sum_{k=1}^{\infty}\sum_{l=1}^{\infty}\mathrm{e}^{-\frac{\beta}{2}(E_i+E_j+E_k+E_l)}\Big(|i+1\rangle_L\otimes|i-1\rangle_R\Big)\delta_{jk}\Big({}_L\langle l+1|\otimes{}_R\langle l-1|\Big)\Big] \\
&= \frac{1}{Z^2_{(1)}}\text{Tr}\Big[\sum_{i=1}^{\infty}\sum_{l=1}^{\infty}\mathrm{e}^{-\frac{\beta}{2}(E_i+E_l)}\Big(|i+1\rangle_L\otimes|i-1\rangle_R\Big)\Big({}_L\langle l+1|\otimes{}_R\langle l-1|\Big)\sum_{j=1}^{\infty}\mathrm{e}^{-\beta E_j}\Big] \\
&= \frac{1}{Z_{(1)}}\text{Tr}\Big[\sum_{i=1}^{\infty}\sum_{l=1}^{\infty}\mathrm{e}^{-\frac{\beta}{2}(E_i+E_l)}\Big(|i+1\rangle_L\otimes|i-1\rangle_R\Big)\Big({}_L\langle l+1|\otimes{}_R\langle l-1|\Big)\Big] \\
&= \text{Tr}[\rho^{(1)}_{LR}] \\
&= 1\,,
\end{aligned} \tag{5.105}$$

showing that coupling to the bath does result in a pure final state. To verify Claim 2 more

precisely, one needs to look at the reduced density matrices which are given by

$$\rho_L^{(1)} = \mathrm{Tr}_R \rho_{LR}^{(1)} = \frac{1}{Z_{(1)}} \sum_{i=1}^{\infty} \mathrm{e}^{-\beta E_i} \, |i+1\rangle_{LL}\langle i+1| \tag{5.106}$$

$$\rho_R^{(1)} = \mathrm{Tr}_L \rho_{LR}^{(1)} = \frac{1}{Z_{(1)}} \sum_{i=1}^{\infty} \mathrm{e}^{-\beta E_i} \, |i-1\rangle_{RR}\langle i-1| \, . \tag{5.107}$$

Looking at these expressions, it can be seen that acting with the $\hat{\mathcal{O}}_{(1)}$ operator on the TFD state, the quantum numbers of the energy eigenstates of the R subsystem got lowered (with 1), while those of the L subsystem got raised (with 1) as required. The system R has lost energy and the system L has gained energy, as required by Claim 2. It is interesting to also notice that while the lowest energy eigenstate in the R subsystem is still the vacuum state $|0\rangle_R$, the lowest energy eigenstate in the L subsystem is now the $|2\rangle_L$ state.

The next claim that we need to check is Claim 3, namely whether the coupling to the bath acts in a way that lowers the entanglement between the two subsystems. Since the density matrix (5.104) is pure, its entropy is still $S(\rho_{LR}^{(1)}) = 0$ by definition. The system is also still entangled, because the state (5.103) cannot be written as a product state. However, the entanglement entropy between the subsystems, namely $S(\rho_R^{(1)}) = S(\rho_L^{(1)})$, could have changed. This can be checked, as before, by using the reduced density matrices, which gives

$$\begin{aligned} S(\rho_R^{(1)}) &= -\mathrm{Tr}[\rho_R^{(1)} \log \rho_R^{(1)}] \\ &= -\sum_{i=1}^{\infty} \lambda_i(\rho_R^{(1)}) \log \lambda_i(\rho_R^{(1)}) \\ &= -\sum_{i=1}^{\infty} \frac{\mathrm{e}^{\beta E_i}}{Z_{(1)}} \log \frac{\mathrm{e}^{\beta E_i}}{Z_{(1)}} \\ &= \frac{1}{Z_{(1)}} \sum_{i=1}^{\infty} \mathrm{e}^{\beta E_i} \left(\beta E_i + \log Z_{(1)}\right) \end{aligned} \tag{5.108}$$

where $\lambda_i(\rho_R^{(1)})$ are the eigenvalues of $\rho_R^{(1)}$. Comparing this to the entanglement entropy (5.94) of the TFD state, it is clear that the entropy has decreased due to the new partition function $Z_{(1)}$ no longer containing one of the energy eigenstates, which is contained in the original partition function Z.

So far we have come up with an operator which reproduces all three claims made in [18] for the properties that the dual theory state should have following the coupling to the bath. However, we have not yet checked the most important property of the operation, namely whether it is unitary. Using the Hermitian conjugate of the $\hat{\mathcal{O}}_{(1)}$ operator , one can show that

the unitarity requirement yields

$$\begin{aligned}
\hat{\mathcal{O}}^{\dagger}_{(1)}\hat{\mathcal{O}}_{(1)} &= \sum_{i=0}^{\infty}\sum_{j=1}^{\infty}\sum_{k=0}^{\infty}\sum_{l=1}^{\infty}\Big(|i\rangle_{LL}\langle i+1|\otimes|j\rangle_{RR}\langle j-1|\Big)\Big(|k+1\rangle_{LL}\langle k|\otimes|l-1\rangle_{RR}\langle l|\Big)\\
&= \sum_{i=0}^{\infty}\sum_{j=1}^{\infty}\sum_{k=0}^{\infty}\sum_{l=1}^{\infty}|i\rangle_{LL}\langle i+1|k+1\rangle_{LL}\langle k|\otimes|j\rangle_{RR}\langle j-1|l-1\rangle_{RR}\langle l|\\
&= \sum_{i=0}^{\infty}\sum_{j=1}^{\infty}\sum_{k=0}^{\infty}\sum_{l=1}^{\infty}\delta_{ik}|i\rangle_{LL}\langle k|\otimes\delta_{jl}|j\rangle_{RR}\langle l|\\
&= \sum_{i=0}^{\infty}\sum_{j=1}^{\infty}|i\rangle_{LL}\langle i|\otimes|j\rangle_{RR}\langle j|\\
&= \sum_{i=0}^{\infty}|i\rangle_{LL}\langle i|\otimes\sum_{j=1}^{\infty}|j\rangle_{RR}\langle j|\\
&= \hat{\mathcal{I}}_L\otimes(\hat{\mathcal{I}}_R-|0\rangle_{RR}\langle 0|)\\
&\neq \hat{\mathcal{I}}_{LR}\,,
\end{aligned}\tag{5.109}$$

where the last step follows from noticing that there is a state missing from identity operator of the L subsystem, namely the ground state $|0\rangle_L$, so $\sum_{i=0}^{\infty}|i\rangle_{LL}\langle i| = \hat{\mathcal{I}}_L \neq \sum_{i=1}^{\infty}|i\rangle_{LL}\langle i|$. Similarly, to be unitary, the operator also needs to satisfy $\hat{\mathcal{O}}_{(1)}\hat{\mathcal{O}}^{\dagger}_{(1)} = 1$, which is also violated. Repeating the above calculation gives $\hat{\mathcal{O}}_{(1)}\hat{\mathcal{O}}^{\dagger}_{(1)} = (\hat{\mathcal{I}}_L - |0\rangle_{LL}\langle 0|)\otimes\hat{\mathcal{I}}_R \neq \hat{\mathcal{I}}_{LR}$. Hence, even though it satisfies all claims we expect from the evolution of the dual theory, this operator, just like $\hat{\mathcal{A}}$, is not unitary.

Although we have used a non-unitary operation, we have still ended up with another pure state.[48] The final state is still a TFD-like state with more-excited energy eigenstates in the L subsystem and less-excited energy eigenstates in the R subsystem formed by transferring a single excitation from R to L. It is interesting to note that such an operator can also produce a state that one could expect from the complete evaporation of the right exterior. A complete evaporation of the black hole right exterior would result in a vacuum state in R. A slightly different version of the $\hat{\mathcal{O}}_{(1)}$ operator can be used to transfer all the excitations from the R subsystem to the L subsystem, ending up with a vacuum in R, while keeping a superposition of excited states in L. This is achieved via the operator $\hat{\mathcal{O}}_{(i)}$, defined as

$$\hat{\mathcal{O}}_{(i)} = \sum_{i=0}^{\infty}\sum_{j=0}^{\infty}|2i\rangle_{LL}\langle i|\otimes|0\rangle_{RR}\langle j|\,.\tag{5.110}$$

Note that, unlike $\hat{\mathcal{O}}_{(1)}$, both summations starts from 0, so the partition function will not have

[48] Note that it is not necessary to use a unitary operator to go from one pure state to another, if one recalls, for example, the projection operator, P. Consider a simple pure state $|\phi\rangle_i = \alpha|0\rangle + |1\rangle$, such that $|\alpha|^2 + |\beta|^2 = 1$. Now, acting on this state with the projection operator $P = |0\rangle\langle 0|$, yields $P|\phi\rangle_i = \alpha|0\rangle$. Of course, this new state is not normalized yet, since $\mathrm{Tr}[P\phi\rangle_i] \neq 1$. Normalizing it yields that the final state is $|\phi\rangle_f = P|\phi\rangle_i/\sqrt{{}_i\langle\phi|P|\phi\rangle_i} = |0\rangle$, which is, again, pure. The projection operator has projected the initial pure state onto the $|0\rangle$ pure state. However, the projection operator is not unitary, since $P^{\dagger} = |0\rangle\langle 0| = P$, so $P^{\dagger}P = P \neq 1$.

to be changed. The operator $\hat{\mathcal{O}}_{(i)}$ acts on the TFD state such that

$$\begin{aligned}\hat{\mathcal{O}}_{(i)}|\text{TFD}\rangle &= \frac{1}{\sqrt{Z}}\sum_{i=0}^{\infty}\sum_{j=0}^{\infty}\sum_{k=0}^{\infty}\mathrm{e}^{-\frac{\beta}{2}E_k}\Big(|2i\rangle_{LL}\langle i|\otimes|0\rangle_{RR}\langle j|\Big)\Big(|k\rangle_L\otimes|k\rangle_R\Big)\\ &= \frac{1}{\sqrt{Z}}\sum_{i=0}^{\infty}\mathrm{e}^{-\frac{\beta}{2}E_i}\,|2i\rangle_L\otimes|0\rangle_R\,. \end{aligned} \tag{5.111}$$

The density matrix of this state is hence given by

$$\rho_{LR}^{(i)} = \frac{1}{Z}\sum_{i=0}^{\infty}\sum_{j=0}^{\infty}\mathrm{e}^{-\frac{\beta}{2}(E_i+E_j)}\Big(|2i\rangle_{LL}\langle 2j|\otimes|0\rangle_{RR}\langle 0|\Big) \tag{5.112}$$

One can see that the state is, in fact, a product state, since it can be written in the form $\rho_{LR}^{(i)} = \rho_L^{(i)}\otimes\rho_R^{(i)}$. Since the state is now a separable state, it is no longer entangled. It is a general property that a pure reduced density matrix $\rho_R^{(i)}$, irrespective of the purity of the other one, namely $\rho_L^{(i)}$, means that the state $\rho_{LR}^{(i)}$ is not entangled. In our case both reduced density matrices are pure and given by

$$\rho_L^{(i)} = \mathrm{Tr}_R\rho_{LR}^{(i)} = \frac{1}{Z}\sum_{i=0}^{\infty}\sum_{j=0}^{\infty}\mathrm{e}^{-\frac{\beta}{2}(E_i+E_j)}\,|2i\rangle_{LL}\langle 2j| \tag{5.113}$$

$$\rho_R^{(i)} = \mathrm{Tr}_L\rho_{LR}^{(i)} = \frac{1}{Z}|0\rangle_{RR}\langle 0|\,\sum_{i=0}\mathrm{e}^{-\beta E_i} = |0\rangle_{RR}\langle 0| \tag{5.114}$$

Starting from the TFD state and completely evaporating one side of the black hole, we have gone from an entangled pure state to an unentangled pure product state. One could, again, motivate this result by considering what a complete evaporation of the one-sided black hole would look like in the bulk. Since the right exterior has evaporated completely, resulting in a vacuum state in R, this means that the black hole on the right side of the wormhole, which initially connected the two subsystems, is now gone. Since the final geometry has a single black hole, there is no wormhole connecting the two boundaries, so the entanglement between them has been destroyed.

Besides the fact that the operator does not satisfy the unitarity condition, another way to show why both this method and the ladder operator method are irreversible is via the following highly simplified example. What we, effectively, want to achieve is reversibly lower and then raise the energy eigenstates of one of the subsystems. We will focus on the R subsystem and assume, for simplicity, that it is $(d+1)$-dimensional; i.e. the energy eigenstates $\{|i\rangle_R\}$ form an orthonormal basis of the $(d+1)$-dimensional Hilbert space, $\mathcal{H}_R$. Consider a generic state in the R subsystem, given by

$$|\psi\rangle_R = \alpha_0|0\rangle_R + \alpha_1|1\rangle_R + \alpha_2|2\rangle_R + \alpha_3|3\rangle_R + \ldots + \alpha_d|d\rangle_R\,, \tag{5.115}$$

such that in order for the state to be properly normalized; i.e. ${}_R\langle\psi|\psi\rangle_R = 1$, requires to impose a condition on the amplitudes α_i, namely that $\sum_{i=0}^{d}|\alpha_i|^2 = 1$. Acting on this state either with the lowering operator $\hat{a}_R$ or with the operator $\sum_{i=1}|i-1\rangle_{RR}\langle i|$ (the part of $\hat{\mathcal{O}}_{(1)}$, which acts as to lower the eigenstates), yields

$$|\psi'\rangle_R = \alpha_1|0\rangle_R + \alpha_2|1\rangle_R + \alpha_3|2\rangle_R + \ldots + \alpha_d|d-1\rangle_R\,, \tag{5.116}$$

which should now be normalized, such that $\sum_{i=1}^{d} |\alpha_i|^2 = 1$. Although this has successfully lowered the eigenstates, one can see that the process is irreversible since we have effectively lost one of the states (by having annihilated the vacuum state), which is not recoverable. This can be seen by performing the reverse process, namely acting either with the raising operator $\hat{a}_R^\dagger$ or with the operator $\sum_{i=0} |i+1\rangle_{RR}\langle i|$ (the part of $\hat{\mathcal{O}}_{(1)}$, which acts as to raise the eigenstates), which gives

$$|\psi''\rangle_R = \alpha_1|1\rangle_R + \alpha_2|2\rangle_R + \alpha_3|3\rangle_R + \ldots + \alpha_d|d\rangle_R \,, \tag{5.117}$$

showing that the vacuum eigenstate $|0\rangle_R$ has been lost from the system. This loss of information is expected from an irreversible and hence a non-unitary model. Additionally, one can see that acting with the lowering operator on the state in (5.115) d times, gives simply $\alpha_d|0\rangle_R$, which is simply the vacuum state (after normalizing). Reversing this process by acting on this vacuum state with the raising operator d times would simply give the highly excited $|d\rangle_R$ state, rather than a superposition of states. Hence, due to the annihilation of the vacuum states, this method would not be able to recover the initial state (5.115).

This naturally gives rise to the question: What if one lowers the energy eigenstates, but never annihilates a vacuum state? Consider starting with the same state in the R subsystem, namely (5.115). Suppose there exists an operator which acts on the state, such that it lowers all energy eigenstates, except for the vacuum state, which is kept the same. An example of such an operator is

$$\hat{\mathcal{Q}} = |0\rangle_{RR}\langle 0| + \sum_{i=1}^{d} |i-1\rangle_{RR}\langle i| \,, \tag{5.118}$$

such that $\hat{\mathcal{Q}}|0\rangle_R = |0\rangle_R$, $\hat{\mathcal{Q}}|1\rangle_R = |0\rangle_R$, $\hat{\mathcal{Q}}|2\rangle_R = |1\rangle_R$ etc. When $\hat{\mathcal{Q}}$ acts on the state in (5.115), it gives

$$\begin{aligned}\hat{\mathcal{Q}}|\psi\rangle_R &= \Big(|0\rangle_{RR}\langle 0| + \sum_{i=1}^{d} |i-1\rangle_{RR}\langle i|\Big)\Big(\alpha_0|0\rangle_R + \alpha_1|1\rangle_R + \alpha_2|2\rangle_R + \alpha_3|3\rangle_R + \ldots + \alpha_d|d\rangle_R\Big) \\ &= \alpha_0|0\rangle_R + \alpha_1|0\rangle_R + \alpha_2|1\rangle_R + \alpha_3|2\rangle_R + \ldots + \alpha_d|d-1\rangle_R \\ &= (\alpha_0+\alpha_1)|0\rangle_R + \alpha_2|1\rangle_R + \alpha_3|2\rangle_R + \ldots + \alpha_d|d-1\rangle_R \,, \end{aligned} \tag{5.119}$$

which should now be normalized according to $|\alpha_0 + \alpha_1|^2 + \sum_{i=2}^{d} |\alpha_i|^2 = 1$. Although the vacuum state was not annihilated this time, reversing the process by simply raising each of the energy eigenstates would, again, result in losing information about this initial vacuum state. This is because using the inverse of the $\hat{\mathcal{Q}}$ cannot only raise the vacuum state with the α_1 prefactor, while not acting on the vacuum state that has the α_0 prefactor. Hence, reversing the process would result in a state similar to (5.117), though with different amplitudes. This is more evident if one considers acting with the $\hat{\mathcal{Q}}^d$ operator, which results in

$$\hat{\mathcal{Q}}^d|\psi\rangle_R = (\alpha_0 + \alpha_1 + \ldots + \alpha_d)|0\rangle_R \,, \tag{5.120}$$

which once normalized would become simply the vacuum state $|0\rangle_R$. As before, reversing this process would not result in a superposition of states, such as in (5.115), but rather a single excited energy eigenstate $|d\rangle_R$. In any way, these operators cause a loss of information when acting on a state, and are hence irreversible.

So far, we have come up with an operator which acts on the initial TFD state, satisfying all claims in [18] for the final state. Although the final state obtained agrees with what is expected from, either partial, or complete one-sided black hole evaporation, the bath operator used to achieve this was shown to be non-unitary. Hence, our proposed model for the evolution in the dual theory is not unitary. However, the evolution of the black hole inside the bulk was shown to be unitary. The questions we need to address now are: What went wrong? What is unitary way to model our bath operator? Is there a unitary bath operator that satisfies all the claims expected from a one-sided unitary black hole evaporation?

What went wrong?
The goal of the previous section was to employ the claims in [18] about the dual of the proposed one-sided black hole evaporation. We also motivated the reason why these claims are indeed what should be expected from the process (if it is unitary). As claimed, a bath operator was found that acted on the pure TFD state and successfully transferred excitations from the R to the L subsystems, lowering their entanglement, resulting in a final pure state. However, the operation found was shown to be non-unitary. The key to resolving this issue lies in recognizing that there are different types of unitary operations, namely *global unitary* and *local unitary* operations. A general local (unitary or non-unitary) operator $\hat{\mathcal{O}}_{\text{Local}}$ is one that can be written as a tensor product of local operations, such that $\hat{\mathcal{O}}_{\text{Local}} = \hat{\mathcal{O}}_L \otimes \hat{\mathcal{O}}_R$. A global operator is one that cannot be written as a tensor product of local operations; i.e. $\hat{\mathcal{O}}_{\text{Global}} \neq \hat{\mathcal{O}}_L \otimes \hat{\mathcal{O}}_R$. Although a global unitary should exist from a pure state of a Hilbert space to another pure state of that same Hilbert space, this is not the type of operator that we have considered so far. Instead, we tried to model the bath operator as a local operator, such that both the partial evaporation operator $\hat{\mathcal{O}}_{(1)}$ in (5.102) and the complete evaporation operator $\hat{\mathcal{O}}_{(i)}$ in (5.110) are local operators. This can be seen more clearly by rewriting them as

$$\begin{aligned}
\hat{\mathcal{O}}_{(1)} &= \sum_{i=0}^{\infty} |i+1\rangle_{LL}\langle i| \otimes \sum_{j=1}^{\infty} |j-1\rangle_{RR}\langle j| = \hat{\mathcal{O}}^L_{(1)} \otimes \hat{\mathcal{O}}^R_{(1)} = (\hat{\mathcal{O}}^L_{(1)} \otimes \hat{\mathcal{I}}^R_{(1)})(\hat{\mathcal{I}}^R_{(1)} \otimes \hat{\mathcal{O}}^R_{(1)}) \\
\hat{\mathcal{O}}_{(i)} &= \sum_{i=0}^{\infty} |2i\rangle_{LL}\langle i| \otimes \sum_{j=0}^{\infty} |0\rangle_{RR}\langle j| = \hat{\mathcal{O}}^L_{(i)} \otimes \hat{\mathcal{O}}^R_{(i)} = (\hat{\mathcal{O}}^L_{(i)} \otimes \hat{\mathcal{I}}^R_{(i)})(\hat{\mathcal{I}}^R_{(i)} \otimes \hat{\mathcal{O}}^R_{(i)})
\end{aligned} \tag{5.121}$$

One might wonder about the reason why a local operator was considered, instead of a global one, since it is global unitarity that is required to validate the operation. The reason we modeled our bath operator as a local operator is due to the way the bath is described to operate in the one-sided black hole evaporation model. The bath is first only coupled to the right exterior to absorb all the radiation from the evaporating black hole, and then only coupled to the left exterior to release all the collected radiation back into the bulk. This is the reason we chose to model the bath via a local operator, which first acts only on the right subsystem via $(\hat{\mathcal{I}}^L_{(i)} \otimes \hat{\mathcal{O}}^R_{(i)})$ and then acts only on the L subsystem via $(\hat{\mathcal{O}}^L_{(i)} \otimes \hat{\mathcal{I}}^R_{(i)})$. To be more precise, since the bath operator acts on each of the subsystems independently of the other subsystem, namely first acting only on R and then acting only on L, it seems to be acting locally.

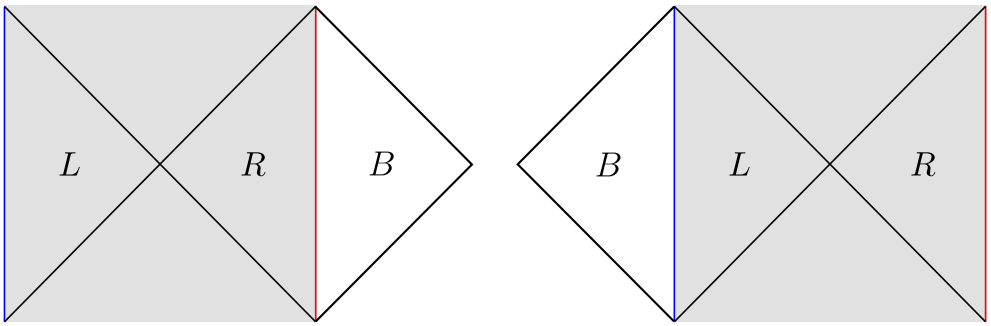

Figure 5.22: The action of the bath operator is local, since the bath operator acts on each of the subsystems independently of the other subsystem. Such a local bath operator, if unitary, will not be able to change the entanglement structure between the two asymptotic CFT theories. The only way for this local bath to achieve the desired lowering of the entanglement entropy due to the black hole evaporation will be if it is a non-unitary operator.

Although the local operation achieved the desired lowering of entanglement, the reason why it is not unitary, and most importantly, why it cannot be unitary, is because local unitary operations cannot change the entanglement structure. We modeled the bath as a local operator, and effectively forced it to act in a way such that it lowered the entanglement, which can only be achieved locally via a non-unitary operation. Hence, if we wish to model the locally-acting bath as a unitary operator, we cannot expect it to change the entanglement between the R and L subsystems. Similarly, if we with to model the bath operation as a unitary operation that indeed changes the entanglement, it cannot be local.

Note that so far we have looked at the entanglement change at the end of the evaporation process. However, the emission from the right exterior happens before the absorption into the left exterior, since the transfer of the radiation is not continuous (the bath is not a traversable wormhole connecting both exterior regions), so bath needs to first be disconnected from R and then connected to L. However, the entanglement entropy should change even before the radiation has been transferred to the left exterior, since the right black hole now has a lower mass (or no mass if it was completely evaporated). This means that we would need to already see entanglement change from the bath operation on just the right exterior. Again, this operation was modeled as the local operator $(\hat{\mathcal{I}}^L_{(i)} \otimes \hat{\mathcal{O}}^R_{(i)})$, which, if indeed causes an entanglement change, cannot be unitary. If we impose it to unitary, it cannot change the entanglement entropy, unless we make it global.

This naturally raises some confusion, since the entanglement between the boundary theories should inevitably change during a one-sided black hole evaporation, precisely because the evaporation would change the geometry and hence the wormhole connecting the two boundaries. Hence, to achieve the one-sided black hole evaporation, we need an operator that is either a **local non-unitary** operator or a **global unitary** operator. Since a non-unitary evolution is not desirable (since it is not reversible), we will focus on the global unitary case.

Of course, as mentioned before, there should indeed exist a global unitary operator that can achieve the one-sided evaporation, while transferring excitation and lowering entanglement, since global purity (of the total state) has been preserved during the process. Such an operator should enable an interaction between the two subsystems. [49] However, this does not necessarily

[49] Note that besides an interaction between the two subsystems, the entanglement between them can also be

mean that this operation can be achieved via the bath, especially by the way it is described to be acting. The questions we wish to address now are: 1) Can a bath be modeled as a global unitary operation? and 2) Can such a global unitary bath achieve a one-sided evaporation?

One might still say that even though that is not how we defined our bath operator, when coupled to the right exterior, the bath somehow ALSO affects the left exterior. However, to address this possibility, one should recall that in the TFD formalism, even though the entanglement between the two boundary CFTs is reflected in the presence of a wormhole in the bulk, the two subsystems in the TFD are non-interacting, and the wormhole is non-traversable. Hence, coupling the bath only to the right exterior should not affect the left exterior, unless there is an interaction between them, and hence a traversable wormhole. Equivalently, acting with an operator on just the R subsystem (i.e. locally), should not affect the L subsystem, unless there is an interaction between them.

It is precisely an interaction between the subsystems that we need our global bath operator to enable, such that it can unitarily decrease the entanglement between the two subsystems. However, we do not seek an interaction via the traversable wormhole inside the bulk, as that would: 1) not necessarily lead to Hawking radiation leaving the right exterior of the wormhole into the bath; 2) defeat the whole purpose of attaching an auxiliary system to the bulk.

One scenario to consider is the coupling of the bath to both exterior regions, as illustrated in Figure 5.23. To achieve an evaporation of only the right exterior, one would need to use different baths (with different temperatures) on each side, such that the left exterior does not evaporate into B_L. However, this also does not imply an interaction between the regions. The baths would need to be disconnected from the bulk, joined together so that the the radiation collected from R into B_R can now be transferred from B_R to B_L, and then re-attached to the bulk again, so that the radiation can not be transferred from B_L to L. This is identical to the previous case, since the evaporation of the right exterior into B_R still does not affect the left exterior, hence acting. This model, however, has been used to study the double-side black hole evaporation, in which case both exterior regions evaporate into the bath [92, 93]

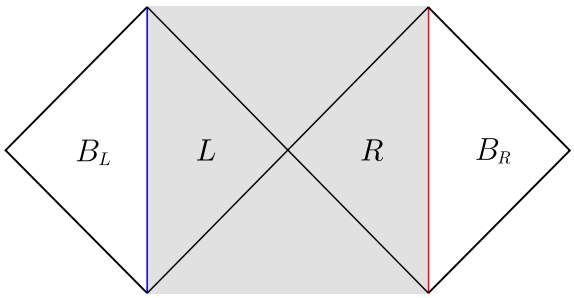

Figure 5.23: A bath attached to both exteriors of the black hole. However, since there is still no interaction between them, this should lead to the same issue. Furthermore, unless the two baths are at different temperatures, this arrangement will not lead in just a one-sided black hole evaporation, but to an evaporation of both black holes, which is not what we require.

destroyed via a measurement on any one of them. However, this is also not a unitary process, since it causes the collapse of the wavefunction, which is not reversible.

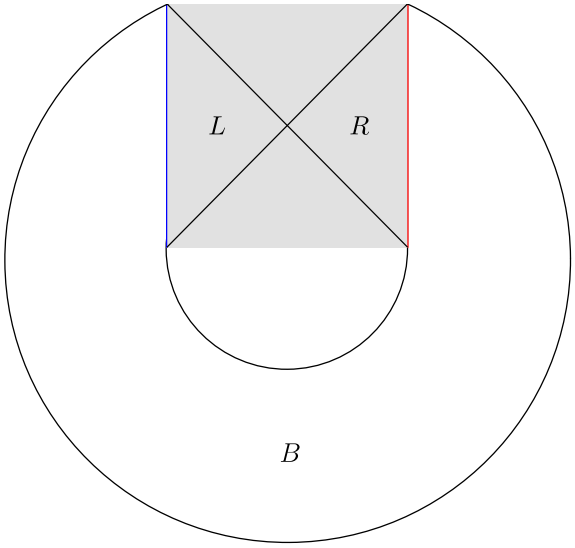

Figure 5.24: A globally-acting bath that causes an interaction between the left and right exterior regions. However, to achieve the one-sided evaporation from the right to the left exterior, the bath would need to have a continuous temperature gradient starting from very low temperature at the right exterior, and having a very high temperature at the left exterior.

A bath that enables an interaction between both subsystems can be one that is coupled to both of them, as illustrated in Figure 5.24, which resembles the traversable wormhole solution. However, the bath is still described by a flat spacetime. The issue now is that if we were to use the same evaporation protocol as the one for the one-sided evaporation, both the right and the left exterior regions will evaporate into the black hole. To have only the right exterior region evaporate, the Hawking radiation to go into the bath and travel to the left exterior, there needs to be a controlled temperature gradient all the way across the bath, such that the temperature of the bath region close to the right exterior is very low (lower than the temperature of the right exterior), while the temperature of the bath region very close to the left exterior is very high (higher than the temperature of the right exterior).

That being said...
It should be noted that a huge assumption was also made in the search for the bath operator, namely the temperature was assumed to be constant. The initial state is an entangled state between two subsystems which are at equal temperatures $T = 1/\beta$. Having moved energy from one system to the other adiabatically; i.e. while keeping the entropy of the total system fixed (at zero), should lead to a change in temperature in each of the two subsystems. One way of seeing this more clearly is that evaporating the black hole, which is dual to R, its mass has decreased, hence changing its temperature. Simultaneously, the mass of the black hole dual to L has gained mass and hence its temperature has also changed. This needs to also be incorporated into the model. That being said, the final state obtained from acting with th complete evaporation bath operator was the vacuum state in the R subsystem, which is at zero temperature, as expected.

Although, the bath operator used to achieve the one-sided evaporation was not unitary, the final state we achieved from acting with this operator on the TFD is indeed what we would expect from the complete evaporation, namely: destroyed entanglement between the previously entangled subsystems of the TFD, and a transfer of all the excitation from the R subsystem to the L subsystem, leaving the former in a zero temperature vacuum state, while the latter is still a superposition of energy eigenstates at some non-zero temperature. Even though the TFD considered did not include an explicit interaction term between the two subsystems, the transfer of classical information from the R to L subsystem, should be possible via the bath, just as it would be possible via the traversable wormhole. This transfer of classical information can be used to model the one-sided evaporation via an LOCC channel, which is a type of quantum teleportation protocol.

5.3.3 Disentangling the TFD via an LOCC channel

The conformal boundaries of the TFD state, namely CFT_L and CFT_R, are non-interacting. The two systems are entangled, and so the geometries associated with them are connected via a wormhole. Since traversable wormholes are not allowed in general relativity, because of the possible faster-than-light signal transfer, it is the non-traversability of the wormhole that ensures there are no interactions between the two TFD subsystems [94]. Nonetheless, due to the entanglement between the two systems, it is natural to wonder if they might be able to somehow "communicate" with each other. Despite the restrictions from general relativity, interactions between the two quantum systems living on the boundaries have been shown to be possible[95]. Due to the dual nature of the eternal AdS black hole, namely its quantum mechanical description, one could introduce an interaction term in the TFD formalism, hence allowing the two systems to interact. This makes it possible for the transfer of classical information between the two boundaries via the resulting traversable wormhole, which can be modelled as a quantum teleportation protocol [91]. The interaction between the two subsystems can be achieved via a double-trace deformation, which yields a symmetric evolution of L and R, and hence of the left and right black hole exterior regions, such that they both increase or decrease in size simultaneously [96]. This does change the entanglement entropy between the L and R subsystems, but it does not describe a one-sided evaporation. The question is: Can quantum teleportation be used to describe the one-sided evaporation model?

In the next section we model the one-sided evaporation by exploring a different type of quantum teleportation protocol, namely an LOCC channel, which does not rely on the double-trace formalism that evolves both subsystems evenly. As we will see, an LOCC channel makes use of classical communication between two entangled systems, and can be used to convert from one pure state to another pure state with a lower entanglement entropy. Although the LOCC channel is not invertible, and hence non-unitary, it is a model for a quantum channel from an entangled TFD state to a disentangled state, which can be used to describe the one-sided evaporation of the AdS black hole.

Review of the LOCC protocol

At the heart of entanglement theory is the notion of the "distant lab", where a multipartite quantum system is distributed over several parties. Two parties, called Alice and Bob, can be at a large distance from each other. They cannot perform global operations on the state they share and are hence restricted to act only locally on their respective subsystems. However, this local action does allow them to perform local measurements and transmit classical data; i.e. share the results of their measurements [97].

In this section we will review this type of quantum operations, which are known as Local Operations Classical Communication (LOCC). The name comes from the fact that these quantum channels are implemented solely through *local operations* and *classical communication*. Local operations (such as a local quantum channel) refer to operations restricted to act only on one subsystem at a time; i.e. not on the density matrix of the multipartite system ρ_{AB}, but only on one of the reduced density matrices (ρ_A or ρ_B). Classical communication describes the exchange of classical data between the subsystems, such as results from a measurement. It has been shown that entanglement cannot be increased via these processes. In particular, if a state ρ_{AB} has been converted to a state ρ'_{AB} via an LOCC, then ρ_{AB} must have at least as much entanglement as ρ'_{AB}, since it cannot be increased via the LOCC.

The basic idea is the following: Alice and Bob share an entangled state. Alice performs a measurement and sends this classical measurement outcome to Bob (via a classical channel). Bob then applies a quantum channel, depending on this measurement, to obtain the desired result. The LOCC protocol can be used to achieve different tasks, such as *state discrimination* (uses communication to distinguish states which have the same reduced density matrices and cannot be distinguished with local measurements alone), *entanglement distillation* (uses LOCC to convert an arbitrary number of copies of weakly-entangled state to a smaller number of maximally entangled pairs) and others.

To properly define an LOCC channel, it is useful to first recall some important concepts in quantum information theory, starting with the notion of a *measurement*, which has been schematically represented in Figure 5.25 [98].

Definition : (Measurement) A measurement on some Hilbert space $\mathcal{H}$ is a function μ that produces an outcome x in some finite set Ω such that

$$\mu : \Omega \to \mathrm{PSD}(\mathcal{H}) \quad \text{and} \quad \sum_{x\in\Omega} \mu(x) = \mathcal{I} \,, \tag{5.122}$$

where PSD stands for *positive semidefinite*. $A \in \mathrm{PSD}(\mathcal{H})$ if A is Hermitian and all its eigenvalues a_i are nonnegative (i.e. $a_i \geq 0$).

For a quantum system in a state ρ, the probability of a certain outcome x following a measurement is given by *Born's rule*, which states

$$P(x) = \mathrm{Tr}[\mu(x)\rho] \,. \tag{5.123}$$

Indeed, using (5.122) yields $\sum_x P(x) = \sum_x \mathrm{Tr}[\mu(x)\rho] = \mathrm{Tr}[\sum_x \mu(x)\rho] = 1$ as required.

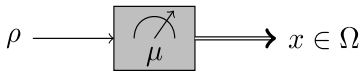

Figure 5.25: Measurement of a quantum state is an operation that acts on a quantum state to produce a classical outcome x [98].

A convenient choice of measurement is the *basis measurement*, which is defined in terms of an arbitrary orthonormal basis $\{|\psi_x\rangle\} \in \mathcal{H}$ as $\mu = |\psi_x\rangle\langle\psi_x|$, in which case the probability of a certain outcome x becomes $P(x) = \langle\psi_x|\rho|\psi_x\rangle$.[50]

So far the state measured was the global state of the quantum system. For a multipartite system, one can also define a measurement on one of the subsystems. For example, for a bipartite state ρ_{AB}, a measurement μ_A can be made on the subsystem A, as illustrated in Figure 5.26.

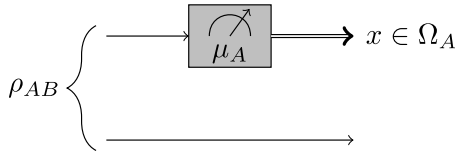

Figure 5.26: Measurement of subsystem A, which acts on subsystem A to give a classical outcome x, but it does not act on the other subsystem [98].

The probability of a specific outcome is then given by

$$P(x) = \mathrm{Tr}[(\mu_A(x) \otimes \mathcal{I}_B)\rho_{AB}] \,, \tag{5.124}$$

which closely resembles Bohr's rule above. It should be noted, for completeness, that joint measurements of the two subsystems are also possible, as illustrated in Figure 5.27. Applying a measurement $\mu_A(x)$ on the subsystem A and a measurement $\mu_B(y)$ on the subsystem B, the probability of outcomes $x \in \Omega_A$ and $y \in \Omega_B$ is given by

$$P(x, y) = \mathrm{Tr}[(\mu_A(x) \otimes \mu_B(y))\rho_{AB}] \tag{5.125}$$

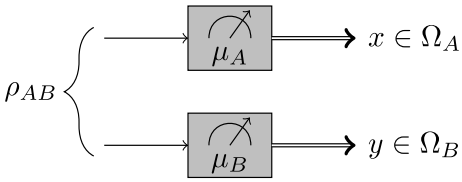

Figure 5.27: Joint measurement of subsystems A and B. The measurement μ_A on subsystem A gives the classical outcome x, while the measurement μ_B on subsystem B gives the classical outcome y [98].

As will be discussed later, local measurements on the subsystems play a key role in the operational principle of the LOCC channel.

Another important operation to consider is the *quantum channel*. As opposed to a classical measurement outcome, the outcome of a quantum channel is a quantum state; i.e. a quantum channel maps quantum states to quantum states, as illustrated in Figure 5.28, where $\Phi[\rho_A] = \rho_B$, namely the channel acts on some state ρ_A to give another state ρ_B. The more formal definition of a quantum channel is given below.

[50] For example, for the qubit state $\rho = |0\rangle\langle 0|$, one can use the basis $\{|0\rangle, |1\rangle\}$. Then $P(0) = \langle 0|\rho|0\rangle = 1$ and $P(1) = \langle 1|\rho|1\rangle = 0$ as expected.

Definition : (Quantum channel) The superoperator[51] $\Phi_{A\to B}$ is a quantum channel; i.e. $\Phi_{A\to B} \in \mathrm{C}(\mathcal{H}_A, \mathcal{H}_B)$, if it is
(a) Completely positive: For all $\mathcal{H}_R$ and $M_{AR} \geq 0$, $\Phi_{A\to B} \in \mathrm{CP}(\mathcal{H}_A, \mathcal{H}_B)$ if $(\Phi_{A\to B} \otimes \mathcal{I}_R)[M_{AR}] \geq 0$
(b) Trace preserving: For all M_A, $\mathrm{Tr}[\Phi_{A\to B}[M_A] = \mathrm{Tr}[M_A]]$.

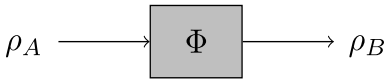

Figure 5.28: A quantum channel Φ maps a state ρ_A to another state ρ_B, such that $\Phi[\rho_A] = \rho_B$ [98].

The trivial quantum channel is the *identity channel* $\mathcal{I}_A$, which maps the state to itself, namely $\mathcal{I}_A[\rho_A] = \rho_A$ (or, equivalently, is the absence of any operation).

The concepts of a measurement (i.e. a classical outcome) and a channel (i.e. a quantum state outcome) can be combined into the notion of an *instrument*. Indeed, an instrument is an operation that produces both a classical outcome and a quantum state, as illustrated in Figure 5.29.

Definition : (Instrument) An instrument is a set of completely positive maps, denoted by $\{\Phi_{A\to B,x}\} \in \mathrm{CP}(\mathcal{H}_A, \mathcal{H}_B)$, such that $\sum_x \Phi_{A\to B,x} \in \mathrm{C}(\mathcal{H}_A, \mathcal{H}_B)$.

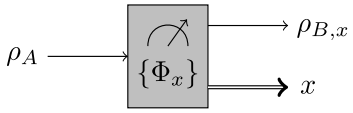

Figure 5.29: An instrument is an operation which acts on a quantum state to produce both a classical output x (as a measurement does) and a quantum state $\rho_{B,x}$ (as a quantum channel does) [98].

Being equipped with the above definitions, one can define an LOCC channel, illustrated in Figure 5.30

Definition : (LOCC channel) A channel $\Xi_{AA'\to BB'}$ is called a one-way LOCC channel from A to B if

$$\Xi_{AA'\to BB'}[\rho_{AB}] = \sum_x (\Phi_{A\to A',x} \otimes \Psi_{B\to B',x})[\rho_{AB}] \,, \tag{5.126}$$

where $\{\Phi_{A\to A',x}\}$ is a collection of instruments acting on the subsystem A to generate a set $\{x\}$ of classical outputs and a set of quantum states, which are sent to the subsystem B. These quantum states are then acted on by a set of quantum channels $\{\Psi_{B\to B',x}\}$, which reproduce the state required by the LOCC protocol.

[51] A superoperator is an operator that maps operators to operators.

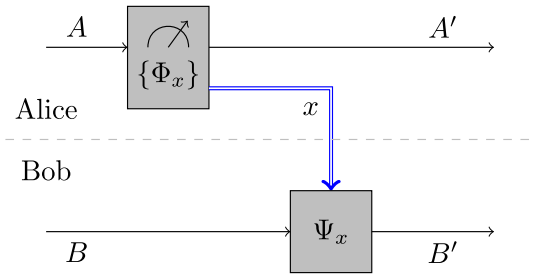

Figure 5.30: The way the LOCC protocol works is that subsystem A acts locally on itself with a set of instruments $\{\Phi_{A\to A',x}\}$, which generate a set $\{x\}$ of classical outputs and a set of quantum states, which are then sent to the subsystem B. These quantum states are then acted on by a set of quantum channels $\{\Psi_{B\to B',x}\}$, which reproduce the state required by the LOCC protocol. [98].

Note, the more familiar quantum teleportation protocol is an example of an LOCC protocol.

Modeling the complete evaporation via an LOCC

In this section, we wish to check if the evolution from the TFD state (5.88) to the completely evaporated disentangled state (5.112) can be described via an LOCC channel. Hence, we wish to check if the following operation is possible:

$$\rho_{RL} \xrightarrow[?]{\text{LOCC}} \rho'_{RL} \,, \tag{5.127}$$

where

$$\rho_{RL} = \frac{1}{Z}\sum_{i=0}^{\infty}\sum_{j=0}^{\infty} \mathrm{e}^{-\frac{\beta}{2}(E_i+E_j)} \Big(|i\rangle_{RR}\langle j| \otimes |i\rangle_{LL}\langle j| \Big) \tag{5.128}$$

$$\rho'_{RL} = \frac{1}{Z}\sum_{i=0}^{\infty}\sum_{j=0}^{\infty} \mathrm{e}^{-\frac{\beta}{2}(E_i+E_j)} \Big(|0\rangle_{RR}\langle 0| \otimes |2i\rangle_{LL}\langle 2j| \Big) \,. \tag{5.129}$$

Since both states ρ_{RL} and ρ'_{RL} are pure, one can use *Nielsen's Theorem*, which provides a way of checking if an LOCC protocol is allowed, by using just the initial and final states.

Theorem : (Nielsen) Let ρ_{RL} and ρ'_{RL} be two pure states on $\mathcal{H}_R \otimes \mathcal{H}_L$. Then the following statements are equivalent:
(a) $\rho_R \prec \rho'_R$.
(b) There exists a one-way LOCC channel Ξ from R to L, such that $\Xi[\rho_{RL}] = \rho'_{RL}$.
Interchanging the roles of the R and L systems, the following statements are also equivalent:
(c) $\rho_L \prec \rho'_L$.
(d) There exists a one-way LOCC channel Ξ from L to R, such that $\Xi[\rho_{RL}] = \rho'_{RL}$.

Nielsen's theorem makes use of *majorization*, denoted by "$\prec$".

Definition : (Majorization) Consider two vectors $x, y \in \mathbb{R}^n$. Then $x \prec y$ ("x is majorized by y" or "y majorizes x") if

$$\sum_{i=1}^{k} x_i^{\downarrow} \leq \sum_{i=1}^{k} y_i^{\downarrow} \quad \text{and} \quad \sum_{i=1}^{n} x_i = \sum_{i=1}^{n} y_i \,, \tag{5.130}$$

where $k \in \{1, 2, \ldots, n-1\}$ and $x_i^{\downarrow}$ is used to denote the eigenvalues of x sorted in a non-increasing order, such that $x_1^{\downarrow} \geq x_2^{\downarrow} \geq \ldots \geq x_n^{\downarrow}$.

We wish to check if there exists an LOCC from R to L, such that $\Xi[\rho_{RL}] = \rho'_{RL}$. By Nielsen's theorem, it is sufficient to verify that $\rho_R \prec \rho'_R$, since the statements (a) and (b) are equivalent. This requires using the "quantum extension" of majorization, which deals with Hermitian operators instead of real vectors.

Definition : (Majorization for Hermitian operators) For two Hermitian operators A and B, with eigenvalues $\lambda(A)$ and $\lambda(B)$ respectively, $A \prec B$ iff $\lambda(A) \prec \lambda(B)$.

Using this definition for the case of the density matrices ρ_R and ρ'_R implies that the majorization between the reduced density matrices can be written as majorization between their eigenvalues, namely $\rho_R \prec \rho'_R \iff \lambda(\rho_R) \prec \lambda(\rho'_R)$. Using the majorization definition (5.130), this gives the following requirement for the existence of the LOCC channel we require:

$$\sum_{i=0}^{k} \lambda_i(\rho_R)^{\downarrow} \leq \sum_{i=0}^{k} \lambda_i(\rho'_R)^{\downarrow} \quad \text{and} \quad \sum_{i=0}^{\infty} \lambda_i(\rho_R) = \sum_{i=0}^{\infty} \lambda_i(\rho'_R) \tag{5.131}$$

To validate this expression, one first needs to evaluate the reduced density matrices and their eigenvalues, which are given by

$$\rho_R = \frac{1}{Z} \sum_{i=0} \mathrm{e}^{-\beta E_i} \, |i\rangle_{RR}\langle i| \quad \text{with} \quad \lambda(\rho_R)^{\downarrow} = \left\{ \frac{\mathrm{e}^{-\beta E_0}}{Z}, \frac{\mathrm{e}^{-\beta E_1}}{Z}, \ldots, \frac{\mathrm{e}^{-\beta E_\infty}}{Z} \right\} \tag{5.132}$$

$$\rho'_R = |0\rangle_{RR}\langle 0| \qquad \text{with} \quad \lambda(\rho'_R)^{\downarrow} = \Big\{ 1, 0, \ldots, 0 \Big\} \,. \tag{5.133}$$

To verify the second condition in (5.131) is sufficient to recall that $Z = \sum_i \mathrm{e}^{-\beta E_i}$ and thus

$$\sum_{i=0}^{\infty} \lambda_i(\rho_R) = 1 = \sum_{i=0}^{\infty} \lambda_i(\rho'_R) \tag{5.134}$$

The first condition in (5.131) can be verified by noticing that $\mathrm{e}^{-\beta E_i}/Z < 1$ for all i. Hence,

$$\sum_{i=0}^{k} \lambda_i(\rho_R)^{\downarrow} = \left[\underbrace{\frac{\mathrm{e}^{-\beta E_0}}{Z}}_{<1} + \underbrace{\frac{\mathrm{e}^{-\beta E_1}}{Z}}_{<1} + \ldots + \underbrace{\frac{\mathrm{e}^{-\beta E_k}}{Z}}_{<1} \right] \leq \Big[1 + 0 + \ldots + 0 \Big] = \sum_{i=0}^{k} \lambda_i(\rho'_R)^{\downarrow} \,, \tag{5.135}$$

with the equality being satisfied only when $k \to \infty$. Hence, $\rho_R \prec \rho'_R$, and by Nielsen's theorem, there exists an LOCC from R to L, such that $\Xi[\rho_{RL}] = \rho'_{RL}$.

Another theorem, which follows from Nielsen's theorem is *Uhlmann's Theorem*, which states that this majorization condition implies the existence of a mixed unitary channel.

Theorem : (Uhlmann) For two Hermitian operators A and B on some Hilbert space $\mathcal{H}$, then $A \prec B$ iff there exists a mixed-unitary channel $\Phi \in C(\mathcal{H})$ such that $\Phi[B] = A$.

A mixed unitary channel is defined as a superposition of unitary channels.

Definition : (Mixed-unitary channel) A channel $\Phi \in \mathrm{C}(\mathcal{H})$ is called mixed-unitary if

$$\Phi[M] = \sum_x q_x U_x M U_x^\dagger \tag{5.136}$$

for a probability distribution q_x and a set of unitaries $U_x \in U(\mathcal{H})$.

However, note that the action of this mixed unitary channel (implied from Uhlmann's theorem) is in the opposite direction to the action of the LOCC (implied from Nielsen's theorem). Although it might seem irrelevant, Uhlmann's theorem will be important in the derivation of the LOCC protocol.

Having established that an LOCC protocol is possible, the aim for the rest of this section is to find the LOCC that converts the TFD state (5.128) into the disentangled state (5.129). This would involve the R subsystem to use an instrument to send classical information obtained locally to the L subsystem. The L subsystem can then apply a unitary channel, again locally, to obtain the desired state. Using the LOCC definition, the LOCC is given by

$$\Xi[\rho_{RL}] = \sum_x (\Phi_{R,x} \otimes \Psi_{L,x})[\rho_{RL}] = \rho'_{RL} \tag{5.137}$$

We begin by finding the instrument $\Phi_{R,x}$. This can be done by using Uhlmann's theorem and the definition (5.136) of a mixed-unitary channel. Since $\rho_R \prec \rho'_R$, this means there exists a mixed unitary channel, such that

$$\rho_R = \sum_x q_x U_{R,x} \rho'_R U_{R,x}^\dagger \,. \tag{5.138}$$

The instrument $\Phi_{R,x}$ is defined as

$$\Phi_{R,x}[M] = Y_{R,x} M Y_{R,x}^\dagger \,, \tag{5.139}$$

where, using (5.138), the unitaries $Y_{R,x}$ can be written as

$$Y_{R,x} = \sqrt{q_x}\sqrt{\rho'_R} U_{R,x}^\dagger \sqrt{\rho_R}^{-1} \,. \tag{5.140}$$

Substituting the expressions for ρ_R (5.132) and ρ'_R (5.133) into (5.138) yields the following equation for the unitaries

$$\frac{1}{Z}\sum_{i=0}^{\infty} \mathrm{e}^{-\beta E_i} \, |i\rangle_{RR}\langle i| = \sum_{x=0}^{\infty} q_x U_{R,x} |0\rangle_{RR}\langle 0| U_{R,x}^\dagger \,, \tag{5.141}$$

which can be written in a matrix form that gives

$$\frac{1}{Z}\begin{pmatrix} \mathrm{e}^{-\beta E_0} & 0 & \cdots & 0 \\ 0 & \mathrm{e}^{-\beta E_1} & \cdots & 0 \\ \vdots & \vdots & \ddots & \vdots \\ 0 & 0 & \cdots & \mathrm{e}^{-\beta E_\infty} \end{pmatrix} = \sum_{x=0}^{\infty} q_x U_{R,x} \begin{pmatrix} 1 & 0 & \cdots & 0 \\ 0 & 0 & \cdots & 0 \\ \vdots & \vdots & \ddots & \vdots \\ 0 & 0 & \cdots & 0 \end{pmatrix} U_{R,x}^{\dagger} \,. \tag{5.142}$$

To obtain the values of q_x and the unitaries $U_{R,x}$ one can use *permutation matrices*. A permutation matrix P is a square binary matrix with a single entry of 1 on each row and column, with the rest being 0. The unit matrix I is a special case of the permutation matrix, with every 1 being on the diagonal of the matrix. There are $n!$ permutation matrices of size $n \times n$, also known as permutation matrices of order n. For example, the permutation matrices of order 2 and 3 are given by

$$n = 2 : \begin{pmatrix} 1 & 0 \\ 0 & 1 \end{pmatrix}, \begin{pmatrix} 0 & 1 \\ 1 & 0 \end{pmatrix} \tag{5.143}$$

$$n = 3 : \begin{pmatrix} 1 & 0 & 0 \\ 0 & 1 & 0 \\ 0 & 0 & 1 \end{pmatrix}, \begin{pmatrix} 1 & 0 & 0 \\ 0 & 0 & 1 \\ 0 & 1 & 0 \end{pmatrix}, \begin{pmatrix} 0 & 1 & 0 \\ 1 & 0 & 0 \\ 0 & 0 & 1 \end{pmatrix}, \begin{pmatrix} 0 & 1 & 0 \\ 0 & 0 & 1 \\ 1 & 0 & 0 \end{pmatrix}, \begin{pmatrix} 0 & 0 & 1 \\ 1 & 0 & 0 \\ 0 & 1 & 0 \end{pmatrix}, \begin{pmatrix} 0 & 0 & 1 \\ 0 & 1 & 0 \\ 1 & 0 & 0 \end{pmatrix} \tag{5.144}$$

Permutation matrices satisfy $PP^T = 1$, hence the transpose of a permutation matrix is its inverse; i.e. $P^{-1} = P^T$. For a matrix M, PM gives a permutation of the rows of M; i.e. P acts as to move along the columns of M. Reversing the order of the multiplication, MP^T gives a permutation of the columns of M; i.e. P acts to move along the rows of M. Using this property, one can use permutation matrices to move along the diagonal of a matrix M via PMP^T. Additionally, since these matrices are real, $P^\dagger = P^T$. This can be used in (5.142) to move the entry 1 of ρ'_R down its diagonal in order to obtain the non-zero diagonal values of ρ_R.

For example, using the permutation matrices of order 2 in (5.143), the 2×2 case of (5.142), namely the case that only includes the contribution from $\{E_0, E_1\}$, given by

$$\frac{1}{Z}\sum_{i=0}^{1} \mathrm{e}^{-\beta E_i} \, |i\rangle_{RR}\langle i| = \sum_{x=0}^{1} q_x U_{R,x} |0\rangle_{RR}\langle 0| U_{R,x}^{\dagger} \,, \tag{5.145}$$

can be solved with

$$q_0 = \mathrm{e}^{-\beta E_0}/Z \;,\; U_{R,0} = U_{R,0}^{\dagger} = \begin{pmatrix} 1 & 0 \\ 0 & 1 \end{pmatrix} \tag{5.146}$$

$$q_1 = \mathrm{e}^{-\beta E_1}/Z \;,\; U_{R,1} = U_{R,1}^{\dagger} = \begin{pmatrix} 0 & 1 \\ 1 & 0 \end{pmatrix} \,. \tag{5.147}$$

Similarly, solving the 3×3 case, namely the one that includes contributions from $\{E_0, E_1, E_2\}$, given by

$$\frac{1}{Z}\sum_{i=0}^{2} \mathrm{e}^{-\beta E_i}\ |i\rangle_{RR}\langle i| = \sum_{x=0}^{2} q_x U_{R,x}|0\rangle_{RR}\langle 0|U_{R,x}^{\dagger}\ , \tag{5.148}$$

requires using only some of the permutation matrices of order 3, and is solved with

$$q_0 = \mathrm{e}^{-\beta E_0}/Z\ ,\ U_{R,0} = U_{R,0}^{\dagger} = \begin{pmatrix} 1 & 0 & 0 \\ 0 & 1 & 0 \\ 0 & 0 & 1 \end{pmatrix} \tag{5.149}$$

$$q_1 = \mathrm{e}^{-\beta E_1}/Z\ ,\ U_{R,1} = U_{R,1}^{\dagger} = \begin{pmatrix} 0 & 1 & 0 \\ 1 & 0 & 0 \\ 0 & 0 & 1 \end{pmatrix} \tag{5.150}$$

$$q_2 = \mathrm{e}^{-\beta E_2}/Z\ ,\ U_{R,2} = \begin{pmatrix} 0 & 1 & 0 \\ 0 & 0 & 1 \\ 1 & 0 & 0 \end{pmatrix}\ ,\ U_{R,2}^{\dagger} = \begin{pmatrix} 0 & 0 & 1 \\ 1 & 0 & 0 \\ 0 & 1 & 0 \end{pmatrix}\ . \tag{5.151}$$

This can be generalized to the $d \times d$ case, which includes all terms $\{E_0, \ldots, E_{d-1}\}$, and is given by

$$\frac{1}{Z}\sum_{i=0}^{d} \mathrm{e}^{-\beta E_i}\ |i\rangle_{RR}\langle i| = \sum_{x=0}^{d} q_x U_{R,x}|0\rangle_{RR}\langle 0|U_{R,x}^{\dagger}\ . \tag{5.152}$$

This general case can be solved in the same way and the solution is given by

$$q_0 = \mathrm{e}^{-\beta E_0}/Z\ ,\ U_{R,0} = U_{R,0}^{\dagger} = \mathcal{I}_d \tag{5.153}$$

$$q_1 = \mathrm{e}^{-\beta E_1}/Z\ ,\ U_{R,1} =: P_{1,2}^{(d)}\ ,\ U_{R,1}^{\dagger} =: P_{1,2}^{(d)\dagger} \tag{5.154}$$

$$\vdots$$

$$q_{d-1} = \mathrm{e}^{-\beta E_{d-1}}/Z\ ,\ U_{R,d-1} =: P_{1,d}^{(d)}\ ,\ U_{R,d-1}^{\dagger} =: P_{1,d}^{(d)\dagger} \tag{5.155}$$

Here we have defined the permutation matrix $P_{1,d}^{(d)}$ as a permutation matrix of order d, which switches row 1 and row d of a $d \times d$ matrix M via $P_{1,d}^{(d)}M$. Hence, it moves the element $(1,1)$ of M to the position of the element $(1,d)$. Similarly, its complex conjugate $P_{1,d}^{(d)\dagger} = P_{1,d}^{(d)T}$ switches column 1 and column d of the matrix M via $MP_{1,d}^{(d)\dagger}$. Hence, it moves the element $(1,1)$ of M to the position of the element $(d,1)$. Acting with both permutation matrices via $P_{1,d}^{(d)}MP_{1,d}^{(d)\dagger}$ acts as to move along the diagonal of M and moves the element $(1,1)$ to the position of the element (d,d). The trivial permutation matrix is the identity matrix, given by $P_{1,1}^{(d)} = \mathcal{I}_d$, such that $P_{1,1}^{(d)}MP_{1,1}^{(d)\dagger}$ does not move the element $(1,1)$. Hence, using the above generalization, equation (5.142) is solved by $q_x = \mathrm{e}^{-\beta E_x}/Z$, $U_{R,x} = P_{1,x+1}^{(x)}$ and $U_{R,x}^{\dagger} = P_{1,x+1}^{(x)\dagger}$.

This can be substituted into (5.140) to find an expression for $Y_{R,x}$, which yields

$$\begin{aligned}
Y_{R,x} &= \sqrt{q_x}\sqrt{\rho'_R}U^\dagger_{R,x}\sqrt{\rho_R}^{-1} \\
&= \mathrm{e}^{-\frac{\beta E_x}{2}}\begin{pmatrix}1&0&\cdots&0\\0&0&\cdots&0\\\vdots&\vdots&\ddots&\vdots\\0&0&\cdots&0\end{pmatrix}P^{(x)\dagger}_{1,x+1}\begin{pmatrix}\mathrm{e}^{\frac{\beta E_0}{2}}&0&\cdots&0\\0&\mathrm{e}^{\frac{\beta E_1}{2}}&\cdots&0\\\vdots&\vdots&\ddots&\vdots\\0&0&\cdots&\mathrm{e}^{\frac{\beta E_\infty}{2}}\end{pmatrix} \\
&= \mathrm{e}^{-\frac{\beta E_x}{2}}\begin{pmatrix}0&\cdots&1&\cdots&0\\0&\cdots&0&\cdots&0\\\vdots&&\vdots&&\vdots\\0&\cdots&0&\cdots&0\end{pmatrix}\begin{pmatrix}\mathrm{e}^{\frac{\beta E_0}{2}}&0&\cdots&0\\0&\mathrm{e}^{\frac{\beta E_1}{2}}&\cdots&0\\\vdots&\vdots&\ddots&\vdots\\0&0&\cdots&\mathrm{e}^{\frac{\beta E_\infty}{2}}\end{pmatrix} \\
&= \mathrm{e}^{-\frac{\beta E_x}{2}}\begin{pmatrix}0&\cdots&\mathrm{e}^{\frac{\beta E_x}{2}}&\cdots&0\\0&\cdots&0&\cdots&0\\\vdots&&\vdots&&\vdots\\0&\cdots&0&\cdots&0\end{pmatrix} \\
&= \begin{pmatrix}0&\cdots&1&\cdots&0\\0&\cdots&0&\cdots&0\\\vdots&&\vdots&&\vdots\\0&\cdots&0&\cdots&0\end{pmatrix}, \qquad (5.156)\\
&\qquad \mathrm{Col}_1 \qquad \mathrm{Col}_{x+1} \qquad \mathrm{Col}_\infty
\end{aligned}$$

where we have used that the square root of a diagonal matrix is obtained by simply taking the square root of all the eigenvalues (diagonal elements). In the third line we have used that the permutation matrix $P^{(x)\dagger}_{1,x+1}$ acts on a matrix M is such that the operation $MP^{(x)\dagger}_{1,x+1}$ moves the first column of the matrix M to the location of its $x+1$ column. Hence, the $Y_{R,x}$ unitary matrices have only one non-zero element such that

$$Y_{R,0} = \begin{pmatrix}1&0&\cdots&0\\0&0&\cdots&0\\\vdots&\vdots&\ddots&\vdots\\0&0&\cdots&0\end{pmatrix}, \; Y_{R,1} = \begin{pmatrix}0&1&\cdots&0\\0&0&\cdots&0\\\vdots&\vdots&\ddots&\vdots\\0&0&\cdots&0\end{pmatrix}, \; \ldots, \; Y_{R,\infty} = \begin{pmatrix}0&0&\cdots&1\\0&0&\cdots&0\\\vdots&\vdots&\ddots&\vdots\\0&0&\cdots&0\end{pmatrix}. \qquad (5.157)$$

These matrices can be written, more conveniently, in the Dirac notation as

$$\begin{aligned}
Y_{R,x} &= |0\rangle\langle x| \\
Y^\dagger_{R,x} &= |x\rangle\langle 0| \, , \qquad (5.158)
\end{aligned}$$

where

$$|0\rangle = \begin{pmatrix}1\\0\\0\\\vdots\\0\end{pmatrix}, \; |1\rangle = \begin{pmatrix}0\\1\\0\\\vdots\\0\end{pmatrix}, \; |2\rangle = \begin{pmatrix}0\\0\\1\\\vdots\\0\end{pmatrix}, \ldots \qquad (5.159)$$

The instrument (5.139) is hence given by

$$\Phi_{R,x}[M] = Y_{R,x} M Y_{R,x}^\dagger = |0\rangle\langle x|M|x\rangle\langle 0| = \langle x|M|x\rangle|0\rangle\langle 0| \tag{5.160}$$

Following the action of the instrument, the state ρ_{RL} transforms into $w_{RL,x}$, given by

$$\begin{aligned}
w_{RL,x} &= (\Phi_{R,x} \otimes \mathcal{I}_L)[\rho_{RL}] \\
&= (Y_{R,x} \otimes \mathcal{I}_L)\rho_{RL}(Y_{R,x}^\dagger \otimes \mathcal{I}_L) \\
&= \Big(|0\rangle\langle x| \otimes \sum_k |k\rangle\langle k|\Big)\rho_{RL}\Big(|x\rangle\langle 0| \otimes \sum_m |m\rangle\langle m|\Big) \\
&= \frac{1}{Z}\sum_{i,j,k,m} \mathrm{e}^{-\frac{\beta}{2}(E_i+E_j)}\Big(|0\rangle\langle x| \otimes |k\rangle\langle k|\Big)\Big(|i\rangle\langle j| \otimes |i\rangle\langle j|\Big)\Big(|x\rangle\langle 0| \otimes |m\rangle\langle m|\Big) \\
&= \frac{1}{Z}\sum_{i,j,k,m} \mathrm{e}^{-\frac{\beta}{2}(E_i+E_j)}\Big(|0\rangle \otimes |k\rangle\Big)\Big(\langle x| \otimes \langle k|\Big)\Big(|i\rangle \otimes |i\rangle\Big)\Big(\langle j| \otimes \langle j|\Big)\Big(|x\rangle \otimes |m\rangle\Big)\Big(\langle 0| \otimes \langle m|\Big) \\
&= \frac{1}{Z}\sum_{i,j,k,m} \Big(|0\rangle \otimes |k\rangle\Big)\underbrace{\delta_{xi}\delta_{ki}}_{\delta_{xk}}\underbrace{\delta_{xj}\delta_{mj}}_{\delta_{xm}}\Big(\langle 0| \otimes \langle m|\Big) \\
&= \frac{1}{Z}\mathrm{e}^{-\beta E_x}\Big(|0\rangle \otimes |x\rangle\Big)\Big(\langle 0| \otimes \langle x|\Big) \\
&= \frac{1}{Z}\mathrm{e}^{-\beta E_x}|0\rangle\langle 0| \otimes |x\rangle\langle x| \,,
\end{aligned} \tag{5.161}$$

such that

$$w_{RL,0} = \begin{pmatrix} 1 & 0 & \cdots & 0 \\ 0 & 0 & \cdots & 0 \\ \vdots & \vdots & \ddots & \vdots \\ 0 & 0 & \cdots & 0 \end{pmatrix}, \; w_{RL,1} = \begin{pmatrix} 0 & 0 & \cdots & 0 \\ 0 & 1 & \cdots & 0 \\ \vdots & \vdots & \ddots & \vdots \\ 0 & 0 & \cdots & 0 \end{pmatrix}, \ldots, w_{RL,\infty} = \begin{pmatrix} 0 & 0 & \cdots & 0 \\ 0 & 0 & \cdots & 0 \\ \vdots & \vdots & \ddots & \vdots \\ 0 & 0 & \cdots & 1 \end{pmatrix} \tag{5.162}$$

The next step in finding the LOCC is to find a unitary channel that can act on this state to give reproduce the state $\rho'_{RL,x}$ as required. This unitary channel is applied by the L subsystem and is defined in terms of the unitary operators $V_{L,x}$ as

$$\Psi_{L,x}[M] = V_{L,x} M V_{L,x}^\dagger \tag{5.163}$$

Demanding that when acted on the state $w_{RL,x}$, the unitary channel correctly constructs the state $\rho'_{RL,x}$ is given by

$$(\mathcal{I}_R \otimes V_{L,x}) w_{RL,x} (\mathcal{I}_R \otimes V_{L,x}^\dagger) = q_x \rho'_{RL} \,. \tag{5.164}$$

To find the unitary matrices $V_{L,x}$ is easier to first trace out the right system in (5.164), which gives

$$V_{L,x} w_{L,x} V_{L,x}^\dagger = q_x \rho'_L \tag{5.165}$$

where $w_{L,x} = \mathrm{Tr}_R[w_{RL,x}] = \frac{\mathrm{e}^{-\beta E_x}}{Z}|x\rangle\langle x|$. Substituting this back into (5.165) gives

$$V_{L,x}|x\rangle\langle x|V_{L,x}^\dagger = \frac{1}{Z}\sum_i\sum_j \mathrm{e}^{-\frac{\beta}{2}(E_i+E_j)}|2i\rangle\langle 2j| \tag{5.166}$$

To solve for the unitary matrices $V_{L,x}$ one can expand can first expand them as

$$V_{L,x} = \sum_m\sum_n V_{mn}^{(x)}|m\rangle\langle n| \ , \tag{5.167}$$

where the basis $|m\rangle$ do not necessarily have to be the energy eigenstates as before, but they will be in this calculation, and the components of the unitaries are $\left(V_{mn}^{(x)}\right)^* = V_{nm}^{(x)}$. Using this expansion and substituting into (5.166) gives

$$\begin{aligned}
\Big(\sum_{mn} V_{mn}^{(x)}|m\rangle\langle n|\Big)|x\rangle\langle x|\Big(\sum_{kl} V_{lk}^{(x)}|k\rangle\langle l|\Big) &= \frac{1}{Z}\sum_i\sum_j \mathrm{e}^{-\frac{\beta}{2}(E_i+E_j)}|2i\rangle\langle 2j| \\
\sum_{k,l,m,n} V_{mn}^{(x)}V_{lk}^{(x)}|m\rangle\langle n|x\rangle\langle x|k\rangle\langle l| &= \frac{1}{Z}\sum_i\sum_j \mathrm{e}^{-\frac{\beta}{2}(E_i+E_j)}|2i\rangle\langle 2j| \\
\sum_{l,m} V_{mx}^{(x)}V_{lx}^{(x)}|m\rangle\langle l| &= \frac{1}{Z}\sum_i\sum_j \mathrm{e}^{-\frac{\beta}{2}(E_i+E_j)}|2i\rangle\langle 2j| \\
\sum_{l,m} V_{mx}^{(x)}V_{lx}^{(x)}\langle n|m\rangle\langle l|k\rangle &= \frac{1}{Z}\sum_i\sum_j \mathrm{e}^{-\frac{\beta}{2}(E_i+E_j)}\langle n|2i\rangle\langle 2j|k\rangle \\
V_{nx}^{(x)}V_{kx}^{(x)} &= \frac{1}{Z}\mathrm{e}^{-\frac{\beta}{2}(E_{n/2}+E_{k/2})} \\
\implies V_{nx}^{(x)} &= \frac{1}{\sqrt{Z}}\mathrm{e}^{-\frac{\beta}{2}E_{n/2}} \ ,
\end{aligned} \tag{5.168}$$

where in the fourth line we have contracted both side of the equation with $\langle n|\ldots|k\rangle$. We find that since all the x dependence is summed over, the unitary matrices $V_{L,x}$ do not depend on the parameter x, so

$$V_{L,x} = \frac{1}{\sqrt{Z}}\sum_n\sum_x \mathrm{e}^{-\frac{\beta}{2}E_{n/2}}|n\rangle\langle x| =: V_L \ . \tag{5.169}$$

The channel is hence also independent of x and given by

$$\begin{aligned}
\Psi_L[M] = V_L M V_L^\dagger &= \frac{1}{Z}\sum_{m,n}\sum_{x,y} \mathrm{e}^{-\frac{\beta}{2}(E_{m/2}+E_{n/2})}|m\rangle\langle x|M|y\rangle\langle n| \\
&= \frac{1}{Z}\sum_{m,n}\sum_{x,y} \mathrm{e}^{-\frac{\beta}{2}(E_{m/2}+E_{n/2})}\langle x|M|y\rangle|m\rangle\langle n|
\end{aligned} \tag{5.170}$$

We can verify that this LOCC channel indeed reproduces the required state by substituting the instrument (5.160) and the channel (5.170) into the definition (5.137) of the LOCC channel,

which gives

$$
\begin{aligned}
&\Xi[\rho_{RL}] = \\
&= \sum_z (\Phi_{R,z} \otimes \Psi_{L,z})[\rho_{RL}] = \\
&= \sum_z (Y_{R,z} \otimes V_L)\rho_{RL}(Y_{R,z}^\dagger \otimes V_L^\dagger) = \\
&= \sum_z \left(|0\rangle_{RR}\langle z| \otimes \Big(\frac{1}{\sqrt{Z}} \sum_m \sum_x \mathrm{e}^{-\frac{\beta}{2}E_{m/2}} |m\rangle_{LL}\langle x| \Big) \right) \rho_{RL} \\
&\qquad\qquad \left(|z\rangle_{RR}\langle 0| \otimes \Big(\frac{1}{\sqrt{Z}} \sum_n \sum_y \mathrm{e}^{-\frac{\beta}{2}E_{n/2}} |y\rangle_{LL}\langle n| \Big) \right) = \\
&= \frac{1}{Z} \sum_z \sum_{m,n} \sum_{x,y} \mathrm{e}^{-\frac{\beta}{2}(E_{m/2}+E_{n/2})} \Big(|0\rangle_{RR}\langle z| \otimes |m\rangle_{LL}\langle x| \Big) \rho_{RL} \Big(|z\rangle_{RR}\langle 0| \otimes |y\rangle_{LL}\langle n| \Big) = \\
&= \frac{1}{Z^2} \sum_z \sum_{m,n} \sum_{x,y} \sum_{i,j} \mathrm{e}^{-\frac{\beta}{2}(E_{m/2}+E_{n/2})} \mathrm{e}^{-\frac{\beta}{2}(E_i+E_j)} \Big(|0\rangle_{RR}\langle z| \otimes |m\rangle_{LL}\langle x| \Big) \Big(|i\rangle_{RR}\langle j| \otimes |i\rangle_{LL}\langle j| \Big) \\
&\qquad\qquad \Big(|z\rangle_{RR}\langle 0| \otimes |y\rangle_{LL}\langle n| \Big) = \\
&= \frac{1}{Z^2} \sum_z \sum_{m,n} \sum_{x,y} \sum_{i,j} \mathrm{e}^{-\frac{\beta}{2}(E_{m/2}+E_{n/2})} \mathrm{e}^{-\frac{\beta}{2}(E_i+E_j)} \Big(|0\rangle_R \otimes |m\rangle_L \Big) \Big({}_R\langle z| \otimes {}_L\langle x| \Big) \\
&\qquad\qquad \Big(|i\rangle_R \otimes |i\rangle_L \Big) \Big({}_R\langle j| \otimes {}_L\langle j| \Big) \Big(|z\rangle_R \otimes |y\rangle_L \Big) \Big({}_R\langle 0| \otimes {}_L\langle n| \Big) = \\
&= \frac{1}{Z^2} \sum_z \sum_{m,n} \sum_{x,y} \sum_{i,j} \mathrm{e}^{-\frac{\beta}{2}(E_{m/2}+E_{n/2})} \mathrm{e}^{-\frac{\beta}{2}(E_i+E_j)} \Big(|0\rangle_R \otimes |m\rangle_L \Big) \underbrace{\delta_{zi}\delta_{xi}}_{\delta_{zx}} \underbrace{\delta_{jz}\delta_{jy}}_{\delta_{zy}} \Big({}_R\langle 0| \otimes {}_L\langle n| \Big) = \\
&= \frac{1}{Z^2} \sum_z \sum_{m,n} \mathrm{e}^{-\frac{\beta}{2}(E_{m/2}+E_{n/2})} \mathrm{e}^{-\beta E_x} \Big(|0\rangle_R \otimes |m\rangle_L \Big) \Big({}_R\langle 0| \otimes {}_L\langle n| \Big) = \\
&= \frac{1}{Z} \sum_{m,n} \mathrm{e}^{-\frac{\beta}{2}(E_{m/2}+E_{n/2})} \Big(|0\rangle_R \otimes |m\rangle_L \Big) \Big({}_R\langle 0| \otimes {}_L\langle n| \Big) = \\
&= \frac{1}{Z} \sum_{m,n} \mathrm{e}^{-\frac{\beta}{2}(E_{m/2}+E_{n/2})} \Big(|0\rangle_{RR}\langle 0| \otimes |m\rangle_{LL}\langle n| \Big) = \\
&= \rho'_{RL}
\end{aligned}
\tag{5.171}
$$

where to see the last equality one can simply relabel $m \to 2i$ and $n \to 2j$.

However, since an LOCC cannot be used to increase entanglement entropy, there is no LOCC channel to model the inverse process, namely from ρ'_{RL} to ρ_{RL}. This can also be seen by verifying that the majorization condition in Nielsen's theorem for the inverse process is not satisfied. Since the channel is not invertible, the process is not unitary.

5.4 Conclusion

In this chapter, we reviewed the recently proposed model for one-sided black hole evaporation [18], which used an auxiliary bath and transparent boundary conditions to allow one-side black hole evaporation. We reviewed the calculations in the bulk, which were based on results in semiclassical JT gravity, to show that the black hole evaporates at an exponential rate, following an inward positive-energy flux, induced from coupling it to the bath. We then reviewed how the generalized gravitational entanglement entropy can be used to show that the proposed black hole evaporation model produces a unitary Page for both the evaporating black hole and the emitted Hawking radiation.

While looking for a way to model this one-sided black hole evaporation in the dual theory, we stumbled onto some confusion as to how it would be possible. We argued that if the action of the bath os modeled as an operator in the dual theory, one-sided evaporation can be achieved vie either a local non-unitary bath operator or a global unitary bath operator. The action of a global bath operator is still unclear, but we have argued that it should involve some interaction between the two exterior regions of the black hole. However, this is not the way we understand the bath to be acting in the original paper, where it seems to be acting only locally.

Assuming such a local bath operator, we also modelled the one-sided black hole evaporation via an LOCC channel, which is non-reversible and hence non-unitary, which as explained, is expected from the operation of such a local bath.

Bibliography

[1] W Israel. "Event horizons in static vacuum spacetimes". In: *Phys. Rev. 164* (1776).

[2] B. Carter. "Axisymmetric black hole has only two degrees of freedom". In: *Phys. Rev. Lett. 26, 331* (1771).

[3] Werner Israel. "Event horizons in static vacuum space-times". In: *Phys. Rev.* 164 (1967), pp. 1776–1779. DOI: 10.1103/PhysRev.164.1776.

[4] Galina Weinstein. *Demons in Black Hole Thermodynamics: Bekenstein and Hawking*. 2021. arXiv: 2102.11209 [physics.hist-ph]. URL: https://arxiv.org/abs/2102.11209.

[5] S. W. Hawking. "Gravitational radiation from colliding black holes". In: *Phys. Rev. Lett.* 26 (1971), pp. 1344–1346. DOI: 10.1103/PhysRevLett.26.1344.

[6] R. Penrose and R. M. Floyd. "Extraction of rotational energy from a black hole". In: *Nature* 229 (1971), pp. 177–179. DOI: 10.1038/physci229177a0.

[7] J. D. Bekenstein. "Black holes and the second law". In: *Lett. Nuovo Cim.* 4 (1972), pp. 737–740. DOI: 10.1007/BF02757029.

[8] Jacob D. Bekenstein. "Black Holes and Entropy". In: *Phys. Rev. D* 7 (8 Apr. 1973), pp. 2333–2346. DOI: 10.1103/PhysRevD.7.2333. URL: https://link.aps.org/doi/10.1103/PhysRevD.7.2333.

[9] James M. Bardeen, B. Carter, and S. W. Hawking. "The Four laws of black hole mechanics". In: *Commun. Math. Phys.* 31 (1973), pp. 161–170. DOI: 10.1007/BF01645742.

[10] S. Hawking. "Black hole explosions?" In: *Nature* 248 (1974), pp. 30–31. DOI: https://doi.org/10.1038/248030a0.

[11] S. W. Hawking. "Black Holes and Thermodynamics". In: *Phys. Rev. D* 13 (1976), pp. 191–197. DOI: 10.1103/PhysRevD.13.191.

[12] S. W. Hawking. "Breakdown of Predictability in Gravitational Collapse". In: *Phys. Rev. D* 14 (1976), pp. 2460–2473. DOI: 10.1103/PhysRevD.14.2460.

[13] S. W. Hawking. "The Quantum Mechanics of Black Holes". In: *Sci. Am.* 236 (1977), pp. 34–49. DOI: 10.1038/scientificamerican0177-34.

[14] S. W. Hawking. "Particle Creation by Black Holes". In: *Commun. Math. Phys.* 43 (1975). Ed. by G. W. Gibbons and S. W. Hawking. [Erratum: Commun.Math.Phys. 46, 206 (1976)], pp. 199–220. DOI: 10.1007/BF02345020.

[15] Jacob D. Bekenstein. *The Limits of Information*. 2001. arXiv: gr-qc/0009019 [gr-qc]. URL: https://arxiv.org/abs/gr-qc/0009019.

[16] Leonard Susskind, Lárus Thorlacius, and John Uglum. "The stretched horizon and black hole complementarity". In: *Physical Review D* 48.8 (Oct. 1993), pp. 3743–3761. ISSN: 0556-2821. DOI: 10.1103/physrevd.48.3743. URL: http://dx.doi.org/10.1103/PhysRevD.48.3743.

[17] Ahmed Almheiri et al. "Black holes: complementarity or firewalls?" In: *Journal of High Energy Physics* 2013.2 (Feb. 2013). ISSN: 1029-8479. DOI: 10.1007/jhep02(2013)062. URL: http://dx.doi.org/10.1007/JHEP02(2013)062.

[18] Ahmed Almheiri et al. "The entropy of bulk quantum fields and the entanglement wedge of an evaporating black hole". In: *Journal of High Energy Physics* 2019.12 (Dec. 2019). ISSN: 1029-8479. DOI: 10.1007/jhep12(2019)063. URL: http://dx.doi.org/10.1007/JHEP12(2019)063.

[19] Ofer Aharony et al. "Large N field theories, string theory and gravity". In: *Physics Reports* 323.3–4 (Jan. 2000), pp. 183–386. ISSN: 0370-1573. DOI: 10.1016/s0370-1573(99)00083-6. URL: http://dx.doi.org/10.1016/S0370-1573(99)00083-6.

[20] Vijay Balasubramanian et al. "Holographic probes of anti–de Sitter spacetimes". In: *Physical Review D* 59.10 (Apr. 1999). ISSN: 1089-4918. DOI: 10.1103/physrevd.59.104021. URL: http://dx.doi.org/10.1103/PhysRevD.59.104021.

[21] Martin Ammon and Johanna Erdmenger. *Gauge/Gravity Duality: Foundations and Applications*. Cambridge University Press, 2015.

[22] Horaiu Năstase. *Introduction to the AdS/CFT Correspondence*. Cambridge University Press, 2015.

[23] Vijay Balasubramanian, Per Kraus, and Albion Lawrence. "Bulk versus boundary dynamics in anti–de Sitter spacetime". In: *Physical Review D* 59.4 (Jan. 1999). ISSN: 1089-4918. DOI: 10.1103/physrevd.59.046003. URL: http://dx.doi.org/10.1103/PhysRevD.59.046003.

[24] Igor R. Klebanov and Edward Witten. "Ads/CFT correspondence and symmetry breaking". In: *Nuclear Physics B* 556.1–2 (Sept. 1999), pp. 89–114. ISSN: 0550-3213. DOI: 10.1016/s0550-3213(99)00387-9. URL: http://dx.doi.org/10.1016/S0550-3213(99)00387-9.

[25] Harold Erbin. "Scalar propagators on adS space". In: (2014). URL: https://api.semanticscholar.org/CorpusID:212632624.

[26] Jared Kaplan. *Lectures on AdS/CFT from the Bottom Up*. 2016. URL: https://sites.krieger.jhu.edu/jared-kaplan/files/2016/05/AdSCFTCourseNotesCurrentPublic.pdf.

[27] P. Di Francesco, P. Mathieu, and D. Senechal. *Conformal Field Theory*. Graduate Texts in Contemporary Physics. New York: Springer-Verlag, 1997. ISBN: 978-0-387-94785-3, 978-1-4612-7475-9. DOI: 10.1007/978-1-4612-2256-9.

[28] David Tong. *Lectures on String Theory*. 2012. arXiv: 0908.0333 [hep-th]. URL: https://arxiv.org/abs/0908.0333.

[29] Alexandre Belin, Jan de Boer, and Jorrit Kruthoff. *Comments on a state-operator correspondence for the torus*. 2018. DOI: https://doi.org/10.21468/SciPostPhys.5.6.060. arXiv: 1802.00006 [hep-th]. URL: https://arxiv.org/abs/1802.00006.

[30] Ralph Blumenhagen and Erik Plauschinn. *Introduction to conformal field theory: with applications to String theory*. Vol. 779. Lect.Notes Phys. 779 (2009), 1-256, 2009. DOI: 10.1007/978-3-642-00450-6.

[31] Daniel Harlow and Douglas Stanford. *Operator Dictionaries and Wave Functions in AdS/CFT and dS/CFT*. 2011. arXiv: 1104.2621 [hep-th]. URL: https://arxiv.org/abs/1104.2621.

[32] D. Harlow. "Jerusalem lectures on black holes and quantum information". In: *Reviews of Modern Physics* 88.1 (Feb. 2016). ISSN: 1539-0756. DOI: 10.1103/revmodphys.88.015002. URL: http://dx.doi.org/10.1103/RevModPhys.88.015002.

[33] Tatsuma Nishioka, Shinsei Ryu, and Tadashi Takayanagi. "Holographic entanglement entropy: an overview". In: *Journal of Physics A: Mathematical and Theoretical* 42.50 (Dec. 2009), p. 504008. ISSN: 1751-8121. DOI: 10.1088/1751-8113/42/50/504008. URL: http://dx.doi.org/10.1088/1751-8113/42/50/504008.

[34] Pasquale Calabrese and John Cardy. "Entanglement entropy and conformal field theory". In: *Journal of Physics A: Mathematical and Theoretical* 42.50 (Dec. 2009), p. 504005. ISSN: 1751-8121. DOI: 10.1088/1751-8113/42/50/504005. URL: http://dx.doi.org/10.1088/1751-8113/42/50/504005.

[35] Horacio Casini and Marina Huerta. *Lectures on entanglement in quantum field theory*. 2023. arXiv: 2201.13310 [hep-th]. URL: https://arxiv.org/abs/2201.13310.

[36] Curtis Callan and Frank Wilczek. "On geometric entropy". In: *Physics Letters B* 333.1–2 (July 1994), pp. 55–61. ISSN: 0370-2693. DOI: 10.1016/0370-2693(94)91007-3. URL: http://dx.doi.org/10.1016/0370-2693(94)91007-3.

[37] Tatsuma Nishioka. "Entanglement entropy: Holography and renormalization group". In: *Reviews of Modern Physics* 90.3 (Sept. 2018). ISSN: 1539-0756. DOI: 10.1103/revmodphys.90.035007. URL: http://dx.doi.org/10.1103/RevModPhys.90.035007.

[38] Matthias Strodtkötter. "Entanglement Entropy in Conformal Field Theory". In: *ETH Zürich* (2013). URL: https://edu.itp.phys.ethz.ch/fs13/cft/EECFT_Strodtkoetter.pdf.

[39] Pasquale Calabrese and John Cardy. "Entanglement entropy and quantum field theory". In: *Journal of Statistical Mechanics: Theory and Experiment* 2004.06 (June 2004), P06002. ISSN: 1742-5468. DOI: 10.1088/1742-5468/2004/06/p06002. URL: http://dx.doi.org/10.1088/1742-5468/2004/06/P06002.

[40] Shinsei Ryu and Tadashi Takayanagi. "Holographic Derivation of Entanglement Entropy from the anti–de Sitter Space/Conformal Field Theory Correspondence". In: *Physical Review Letters* 96.18 (May 2006). ISSN: 1079-7114. DOI: 10.1103/physrevlett.96.181602. URL: http://dx.doi.org/10.1103/PhysRevLett.96.181602.

[41] Aitor Lewkowycz and Juan Maldacena. "Generalized gravitational entropy". In: *Journal of High Energy Physics* 2013.8 (Aug. 2013). ISSN: 1029-8479. DOI: 10.1007/jhep08(2013)090. URL: http://dx.doi.org/10.1007/JHEP08(2013)090.

[42] S.S. Gubser, I.R. Klebanov, and A.M. Polyakov. "Gauge theory correlators from non-critical string theory". In: *Physics Letters B* 428.1–2 (May 1998), pp. 105–114. ISSN: 0370-2693. DOI: 10.1016/s0370-2693(98)00377-3. URL: http://dx.doi.org/10.1016/S0370-2693(98)00377-3.

[43] Edward Witten. *Anti De Sitter Space And Holography*. 1998. arXiv: hep-th/9802150 [hep-th]. URL: https://arxiv.org/abs/hep-th/9802150.

[44] Xi Dong. "The gravity dual of Rényi entropy". In: *Nature Communications* 7.1 (Aug. 2016). ISSN: 2041-1723. DOI: 10.1038/ncomms12472. URL: http://dx.doi.org/10.1038/ncomms12472.

[45] Dmitri V Fursaev. "Proof of the holographic formula for entanglement entropy". In: *Journal of High Energy Physics* 2006.09 (Sept. 2006), pp. 018–018. ISSN: 1029-8479. DOI: 10.1088/1126-6708/2006/09/018. URL: http://dx.doi.org/10.1088/1126-6708/2006/09/018.

[46] Matthew Headrick. "Entanglement Rényi entropies in holographic theories". In: *Physical Review D* 82.12 (Dec. 2010). ISSN: 1550-2368. DOI: 10.1103/physrevd.82.126010. URL: http://dx.doi.org/10.1103/PhysRevD.82.126010.

[47] G. W. Gibbons and S. W. Hawking. "Action integrals and partition functions in quantum gravity". In: *Phys. Rev. D* 15 (10 May 1977), pp. 2752–2756. DOI: 10.1103/PhysRevD.15.2752. URL: https://link.aps.org/doi/10.1103/PhysRevD.15.2752.

[48] James W. York. "Role of Conformal Three-Geometry in the Dynamics of Gravitation". In: 28.16 (Apr. 1972), pp. 1082–1085. DOI: 10.1103/PhysRevLett.28.1082.

[49] Peng Cheng. "Gauge theories with nontrivial boundary conditions: Black holes". In: *Physical Review D* 107.12 (June 2023). ISSN: 2470-0029. DOI: 10.1103/physrevd.107.125022. URL: http://dx.doi.org/10.1103/PhysRevD.107.125022.

[50] Thomas Hartman. "Lectures on Quantum Gravity and Black Holes". In: *Cornell University* (2015). URL: http://www.hartmanhep.net/topics2015/gravity-lectures.pdf.

[51] Veronika E Hubeny, Mukund Rangamani, and Tadashi Takayanagi. "A covariant holographic entanglement entropy proposal". In: *Journal of High Energy Physics* 2007.07 (July 2007), pp. 062–062. ISSN: 1029-8479. DOI: 10.1088/1126-6708/2007/07/062. URL: http://dx.doi.org/10.1088/1126-6708/2007/07/062.

[52] Thomas Faulkner, Aitor Lewkowycz, and Juan Maldacena. "Quantum corrections to holographic entanglement entropy". In: *Journal of High Energy Physics* 2013.11 (Nov. 2013). ISSN: 1029-8479. DOI: 10.1007/jhep11(2013)074. URL: http://dx.doi.org/10.1007/JHEP11(2013)074.

[53] Netta Engelhardt and Aron C. Wall. "Quantum extremal surfaces: holographic entanglement entropy beyond the classical regime". In: *Journal of High Energy Physics* 2015.1 (Jan. 2015). ISSN: 1029-8479. DOI: 10.1007/jhep01(2015)073. URL: http://dx.doi.org/10.1007/JHEP01(2015)073.

[54] S. W. Hawking. "Information loss in black holes". In: *Physical Review D* 72.8 (Oct. 2005). ISSN: 1550-2368. DOI: 10.1103/physrevd.72.084013. URL: http://dx.doi.org/10.1103/PhysRevD.72.084013.

[55] Peng Zhao. "Black Holes in Anti-de Sitter Spacetime". In: 2009. URL: https://api.semanticscholar.org/CorpusID:45636491.

[56] M. Socolovsky. *Schwarzschild Black Hole in Anti-De Sitter Space*. 2017. arXiv: 1711.02744 [gr-qc]. URL: https://arxiv.org/abs/1711.02744.

[57] Ru Ling, Hao Xu, and Yen Chin Ong. "How anti-de Sitter black holes reach thermal equilibrium". In: *Physics Letters B* 826 (Mar. 2022), p. 136896. ISSN: 0370-2693. DOI: 10.1016/j.physletb.2022.136896. URL: http://dx.doi.org/10.1016/j.physletb.2022.136896.

[58] S. J. Avis, C. J. Isham, and D. Storey. "Quantum Field Theory in anti-De Sitter Space-Time". In: *Phys. Rev. D* 18 (1978), p. 3565. DOI: 10.1103/PhysRevD.18.3565.

[59] Gary T. Horowitz and Jorge E. Santos. *Geons and the Instability of Anti-de Sitter Spacetime*. 2014. arXiv: 1408.5906 [gr-qc]. URL: https://arxiv.org/abs/1408.5906.

[60] Krishan Saraswat and Niayesh Afshordi. "Quantum nature of black holes: fast scrambling versus echoes". In: *Journal of High Energy Physics* 2020.4 (Apr. 2020). ISSN: 1029-8479. DOI: 10.1007/jhep04(2020)136. URL: http://dx.doi.org/10.1007/JHEP04(2020)136.

[61] Budhaditya Bhattacharjee, Chethan Krishnan, and Debajyoti Sarkar. "HKLL for the non-normalizable mode". In: *Journal of High Energy Physics* 2022.12 (Dec. 2022). ISSN: 1029-8479. DOI: 10.1007/jhep12(2022)075. URL: http://dx.doi.org/10.1007/JHEP12(2022)075.

[62] Daniel Harlow. *TASI Lectures on the Emergence of the Bulk in AdS/CFT*. 2018. arXiv: 1802.01040 [hep-th]. URL: https://arxiv.org/abs/1802.01040.

[63] Eric Mintun, Joseph Polchinski, and Vladimir Rosenhaus. "Bulk-Boundary Duality, Gauge Invariance, and Quantum Error Corrections". In: *Physical Review Letters* 115.15 (Oct. 2015). ISSN: 1079-7114. DOI: 10.1103/physrevlett.115.151601. URL: http://dx.doi.org/10.1103/PhysRevLett.115.151601.

[64] Ben Freivogel, Ro Jefferson, and Laurens Kabir. "Precursors, gauge invariance, and quantum error correction in AdS/CFT". In: *Journal of High Energy Physics* 2016.4 (Apr. 2016), pp. 1–26. ISSN: 1029-8479. DOI: 10.1007/jhep04(2016)119. URL: http://dx.doi.org/10.1007/JHEP04(2016)119.

[65] Douglas Adams. "The Hitchhiker's Guide to the Galaxy". In: (1995).

[66] Jorge V Rocha. "Evaporation of large black holes in AdS: coupling to the evaporon". In: *Journal of High Energy Physics* 2008.08 (Aug. 2008), pp. 075–075. ISSN: 1029-8479. DOI: 10.1088/1126-6708/2008/08/075. URL: http://dx.doi.org/10.1088/1126-6708/2008/08/075.

[67] Geoffrey Penington. *Entanglement Wedge Reconstruction and the Information Paradox*. 2020. arXiv: 1905.08255 [hep-th]. URL: https://arxiv.org/abs/1905.08255.

[68] Thomas G. Mertens. "Towards black hole evaporation in Jackiw-Teitelboim gravity". In: *Journal of High Energy Physics* 2019.7 (July 2019). ISSN: 1029-8479. DOI: 10.1007/jhep07(2019)097. URL: http://dx.doi.org/10.1007/JHEP07(2019)097.

[69] Julius Engelsöy, Thomas G. Mertens, and Herman Verlinde. "An investigation of AdS_2 backreaction and holography". In: *JHEP* 07 (2016), p. 139. DOI: 10.1007/JHEP07(2016)139. arXiv: 1606.03438 [hep-th].

[70] Thomas Strobl. *Gravity in Two Spacetime Dimensions*. 2000. arXiv: hep-th/0011240 [hep-th]. URL: https://arxiv.org/abs/hep-th/0011240.

[71] Sean M. Carroll. *Spacetime and Geometry: An Introduction to General Relativity*. Cambridge University Press, 2019.

[72] Thomas G. Mertens and Gustavo J. Turiaci. "Solvable models of quantum black holes: a review on Jackiw–Teitelboim gravity". In: *Living Reviews in Relativity* 26.1 (July 2023). ISSN: 1433-8351. DOI: 10.1007/s41114-023-00046-1. URL: http://dx.doi.org/10.1007/s41114-023-00046-1.

[73] Roman Jackiw. "Lower dimensional gravity". In: *Nuclear Physics B* 252 (1985), pp. 343–356. ISSN: 0550-3213. DOI: https://doi.org/10.1016/0550-3213(85)90448-1. URL: https://www.sciencedirect.com/science/article/pii/0550321385904481.

[74] C. Teitelboim. "Gravitation and Hamiltonian Structure in Two Space-Time Dimensions". In: *Phys. Lett. B* 126 (1983), pp. 41–45. DOI: 10.1016/0370-2693(83)90012-6.

[75] Ahmed Almheiri and Joseph Polchinski. "Models of AdS_2 backreaction and holography". In: *JHEP* 11 (2015), p. 014. DOI: 10.1007/JHEP11(2015)014. arXiv: 1402.6334 [hep-th].

[76] Henry Maxfield. "Lectures on black hole information and spacetime wormholes". In: *CERN Winter School on Supergravity, Strings and Gauge Theory* (2021). URL: https://indico.cern.ch/event/970492/contributions/4156436/attachments/2183572/3689048/BHWHlecturesPart1.pdf.

[77] Srijit Bhattacharjee, Subhodeep Sarkar, and Arpan Bhattacharyya. "Scalar perturbations of black holes in Jackiw-Teitelboim gravity". In: *Physical Review D* 103.2 (Jan. 2021). ISSN: 2470-0029. DOI: 10.1103/physrevd.103.024008. URL: http://dx.doi.org/10.1103/PhysRevD.103.024008.

[78] Luca V. Iliesiu and Gustavo J. Turiaci. "The statistical mechanics of near-extremal black holes". In: *Journal of High Energy Physics* 2021.5 (May 2021). ISSN: 1029-8479. DOI: 10.1007/jhep05(2021)145. URL: http://dx.doi.org/10.1007/JHEP05(2021)145.

[79] Evita Verheijden and Erik Verlinde. "From the BTZ black hole to JT gravity: geometrizing the island". In: *Journal of High Energy Physics* 2021.11 (Nov. 2021). ISSN: 1029-8479. DOI: 10.1007/jhep11(2021)092. URL: http://dx.doi.org/10.1007/JHEP11(2021)092.

[80] Juan Maldacena, Douglas Stanford, and Zhenbin Yang. *Conformal symmetry and its breaking in two dimensional Nearly Anti-de-Sitter space*. 2016. arXiv: 1606.01857 [hep-th]. URL: https://arxiv.org/abs/1606.01857.

[81] Juan F. Pedraza et al. "Semi-classical thermodynamics of quantum extremal surfaces in Jackiw-Teitelboim gravity". In: *Journal of High Energy Physics* 2021.12 (Dec. 2021). ISSN: 1029-8479. DOI: 10.1007/jhep12(2021)134. URL: http://dx.doi.org/10.1007/JHEP12(2021)134.

[82] Akash Goel et al. "Classifying boundary conditions in JT gravity: from energy-branes to -branes". In: *Journal of High Energy Physics* 2021.4 (Apr. 2021). ISSN: 1029-8479. DOI: 10.1007/jhep04(2021)069. URL: http://dx.doi.org/10.1007/JHEP04(2021)069.

[83] Julian De Vuyst and Thomas G. Mertens. "Operational islands and black hole dissipation in JT gravity". In: *Journal of High Energy Physics* 2023.1 (Jan. 2023). ISSN: 1029-8479. DOI: 10.1007/jhep01(2023)027. URL: http://dx.doi.org/10.1007/JHEP01(2023)027.

[84] Kanato Goto, Thomas Hartman, and Amirhossein Tajdini. "Replica wormholes for an evaporating 2D black hole". In: *Journal of High Energy Physics* 2021.4 (Apr. 2021). ISSN: 1029-8479. DOI: 10.1007/jhep04(2021)289. URL: http://dx.doi.org/10.1007/JHEP04(2021)289.

[85] Ahmed Almheiri et al. "The Page curve of Hawking radiation from semiclassical geometry". In: *Journal of High Energy Physics* 2020.3 (Mar. 2020). ISSN: 1029-8479. DOI: 10.1007/jhep03(2020)149. URL: http://dx.doi.org/10.1007/JHEP03(2020)149.

[86] Thomas M. Fiola et al. "Black hole thermodynamics and information loss in two dimensions". In: *Physical Review D* 50.6 (Sept. 1994), pp. 3987–4014. ISSN: 0556-2821. DOI: 10.1103/physrevd.50.3987. URL: http://dx.doi.org/10.1103/PhysRevD.50.3987.

[87] Ahmed Almheiri et al. "The entropy of Hawking radiation". In: *Reviews of Modern Physics* 93.3 (July 2021). ISSN: 1539-0756. DOI: 10.1103/revmodphys.93.035002. URL: http://dx.doi.org/10.1103/RevModPhys.93.035002.

[88] Yasuhiro Sekino and L Susskind. "Fast scramblers". In: *Journal of High Energy Physics* 2008.10 (Oct. 2008), pp. 065–065. ISSN: 1029-8479. DOI: 10.1088/1126-6708/2008/10/065. URL: http://dx.doi.org/10.1088/1126-6708/2008/10/065.

[89] Ahmed Almheiri. "Unitary Semiclassical Black Hole Evaporation". In: *Strings Conference, Belgium* (2019). URL: https://member.ipmu.jp/yuji.tachikawa/stringsmirrors/2019/4_A_Almheiri.pdf.

[90] Juan Maldacena. "Eternal black holes in anti-de Sitter". In: *Journal of High Energy Physics* 2003.04 (Apr. 2003), pp. 021–021. ISSN: 1029-8479. DOI: 10.1088/1126-6708/2003/04/021. URL: http://dx.doi.org/10.1088/1126-6708/2003/04/021.

[91] Juan Maldacena, Douglas Stanford, and Zhenbin Yang. "Diving into traversable wormholes". In: *Fortschritte der Physik* 65.5 (May 2017). ISSN: 1521-3978. DOI: 10.1002/prop.201700034. URL: http://dx.doi.org/10.1002/prop.201700034.

[92] Ahmed Almheiri, Raghu Mahajan, and Juan Maldacena. *Islands outside the horizon*. 2023. arXiv: 1910.11077 [hep-th]. URL: https://arxiv.org/abs/1910.11077.

[93] Ahmed Almheiri et al. "Replica wormholes and the entropy of Hawking radiation". In: *Journal of High Energy Physics* 2020.5 (May 2020). ISSN: 1029-8479. DOI: 10.1007/jhep05(2020)013. URL: http://dx.doi.org/10.1007/JHEP05(2020)013.

[94] Ashis Saha and Sunandan Gangopadhyay. "Quantum chaos in the presence of nonconformality". In: *Phys. Rev. D* 110 (2 July 2024), p. 026025. DOI: 10.1103/PhysRevD.110.026025. URL: https://link.aps.org/doi/10.1103/PhysRevD.110.026025.

[95] Ping Gao, Daniel Louis Jafferis, and Aron C. Wall. "Traversable wormholes via a double trace deformation". In: *Journal of High Energy Physics* 2017.12 (Dec. 2017). ISSN: 1029-8479. DOI: 10.1007/jhep12(2017)151. URL: http://dx.doi.org/10.1007/JHEP12(2017)151.

[96] Pouria Dadras. *Disentangling the thermofield-double state*. 2021. arXiv: 1905.02305 [hep-th]. URL: https://arxiv.org/abs/1905.02305.

[97] Eric Chitambar et al. "Everything You Always Wanted to Know About LOCC (But Were Afraid to Ask)". In: *Communications in Mathematical Physics* 328.1 (Mar. 2014), pp. 303–326. ISSN: 1432-0916. DOI: 10.1007/s00220-014-1953-9. URL: http://dx.doi.org/10.1007/s00220-014-1953-9.

[98] Michael Walter and Maris Ozols. "Lectures Notes on Quantum Information Theory". In: (2022). URL: https://qi.rub.de/courses/qit21/qit22.pdf.